The Dissertation Committee for Ben Barrett Hopkins Certifies that this is the approved version of the following dissertation:

The *P. furiosus* Mre11/Rad50 Complex Facilitates 5' Strand Resection by the HerA Helicase and NurA Nuclease at a DNA Double-Strand Break

Committee:

Tanya T. Paull, Supervisor

Jaquelin P. Dudley

David E. Graham

Makkuni Jayaram

Y. Whitney Yin

The *P. furiosus* Mre11/Rad50 Complex Facilitates 5' Strand Resection by the HerA Helicase and NurA Nuclease at a DNA Double-Strand Break

by

Ben Barrett Hopkins, B.S.; M.S.

Dissertation

Presented to the Faculty of the Graduate School of

The University of Texas at Austin

in Partial Fulfillment

of the Requirements

for the Degree of

Doctor of Philosophy

The University of Texas at Austin

May 2010

Dedication

I dedicate this dissertation to Kim and my family.

Acknowledgements

First and foremost, I would like to thank Dr. Tanya Paull for her continual support and constant encouragement throughout my graduate career. Her insights and advice have been key to my success as a graduate student. I am especially grateful for the freedom to explore and pursue various ideas in her laboratory, which has allowed me to grow tremendously as a researcher.

I would also like to thank all past and present members of the Paull lab: Venu, Rajashree, Qiong, Zhi, Jeff, Ji-hoon, Bettina, Mike, Matt, Melissa, Mingjuan, Elena, Soo-hyun, Julie, Chelsea, and Nodar for their comments and suggestions about my work and for making the lab an enjoyable place to be. I would especially like to thank Zhi for his help in performing and analyzing quantitative PCR experiments.

A special thanks to my dissertation committee, Drs. Jaquelin Dudley, David Graham, Makkuni Jayaram, and Whitney Yin for their invaluable comments on my work.

Most importantly, I would like to thank my family. I cannot thank them enough for all of the support and encouragement they have given me throughout my life. And finally, the person whom I am most thankful for is my wife Kim who has provided me an endless source of love, support, and happiness. Without her, I would not be the person I am today.

The *P. furiosus* Mre11/Rad50 Complex Facilitates 5' Strand Resection by the HerA Helicase and NurA Nuclease at a DNA Double-Strand Break

Publication No._____

Ben Barrett Hopkins, Ph.D.

The University of Texas at Austin, 2010

Supervisor: Tanya T. Paull

The Mre11/Rad50 complex has been implicated in the early steps of DNA double-strand break (DSB) repair through homologous recombination in several organisms. However, the enzymatic properties of this complex are incompatible with the generation of 3' single-stranded DNA for recombinase loading and strand exchange. In thermophilic Archaea, the *mre11* and *rad50* genes cluster in an operon with genes encoding a bidirectional DNA helicase, HerA, and a 5' to 3' exonuclease, NurA, suggesting these four enzymes function in a common pathway. I show that purified Mre11 and Rad50 from *Pyrococcus furiosus* act cooperatively with HerA and NurA to resect the 5' strand at a DNA end under physiological conditions *in vitro* where HerA and NurA alone do not show detectable activity. Furthermore, I demonstrate that HerA and NurA physically interact, and this interaction stimulates both helicase and nuclease

activities. The products of HerA/NurA long-range resection are oligonucleotide products and HerA/NurA activity demonstrates both sequence specificity and a preference to cut at a specific distance from the DNA end. I demonstrate a novel activity of Mre11/Rad50 to make an endonucleolytic cut on the 5' strand, which is consistent with a role for the Mre11 nuclease in the removal of 5' protein conjugates. I also show that Mre11/Rad50 stimulates HerA/NurA-mediated resection through two different mechanisms. The first involves an initial Mre11 nucleolytic processing event of the DNA to generate a 3' ssDNA overhang, which is then resected by HerA/NurA in the absence of Mre11/Rad50. The second mechanism likely involves local unwinding of the DNA end in a process dependent on Rad50 ATPase activity. I propose that this unwinding step facilitates binding of HerA/NurA to the DNA end and efficient resection of the break. Furthermore, the binding affinity of NurA for 3' overhang and unwound DNA end substrates partially explains the efficiency of the two resection mechanisms. Lastly, 3' single-stranded DNA generated by these enzymes can be used by the Archaeal RecA homolog RadA to catalyze strand exchange. This work elucidates how the conserved Mre11/Rad50 complex promotes DNA end resection in Archaea, and may serve as a model for DSB processing in eukaryotes.

Table of Contents

List of Figures xi

CHAPTER 1: INTRODUCTION **1**

DNA damage and the cellular damage response 1

The cellular response to DNA damage 2

DSB repair mechanisms.....3

Homologous Recombination 4

Mre11-Rad50-Xrs2 and DNA break repair 9

Mre11 13

Rad50 14

Nbs1/Xrs2 16

Factors involved with Mre11/Rad50 in DNA repair 18

Hypothesis and Goals 20

CHAPTER 2: THE *P. FURIOSUS* MRE11/RAD50 COMPLEX PROMOTES 5' STRAND RESECTION AT A DNA DOUBLE-STRAND BREAK **23**

Introduction.....23

Results.....27

HerA and NurA physically and functionally interact 27

The Mre11/Rad50 complex stimulates DNA degradation with HerA and NurA 30

The directionality of Mre11/Rad50/HerA/NurA resection is 5' to 3' 33

MR generates short 3' overhangs through 5' strand endonucleolytic activity38

3' ssDNA generated by *Pf*MRHN is used by RadA in strand exchange 44

Discussion.....48

HerA and NurA.....49

Catalytic activities of Mre11 and Rad50 in strand resection 49

Metal ion specificity of Mre11 51

Joint molecule formation in concert with RadA 52

Experimental Procedures 57

Expression constructs.....57

Protein expression and purification 57

Gel filtration.....58

Nuclease assays with labeled DNA substrates.....59

Oligonucleotide DNA substrates 59

Preparation of oligonucleotide and DNA substrates.....60

Helicase assays.....61

ATPase assays.....62

Nuclease assays analyzed by non-denaturing Southern hybridization 62

Processing of gels and membranes for Southern hybridization.....63

Primer extension 63

Joint molecule and strand invasion assays.....63

CHAPTER 3: CHARACTERIZATION OF 5' STRAND RESECTION AND MRE11/RAD50 STIMULATION 65

Introduction.....65

Results.....67

5' resection by Mre11/Rad50 and HerA/NurA result in distinct oligonucleotide products.....67

Structure-specific cleavage by Mre11/Rad50 and HerA/NurA 75

Mre11/Rad50 facilitates HerA/NurA resection through a combination of end-processing and recruitment mechanisms 80

Discussion.....87

HerA/NurA resection is regulated by both sequence and distance from the DNA end.....88

Mre11/Rad50 endonucleolytic activity is consistent with 5' conjugate removal *in vivo* and preferentially cuts at sequences with unusual structure 89

Mre11/Rad50 contributes to resection through initial nucleolytic processing, partial unwinding of the DNA end, and recruitment of NurA to DNA90

Experimental Procedures 97
Protein expression and purification 97
Nuclease assays with labeled DNA substrates.....97
Two-stage *in vitro* resection assays 99
Quantitative PCR 99
Gel shift binding assays 101

CHAPTER 4: CONCLUSIONS AND FUTURE DIRECTIONS **102**

Mre11/Rad50 in DSB repair 102
Mre11/Rad50 and HerA/NurA cooperate to resect the 5' strand 103
Combined helicase/nuclease activity in DNA repair 104
Functional role of Mre11/Rad50.....108
Mre11 nuclease role in resection 109
Rad50 ATP-dependent activities in repair.....111
Strand exchange by the RadA recombinase.....114
Future work.....115
Concluding remarks.....117

References.....119

Vita 130

List of Figures

Figure 1.1: Schematic of DSB repair pathways. 5
Figure 1.2: Schematic of RecBCD catalyzed resection and Chi recognition. 9
Figure 1.3: Schematic representation of human Mre11, Rad50, and Nbs1 proteins. 12
Figure 2.1: *P. furiosus* NurA and HerA interact physically. 28
Figure 2.2: HerA and NurA stimulates the nuclease and helicase activities cooperatively. 29
Figure 2.3: HerA and NurA degrade dsDNA cooperatively with Mre11/Rad50 in magnesium. 33
Figure 2.4: Mre11, Rad50, HerA, and NurA function cooperatively to resect the 5' strand of a DSB. 35
Figure 2.5: Mre11, Rad50, HerA, and NurA resects the 5' strand and not the 3' strand. 37
Figure 2.6: Mre11/Rad50 nuclease activity generates short 3' overhangs. 40
Figure 2.7: Mre11/Rad50 5' endonucleolytic activity occurs in magnesium and is dependent on 3'-5' exonuclease activity. 44
Figure 2.8: Mre11, Rad50, HerA, and NurA together with RadA catalyze homologous strand exchange. 47
Figure 2.9: Schematic model of *Pf*MRHN resection process. 55
Figure 3.1: Mre11/Rad50 and HerA/NurA catalyze the removal of oligonucleotides from the 5' strand and Mre11/Rad50 stimulates HerA/NurA 5' strand resection. 69
Figure 3.2: Mre11/Rad50 demonstrates sequence specificity. 73
Figure 3.3: HerA/NurA resection demonstrates sequence specificity as well as distance-dependent activity. 74
Figure 3.4: Mre11/Rad50 makes an endonucleolytic cut 3' to a poly(T) sequence and is stimulated by HerA. 78
Figure 3.5: Mre11/Rad50 cleavage near a 5' end occurs through endonuclease, not exonuclease activity. 79
Figure 3.6: Mre11 nucleolytic processing facilitates resection by HerA/NurA. 81
Figure 3.7: Quantitation by qPCR of single-stranded DNA produced by resection. 83
Figure 3.8: NurA binds preferentially to DNA with long 3' overhangs or unwound strands. 85
Figure 3.9: Model of 5' strand resection catalyzed by *P. furiosus* Mre11/Rad50, HerA, and NurA. 94

CHAPTER 1: INTRODUCTION

DNA damage and the cellular damage response

Genomic integrity is critical to the survival and reproduction of all organisms. To ensure that their DNA remains free of lesions, cells have evolved various pathways to detect and rapidly repair multiple forms of DNA damage. DNA damage can be caused by normal cellular processes, such as incorrect base incorporation during DNA replication and oxidative base damage due to the formation of reactive oxygen species during metabolism. DNA is also constantly exposed to exogenous sources of damage, which include ultraviolet (UV) and ionizing radiation (IR) and base-modifying chemicals. With these different sources of damage comes a wide variety of lesions, from mismatches, base loss, base modification, protein-DNA adducts, and DNA breaks.

DNA double-strand breaks (DSB) are one of the most cytotoxic forms of DNA damage, and can arise when the DNA replication machinery encounters a single-strand DNA break as well as during programmed cellular processes such as V(D)J recombination and meiosis. DSBs are also formed by extrinsic factors such as exposure to IR and radiomimetic compounds. If these potentially lethal DSBs remain unrepaired, chromosomal translocation and genomic instability will ensue and lead to tumorigenesis in multicellular organisms or death. Thus, the cell needs to tightly regulate these programmed DSB events and has evolved efficient DSB repair pathways.

The cellular response to DNA damage

In eukaryotes, the earliest step in the cellular DNA damage response is the detection of the DNA break by sensor proteins and the subsequent activation of signal transduction pathways. Sensor proteins activate kinases of the phosphatidylinositol 3-kinase like (PIKK) family, which amplify signals by phosphorylating effector kinases, such as Chk1 and Chk2. These effector kinases are then necessary for phosphorylating key cellular factors involved in cell cycle arrest and DNA repair. A third damage response pathway is the activation of the apoptotic program, but reasons for activation of this particular pathway in the presence of DNA breaks are currently unknown. However, certain cell types will preferably undergo apoptosis after induction of DSBs (Cann and Hicks, 2007). Importantly, the signal amplification by multiple kinases ensures that the presence of a single DSB will be rapidly detected and repaired (Shiloh, 2003).

In human cells, DSBs are bound by the Mre11/Rad50/Nbs1 (MRN) complex or the Ku70/Ku80 heterodimer sensor proteins. MRN activates the ATM kinase, which phosphorylates Chk2 and activates repair through the homologous recombination (HR) pathway. The Ku70/Ku80 sensor recruits and activates DNA-PKcs to phosphorylate proteins involved in the non-homologous end joining pathway (NHEJ). HR and NHEJ differ greatly in their repair mechanism and mutagenicity.

DSB repair mechanisms

Repair of DSBs occurs through two main pathways: non-homologous end joining (NHEJ) and homologous recombination (HR). During NHEJ, the two DNA ends are directly ligated together and nucleolytic processing of the breaks prior to ligation often results in permanent loss of genetic material. NHEJ is also active throughout the cell cycle, but is the main pathway for DSB repair during G_1 and early-S phase and is the predominant repair pathway in mammalian cells (Takata et al., 1998). In contrast, HR utilizes a homologous DNA sequence to facilitate DSB repair with high fidelity and is regulated by cyclin-dependent kinases (CDK) to occur in the S and G_2 phases of the cell cycle when sister chromatids are available to serve as the repair template (Aylon et al., 2004; Ira et al., 2004; Jazayeri et al., 2006). HR appears to be the dominant pathway in yeast and prokaryotes (Kowalczykowski et al., 1994; Shrivastav et al., 2008). The preference for repair by HR in yeast has been hypothesized to be due to the high density of coding genes and the need to maintain genome integrity. On the other hand, mammals have a lower percentage of coding genes as well as repetitive sequences, which may be dangerous for HR (Aylon et al., 2004).

Despite the clear differences between HR and NHEJ, these two pathways can compensate for one another as inactivation of one repair pathway results in a shift to the other DSB repair pathway. This was demonstrated in mammalian cells with defective NHEJ that the repair pathway was biased toward HR (Delacote et al., 2002). Takeda and colleagues also showed that either NHEJ or HR pathways repair IR-induced DSBs when either pathway is disabled in DT40 chicken B-cells (Takata et al., 1998). Although NHEJ

and HR repair pathways differ, the Mre11/Rad50/Nbs1 complex is known to be active in both processes (Shrivastav et al., 2008).

HOMOLOGOUS RECOMBINATION

Homologous recombination is the preferred pathway for DSB repair in yeast and prokaryotes (Kowalczykowski et al., 1994; Shrivastav et al., 2008). In contrast to the NHEJ pathway, HR does not result in loss of genetic material because it utilizes a homologous DNA template to facilitate repair. Thus, HR is considered a high fidelity, error-free repair pathway (Fig. 1.1). Repair by HR is a tightly regulated process that occurs in S and G_2 phases of the cell cycle when DNA replication has produced sister chromatids, which are the preferred substrate for HR (Aylon et al., 2004; Ira et al., 2004).

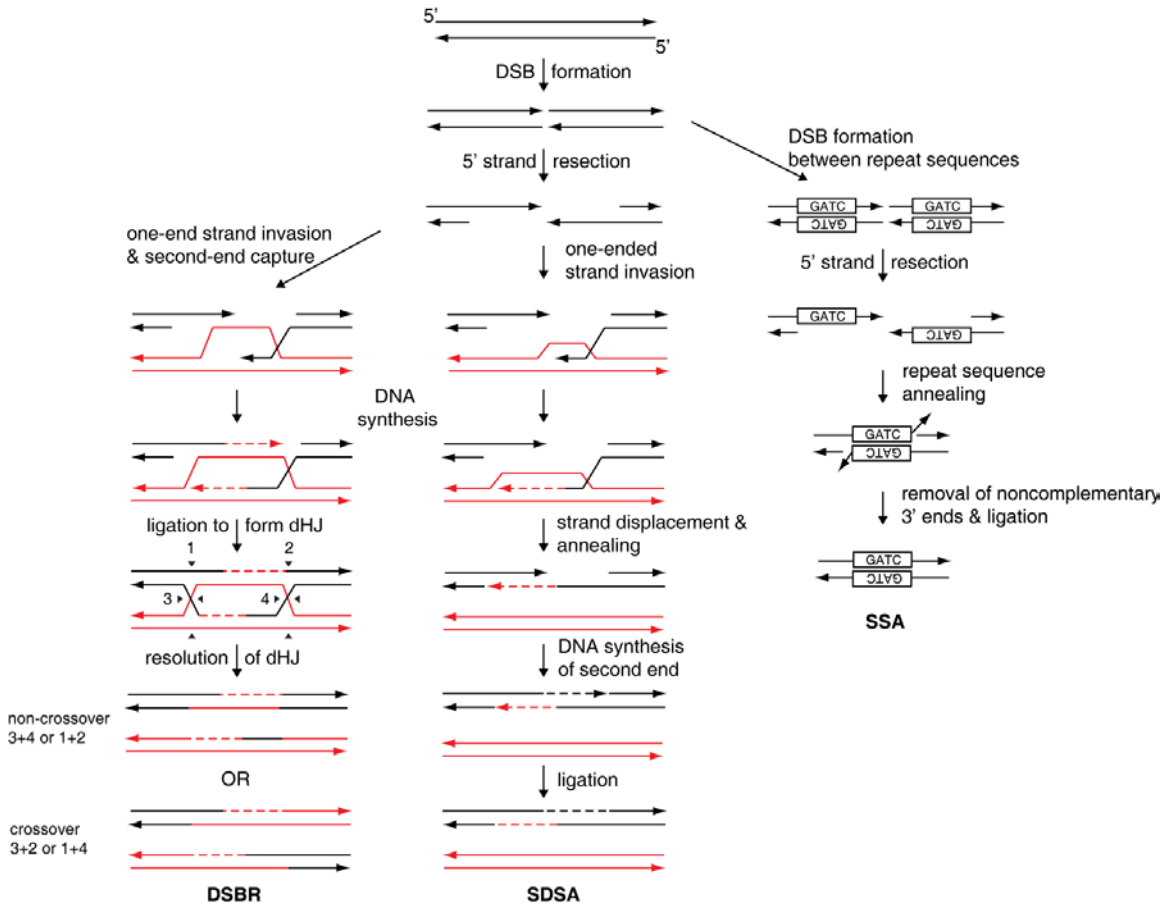

Figure 1.1: Schematic of DSB repair pathways.
Double-strand break repair (DSBR), synthesis dependent strand annealing (SDSA), and single-strand annealing (SSA). The 3' end of DNA is indicated by an arrowhead. Dotted lines indicate newly synthesized DNA. The red DNA is a homologous sequence to the black DNA. "dHJ" is double Holliday junction. Figure adapted from (Symington, 2002).

RecBCD

In *E. coli*, the processing of DSBs for HR is performed by the RecBCD heterotrimeric complex (Dillingham and Kowalczykowski, 2008; Kowalczykowski et al., 1994; Kuzminov, 1999; Smith, 2001) (Figure 1.2). The genetics and biochemistry of

RecBCD indicate that this complex is critical for the repair of DSBs in bacterial cells. Genes encoding *recB and recD* are in an operon with the *recC* gene nearby. The RecB subunit has been shown to possess an N-terminal ATP-dependent 3'-5' helicase activity as well as a C-terminal nuclease domain (Boehmer and Emmerson, 1992; Yu et al., 1998). The RecD subunit is also an ATP-dependent DNA helicase, but unwinds the DNA strands in a 5'-3' polarity (Dillingham et al., 2003; Taylor and Smith, 2003). The RecC component of the complex serves as a scaffold for both RecB and RecD subunits and also utilizes a "pin" structure to separate the DNA duplex (Singleton et al., 2004). RecC is responsible for the detection of the Chi octamer sequence (Singleton et al., 2004) (Fig. 1.2B and Fig. 1.2C).

As a complex, RecBCD binds with high affinity to DNA ends, translocates along the duplex at high velocity, and either degrades both 3' and 5' strands asymmetrically or unwinds the two strands depending on the reaction conditions (Kowalczykowski et al., 1994; Smith, 2001). The RecBCD complex exhibits the unique ability to be regulated by the DNA sequence Chi (5'-GCTGGTGG-3'), at which the complex pauses for ~5 seconds before translocating along DNA approximately 2-fold slower compared to the velocity before Chi (Handa et al., 2005; Spies et al., 2003). The complex then either degrades the 5' strand specifically or induces a nick at Chi (Fig. 1.2A). How Chi brings about this change in activity is currently debated, but it has been suggested that Chi may induce a switch in lead helicase (Spies et al., 2007). Irrespective of how Chi affects RecBCD activity, both processes result in a 3' single-stranded (ss) DNA, which is coated by RecA through direct recruitment by RecB (Spies and Kowalczykowski, 2006).

The RecBCD complex thus consists of a 5'-3' and 3'-5' DNA helicase and a multi-functional nuclease that binds DNA at break sites and begins to degrade or unwind the two strands until it reaches a Chi site on the 3' strand. Recognition of Chi by the RecBCD complex activates RecA recombinase loading by RecBCD onto the 3' strand, which results in RecA-3'ssDNA filaments. These RecA-filaments are involved in searching for a homologous template and catalyze strand invasion at that site. The newly invaded RecA-filament provides the 3' hydroxyl necessary to prime DNA synthesis across the break. Following DNA synthesis, the extended 3' strands are ligated, creating a double Holliday junction (dHJ). Symmetrical or asymmetrical cleavage by the RuvC resolvase results in repair (Kowalczykowski et al., 1994). This mechanism is shown schematically in Figure 1.1 DSBR pathway.

Despite the clear involvement of RecBCD in the DSB repair process in bacteria, no sequence homologs are found in organisms outside of bacteria. A major area of research has been the identification of RecBCD-functional homologs in other organisms. Studies in budding yeast have suggested that a complex containing Mre11-Rad50-Xrs2 (MRX) may be involved in the processing of DNA breaks to facilitate repair.

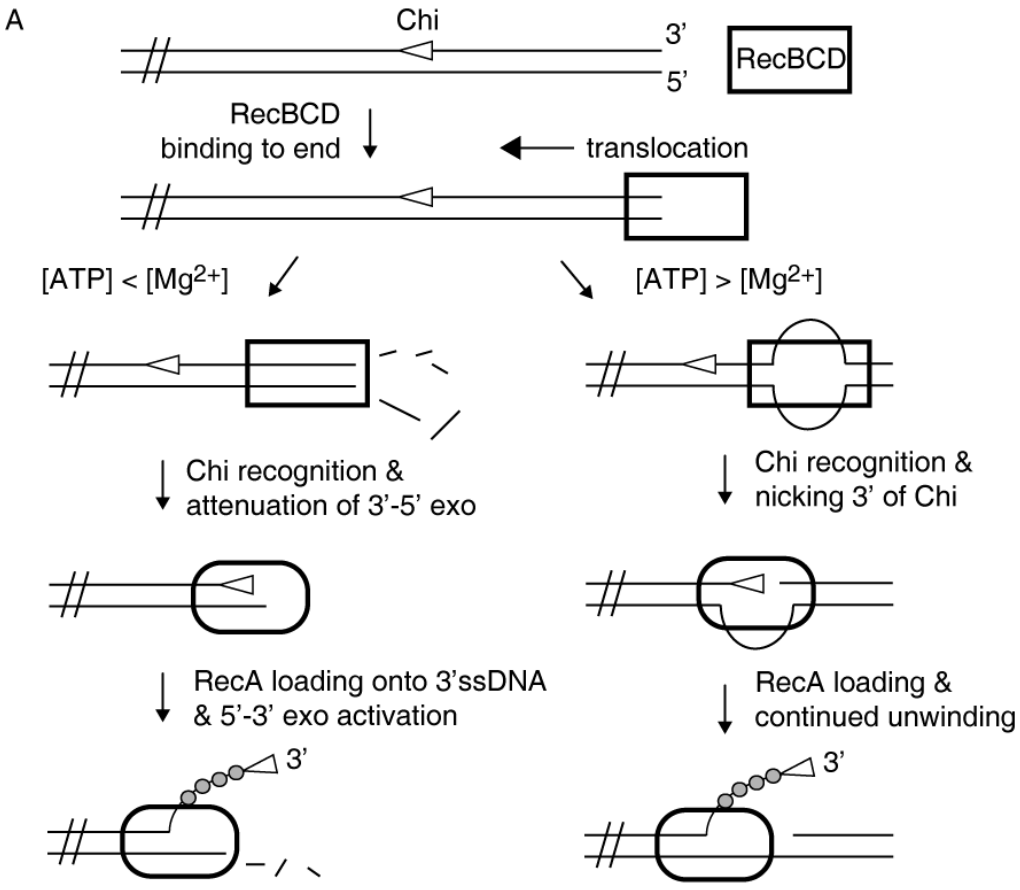
A
Chi
3'
5'
RecBCD
RecBCD
binding to end
translocation
[ATP] < [Mg2+]
[ATP] > [Mg2+]
Chi recognition &
attenuation of 3'-5' exo
Chi recognition &
nicking 3' of Chi
RecA loading onto 3'ssDNA
& 5'-3' exo activation
RecA loading &
continued unwinding
3'
3'

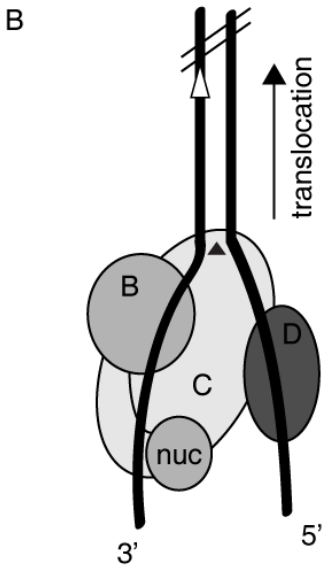
B
translocation
B
D
C
nuc
3'
5'

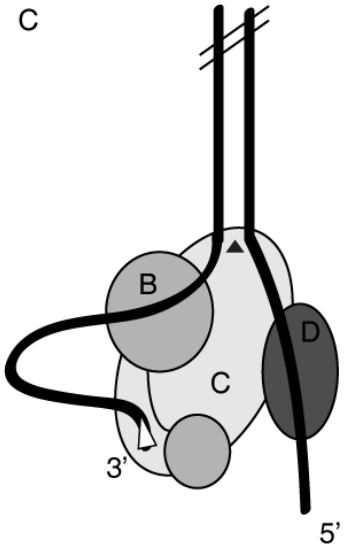
C
B
D
C
3'
5'

Figure 1.2: Schematic of RecBCD catalyzed resection and Chi recognition. (**A**) RecBCD (square rectangle) binds to a DSB end with high affinity and translocates along the duplex. Under conditions where the magnesium are higher than ATP concentrations ([ATP] < [Mg^{2+}], left pathway), RecBCD will asymmetrically degrade both 3' and 5' strands until it reaches the Chi sequence (open triangle) on the 3' strand. Chi induces a change in RecBCD (rounded rectangle), so that it begins to degrade the 5' strand specifically. RecBCD then initiates loading of RecA (gray circles) onto the Chi-terminated 3' ssDNA. Under conditions where the magnesium concentration is less than ATP ([ATP] > [Mg^{2+}], right pathway), RecBCD will unwind the two strands until it reaches Chi. Chi induces a change in RecBCD (rounded rectangle) so that it introduces a nick 3' to Chi. RecBCD then continues to unwind the two strands and begins to load RecA onto the Chi-terminated 3' ssDNA. (**B**) Figure showing the approximate locations of RecBCD relative to each other and DNA. RecC binds both RecB (3'-5' helicase and nuclease) and RecD (5'-3' helicase). RecC also possesses a "pin" structure (small black triangle) which is involved in splitting the DNA duplex. (**C**) When RecBCD reaches Chi (open triangle), binding of Chi to a region on RecC induces a change in RecBCD enzymatic activities. Figure adapted from (Singleton et al., 2004; Smith, 2001).

Mre11-Rad50-Xrs2 and DNA break repair

Mre11, Rad50, and Xrs2 are members of the Rad52 epistasis group of genes and were initially identified in genetic screens in *S. cerevisiae*. Mutations in *MRE11, RAD50,* or *XRS2* confer decreased ionizing radiation survival, meiotic recombination deficiency, and slow vegetative growth (Symington, 2002). The gene products were later shown to interact *in vivo* and form the heterotrimeric complex MRX (Usui et al., 1998). Mre11 and Rad50 are universally conserved in all kingdoms of life, but the third component, Xrs2 in *S. cerevisiae* and Nbs1 in *S. pombe* and mammals, is restricted to eukaryotes. The MRX complex plays a role in many aspects of DNA metabolism; including, initiation and processing of meiotic DSBs, DNA end joining, telomere maintenance, and DNA damage checkpoint signaling (Symington, 2002).

MRE11, RAD50, and *XRS2* were initially identified in genetic screens for mutations that blocked meiosis and increased sensitivity to ionizing radiation (Ajimura et al., 1993; Game and Mortimer, 1974; Ivanov et al., 1992). Work by the Szostak and Kleckner labs demonstrated that yeast meiosis was initiated by a programmed DSB, which was subsequently processed to reveal long 3' ssDNA (Cao et al., 1990; Sun et al., 1989; Sun et al., 1991). The formation of meiotic DSBs was later shown to be formed by Spo11, a Type II like topoisomerase, which is covalently linked through an active site tyrosine residue to the 5' strands (Bergerat et al., 1997; Keeney et al., 1997). Deletions of components of the MRX complex prevent Spo11-dependent meiotic DSB formation, suggesting that MRX is a necessary component for Spo11-initated DSB formation (Cao et al., 1990).

Hypomorphic mutations in *RAD50* and *MRE11 (rad50S* and *mre11S)* allow the formation of Spo11-DSBs but prevent processing at these breaks (Alani et al., 1990; Nairz and Klein, 1997; Tsubouchi and Ogawa, 1998). Keeney and colleagues later showed that Spo11-DNA adducts are removed by an endonucleolytic mechanism where Spo11 remains attached to oligonucleotides between 24-40 nt and 10-15 nt long (Neale et al., 2005). Transient association of MRX to Spo11 breaks *in vivo* (Borde et al., 2004) suggests that the nuclease activity of Mre11 makes the endonucleolytic cut. This was indeed shown to be the case in *S. pombe* where Mre11 along with a second cofactor Ctp1 was required for Rec12 (the Spo11 ortholog) removal (Hartsuiker et al., 2009; Milman et al., 2009; Rothenberg et al., 2009).

Consistent with these findings, earlier work demonstrated that mutations within Mre11 that disrupt nuclease activity prevent meiotic recombination, but surprisingly did

not affect yeast mating-type recombination or DNA end joining (Moreau et al., 1999). Mitotic yeast mating-type switching involves the formation of DSB by the HO-endonuclease at the *MAT* locus and requires DNA processing of the break. Previous work by James Haber and co-workers demonstrated that null strains of *rad50* and *xrs2* are still competent for mating-type switching, but are delayed approximately 30 mins – 1 hr in comparison to wild-type yeast (Ivanov et al., 1994), suggesting a direct role for the MRX complex in processing DSB ends.

Orthologs of Mre11 and Rad50 and the functional homolog of Xrs2, Nbs1, have also been identified in mammals (Figure 1.3). Similar to the MRX complex, these three proteins interact to form the MRN complex (Dolganov et al., 1996). Knockouts of any of these three components results in embryonic lethality in mice (Luo et al., 1999; Xiao and Weaver, 1997; Zhu et al., 2001) and knockdown of Mre11 in chicken DT40 cells results in cell death (Yamaguchi-Iwai et al., 1999), supporting an essential function for MRN in mammalian development. Human patients harboring mutations in *MRE11* and *NBS1* suffer from the diseases Ataxia-Telangiectasia Like Disorder (A-TLD) and Nijmegen breakage syndrome (NBS), respectively. These two diseases share similarities to Ataxia-Telangiectasia where the gene encoding ATM is mutated (Shiloh, 2003). Clinically, patients of these chromosome instability diseases exhibit immunodeficiency and cancer predisposition. On the cellular level, chromosomal breaks and translocations are often observed, as well as increased sensitivity to ionizing radiation, and radioresistant DNA synthesis. Overall, these data demonstrate a central role of the MRN/X complex in critical cellular DNA metabolism pathways.

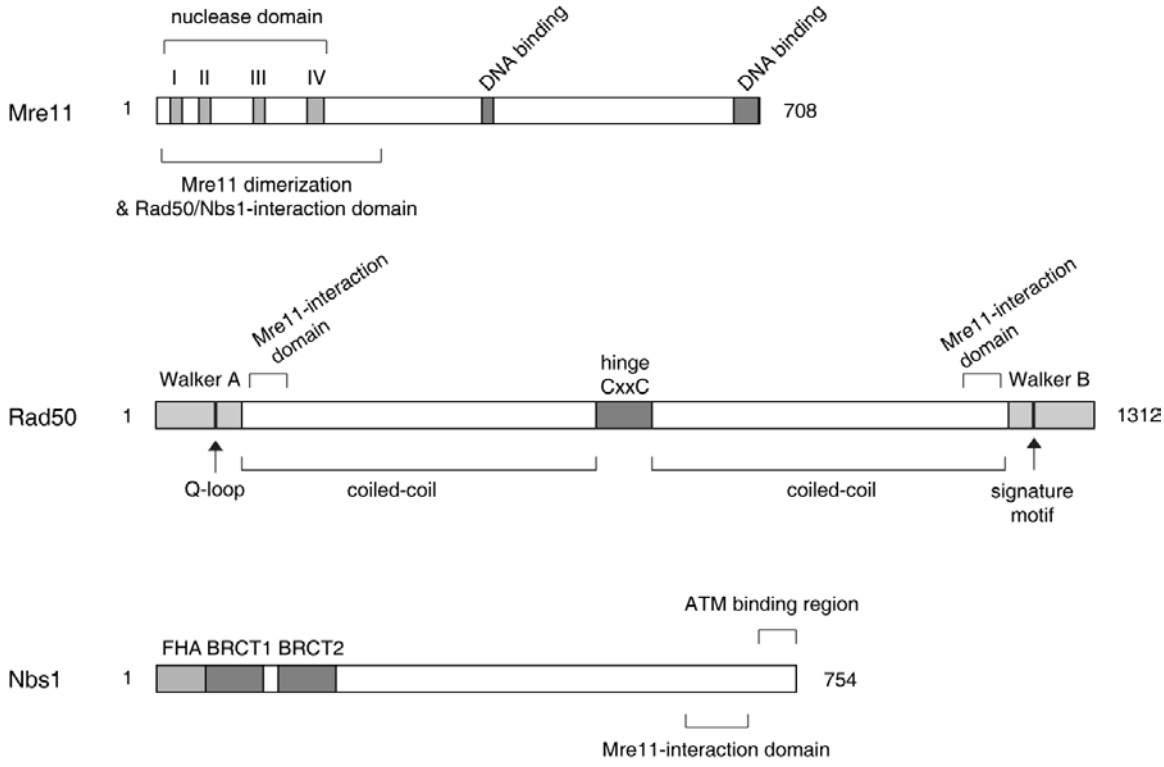

Figure 1.3: Schematic representation of human Mre11, Rad50, and Nbs1 proteins. Mre11 contains four phosphodiesterase motifs (I-IV) at its N-terminus forming the nuclease domain. The nuclease domain overlaps with the Mre11 dimerization and Rad50/Nbs1-interaction domains. Mre11 also has two separate DNA binding motifs at the middle and C-terminus. Rad50 contains N-terminal Walker A and C-terminal Walker B domains which are separated by long coiled-coil regions and a hinge domain. The Walker A and B domains associate with each other to form the active site. The locations of the Q-loop and signature motif and Mre11-interaction domains are indicated. Nbs1 possesses an N-terminal Forkhead-associated (FHA) and two tandem BRCA1-carboxy terminal (BRCT) domains (BRCT1 & BRCT2). Both FHA and BRCT domains are involved in phosphorylated-peptide binding. The ATM and Mre11-binding regions are indicated. The numbers indicate the amino acid number. Figure adapted from (Symington, 2002).

MRE11

The *MRE11* gene encodes for a 692 amino acid (aa) protein in yeast and a 708 aa protein in humans and is critical to the formation of the MRX/MRN complex as Mre11 makes contacts to both the Rad50 and Xrs2/Nbs1 components (Usui et al., 1998). The amino-terminal half of Mre11 is comprised of four separate phosphodiesterase motifs (I-IV) and two DNA-binding motifs in the middle and carboxyl-terminus of the protein (Figure 1.3). Yeast and human Mre11 share homology to the *E. coli* SbcD protein, which forms a complex with SbcC, the *E. coli* Rad50 homolog (Connelly and Leach, 1996). The SbcCD complex was shown to have ATP-dependent dsDNA 3'-5' exonuclease and ATP-independent ssDNA endonuclease activity and requires manganese as the divalent cation (Connelly et al., 1999; Connelly et al., 1997). *In vitro* characterization of Mre11 from yeast and humans demonstrate that Mre11 is also a manganese-dependent 3'-5' dsDNA exonuclease and ssDNA endonuclease, but does not require ATP hydrolysis (Paull and Gellert, 1998; Trujillo and Sung, 2001).

X-ray crystallography studies of a *Pyrococcus furiosus* Mre11 fragment (residues 1-342 of 426 aa) indicate that two manganese ions are coordinated in close proximity by a total of seven amino acid residues, mostly from the four phosphodiesterase motifs (Hopfner et al., 2001). Thus, mutation of conserved aspartic acid or histidine residues within these phosphodiesterase motifs often results in inactivation of Mre11 nuclease activity, as many of these residues are involved in metal-ion coordination or transition state stabilization. Mre11 has been shown by yeast two-hybrid and size-exclusion chromatography to form dimers or higher order multimers (Furuse et al., 1998; Johzuka

and Ogawa, 1995; Paull and Gellert, 1998), and this Mre11 multimerization was shown to be mediated through an N-terminal hydrophobic region in both *P. furiosus* and *S. pombe* Mre11 (Williams et al., 2008).

Considering that each Mre11 monomer has the capacity to bind DNA ends, Mre11-Mre11 complexes may potentially bridge two DNA break ends to facilitate repair through the end joining pathway. Evidence supporting this notion comes from crystallographic data of *P. furiosus* Mre11-Mre11 dimers bound to two DNA ends (Williams et al., 2008), and *in vitro* data demonstrating Mre11 alone is able to facilitate end joining of both complementary 5' or 3' overhang and noncomplementary 5' overhang DNA; however, an Mre11-nuclease mutant was unable to join mismatched 5' overhang ends (Paull and Gellert, 1998, 2000). The ability of Mre11 to mediate end joining between two non-cohesive ends by nucleolytically degrading the 3' strand is further supported by the observation that addition of noncomplementary overhang DNA enhances Mre11 3'-5' exonuclease activity, but not a complementary sequence (Paull and Gellert, 2000). Recent work also indicates that mutations that block Mre11 dimer formation also destabilize ss and dsDNA binding and confer a mild sensitivity to DNA damaging agents, indicating a role for Mre11 dimer formation in repair (Williams et al., 2008).

RAD50

The Rad50 protein is a large protein of 1312 aa in yeast and humans and has an unusual architecture. The amino- and carboxy-termini form globular head domains with

Walker A (N-terminus) and Walker B (C-terminus) domains, which are separated by long coiled coils regions with a hinge region containing a zinc-binding Cys-x-x-Cys (CxxC) motif (Hopfner et al., 2002) (Figure 1.3). These coiled-coil segments fold back on themselves, forming an anti-parallel coiled coil with the zinc-hook at the apex and the two Walker A and B domains adjacent to each other. The Walker A/B head domains contain the catalytic residues necessary for nucleotide binding and hydrolysis, respectively. In addition, the amino-terminus also contains a Q-loop and the carboxyl-terminus contains a signature motif, characteristics of the ATP-binding cassette (ABC) transporter superfamily. The two N- and C-terminal ATPase head domains and the extensive coiled coils, which separate the two domains, make Rad50 architectually similar to Structural Maintenance of Chromosomes (SMC) proteins. These proteins include the condensin and cohesin proteins involved in chromosome condensation and sister chromatid cohesion, respectively.

Mutations in Rad50 indicate its importance in both homologous chromosome synapsis and meiotic recombination (Alani et al., 1990) and its unusual structure as well as adenylate cyclase activity may be involved in tethering DNA homologs/sister chromatids following DSB formation (Bhaskara et al., 2007; Lobachev et al., 2004). Biophysical studies of Rad50 from *P. furiosus* indicate that the N- and C-terminal ATPase head domains dimerize with an ATPase head domain from a second Rad50 molecule in the presence of ATP and this dimerization is critical for DNA binding (Hopfner et al., 2000b). The binding site for Mre11 on Rad50 maps to the first 40 amino acids of the coiled coil adjacent to the ATPase domain (Hopfner et al., 2001), which

suggests that the Mre11 dimer may help to bind two Rad50 ATPase domains in close proximity in the absence of ATP.

Electron microscopy of Mre11/Rad50 complexes from humans show that the coiled coils that protrude from the ATPase head domains can extend 600 Å (de Jager et al., 2001; Hopfner et al., 2001) which can bind DNA breaks (between sister chromatids, homologous chromosomes, or intra-chromatid) up to 1,200 Å when two Rad50 molecules are linked through the zinc-hook to facilitate repair. This may indeed be the case as mutations in the zinc-hook of budding yeast Rad50 resulted in increased sensitivity to ionizing radiation; however, this phenotype may be partly due to MRX complex instability (Hopfner et al., 2002). Thus, Rad50 contributes to DNA repair both enzymatically and structurally.

NBS1/XRS2

The Mre11/Rad50 complex contains a third component, Nbs1 in mammals and *S. pombe* and Xrs2 in *S. cerevisiae* (Figure 1.3). A homolog of Nbs1/Xrs2 is absent in the Archaeal and bacterial complexes. This third subunit of the Mre11/Rad50 complex is a non-enzymatic component, but contributes to the complex as an enzyme regulator and serves to recruit other proteins to sites of DNA damage. In agreement with this, mammalian Nbs1 was previously reported to be essential for DNA repair (Tauchi et al., 2002). Human Nbs1 is a 754 aa protein, whereas the *S. pombe* version is 613 aa. *S. cerevisiae* Xrs2 is an 854 aa protein.

Both Nbs1 and Xrs2 contain N-terminal forkhead-associated (FHA) domains which are involved in binding of phosphorylated proteins. However, only Nbs1 contains two tandem BRCA1 carboxy-terminal (BRCT) domains which are also involved in phospho-protein interactions, immediately C-terminal to the FHA domain. Several groups have shown recently that the FHA domains of *S. pombe* Nbs1 bind to phosphorylated Ctp1 to regulate the repair process (Lloyd et al., 2009; Williams et al., 2009). Nbs1 interacts with Mre11 through the C-terminus of Nbs1 and also recruits ATM to DNA breaks through its C-terminal 50 aa (Falck et al., 2005; You et al., 2005). Nbs1 and Xrs2 have also been shown *in vitro* to modulate Mre11/Rad50 activities, including nucleotide-dependent DNA binding, ATP-dependent 3' overhang cutting, and ATP-dependent DNA unwinding (Lee et al., 2003; Paull and Gellert, 1999; Trujillo et al., 2003).

Nbs1 also contains a nuclear localization sequence and is implicated in DNA damage foci formation (Desai-Mehta et al., 2001; Tauchi et al., 2001; Tseng et al., 2005). In addition, Nbs1 was shown to be recruited to casein kinase 2 (CK2) phosphorylated Mdc1 at sites of damage *in vivo* (Chapman and Jackson, 2008; Melander et al., 2008; Spycher et al., 2008; Wu et al., 2008) through interactions with both FHA and BRCT domains of Nbs1 (Williams et al., 2009), and this Nbs1-Mdc1 interaction is critical to the DSB-induced S-phase checkpoint (Wu et al., 2008). Despite being the only non-enzymatic component of the Mre11/Rad50 complex, Nbs1/Xrs2 plays critical regulatory roles in the heterotrimeric complex. It also serves to recruit important proteins in the signaling and repair pathways and helps to localize these factors to DSBs.

Factors involved with Mre11/Rad50 in DNA repair

In yeast, meiotic recombination is initiated by DSBs introduced by Spo11 at meiotic hotspots. Spo11 forms these breaks by covalently attaching itself through a reactive tyrosine residue to the 5' strand (Bergerat et al., 1997). Removal of these Spo11-adducts is a prerequisite for 5' resection and recombination. However, mutations in *RAD50* (*rad50S*) and *SAE2* prevent the endonucleolytic removal of Spo11 adducts from DNA, suggesting that the MRX does not remove Spo11 adducts alone in *S. cerevisiae* (Keeney and Kleckner, 1995; McKee and Kleckner, 1997; Prinz et al., 1997). Sae2 was also shown to be involved with the MRX complex in the repair of hairpin structures in mitotic cells (Lobachev et al., 2002), and it was later discovered by work in our lab that Sae2 is itself an endonuclease that functionally cooperates with MRX in processing hairpin ends (Lengsfeld et al., 2007).

Sae2 was shown to localize rapidly to sites of DSBs *in vivo* (Lisby et al., 2004) and *sae2Δ* yeast were impaired in repairing an HO-induced DSB (Clerici et al., 2005), suggesting Sae2 involvement in DSB repair. Sae2 is also a target of phosphorylation by Mec1 and Tel1 as well as CDK (Baroni et al., 2004; Huertas et al., 2008). These phosphorylation events of Sae2 are proposed to regulate its activity in response to the cell cycle and the presence of damage, but the order of Mec1/Tel1 and CDK phosphorylation is currently unknown.

CtIP and Ctp1 have been identified as orthologs of Sae2 in mammals and *S. pombe*, respectively. Expression of both CtIP and Ctp1 are affected by the cell cycle phase, with highest expression in S/G_2 corresponding to phosphorylation by CDKs, thus restricting their repair activities to the S/G_2 phases (Huertas and Jackson, 2009; Limbo et

al., 2007; Yun and Hiom, 2009). Although both CtIP and Ctp1 are implicated in homologous recombination repair, only CtIP has been shown to be necessary for repair through microhomology-mediated end joining (MMEJ) (Limbo et al., 2007; Sartori et al., 2007; Yun and Hiom, 2009). CtIP is phosphorylated by ATM on Ser664 and Ser745 in response to DNA damage, and this phosphorylation event is critical for the dissociation of Brca1 from the CtIP/Brca1 complex (Li et al., 2000). In addition, ATM kinase activity recently was shown to be important for the recruitment of *Xenopus* CtIP to damaged chromatin (You et al., 2009). Due to phosphorylation in response to damage and its function in repair, CtIP may coordinate the signaling and repair of DNA damage.

The Mre11/Rad50 complex is known to localize to sites of DSBs *in vivo* and dissociate after repair has been initiated (Lisby et al., 2004; Shroff et al., 2004). Based on the interaction between the MRN/X complex and CtIP/Sae2, it is highly likely that CtIP/Sae2 activity is also restricted to the immediate vicinity of the break. The confinement of MRN/X and CtIP/Sae2 to DNA ends raises the question of what enzymes are responsible for extensive resection far from the initial DSB and what is the role of the Mre11/Rad50 complex in regulating this process.

Recent work in budding yeast has identified redundant pathways that are involved in extensive 5’ strand resection: Exo1 and Dna2/Sgs1 (Mimitou and Symington, 2008; Zhu et al., 2008). Both Exo1 and Dna2 are 5’-3’ exonucleases and Sgs1 is a RecQ-family DNA helicase. Chromatin immunoprecipitation (ChIP) experiments also demonstrate that Sgs1 and Dna2 are found further from the DSB in a time-dependent manner, in contrast to Mre11 DSB localization (Shroff et al., 2004; Zhu et al., 2008). Taken together, the observation that the Mre11/Rad50 complex functions with many other cellular factors

indicates that MR is not solely responsible for DSB repair, but its role in the repair process remains unknown.

Hypothesis and Goals

The precise role of the Mre11/Rad50 complex in meiosis and DNA double-strand break repair pathways has yet to be determined. Much of our understanding of the Mre11/Rad50 role in the repair process has been provided by genetic studies in budding and fission yeast, which provides clues into Mre11/Rad50 *in vivo* function without defining Mre11/Rad50 biochemical activity. The underlying observation from studies in yeast is that Mre11/Rad50 does not function alone.

In yeast meiosis, Mre11/Rad50 along with Spo11 and many other proteins are involved in generating the critical double-strand breaks that initiate meiosis (Keeney, 2001). After the break is formed, Mre11/Rad50 and the cofactor Sae2/Ctp1 are required for the endonucleolytic removal of Spo11-conjugates (Hartsuiker et al., 2009; Milman et al., 2009; Neale et al., 2005; Rothenberg et al., 2009). To further support the notion that Mre11/Rad50 does not function alone in the double-strand break repair pathway, Exo1 and Sgs1/Dna2 have been identified as redundant pathways to generate recombinogenic 3’ single-stranded DNA for homologous recombination in yeast (Mimitou and Symington, 2008; Zhu et al., 2008). However, despite these studies that demonstrate Mre11/Rad50 involvement in meiosis and the repair of DNA double-strand breaks, the biochemical function of Mre11/Rad50 has yet to be resolved.

To investigate the role of Mre11/Rad50 in the DNA repair process, I undertook an *in vitro* approach using recombinant, purified proteins from *Pyrococcus furiosus*. The reasoning for studying proteins from this organism is three-fold: firstly, hyperthermophilic Archaea have been shown to possess an efficient DSB repair pathway, which confers high resistance to ionizing radiation and extreme temperatures (DiRuggiero et al., 1997; Gerard et al., 2001; Peak et al., 1995). Secondly, the *mre11* and *rad50* genes are found in an operon with two genes *herA* and *nurA*, which encode a DNA helicase and 5'-3' exonuclease, respectively (Constantinesco et al., 2002; Constantinesco et al., 2004; Manzan et al., 2004). The genomic organization of genes in prokaryotes into operons often suggests that the gene products are involved in a similar biochemical pathway. Further support for an interaction between these gene products is based on the observation in *Methanobacterium thermoautotrophicus* where the HerA gene is split and the C-terminal half is fused to Mre11 (Constantinesco et al., 2004; Manzan et al., 2004). Purified HerA was reported to be a dsDNA-stimulated ATPase and ATP-dependent bipolar DNA helicase (Constantinesco et al., 2004; Manzan et al., 2004). HerA from *P. abyssi* was also shown by gel filtration chromatography and electron microscopy to form hexameric ring structures (Manzan et al., 2004). NurA from *S. acidocaldarius* demonstrates manganese-dependent ssDNA endonuclease as well as 5'-3' exonuclease activity (Constantinesco et al., 2002). This genomic organization as well as the associated enzymatic activities are reminiscent of the bacterial RecBCD system, suggesting that Mre11/Rad50/HerA/NurA may interact to repair DNA breaks *in vivo*. Thirdly, until recently, all of the solved crystal structures of Mre11 and Rad50 have been of *P. furiosus* proteins (Hopfner et al., 2002; Hopfner et al., 2001; Hopfner et al., 2000b).

Based on the discovery of the *herA*, *nurA*, *mre11*, and *rad50* operon in many hyperthermophilic Archaea and previous work indicating a role for the Mre11/Rad50 complex in DNA double-strand break repair, I hypothesize that the Mre11/Rad50 complex along with HerA and NurA enzymes function cooperatively to resect the 5' strand of a DNA double-strand break. I also hypothesize that the exposed 3' ssDNA is sufficient for RadA recombinase binding and the RadA-ssDNA filament catalyzes strand exchange when a homologous DNA sequence is present.

The work described here characterizes the individual activities of the Mre11/Rad50 complex, HerA, and NurA from *P. furiosus in vitro*. The synergistic effects of these proteins are determined as well as physical interactions between these enzymes. I also demonstrated that 5' strand resection occurs in two distinct stages, where HerA and NurA are responsible for long-range resection and Mre11/Rad50 is involved in the initial processing of DNA ends and activation of HerA/NurA. Furthermore, I demonstrated formation of a joint molecule intermediate when the RadA recombinase and a homologous DNA sequence are included together with Mre11/Rad50, HerA, and NurA. Thus, I successfully reconstituted the first several stages of homologous recombination—from 5' strand resection to strand exchange between homologous sequences—using purified proteins *in vitro*. Based on my work, I propose a model for 5' strand resection, and believe this system provides insights into how DSB repair functions in higher organisms.

CHAPTER 2: THE *P. FURIOSUS* MRE11/RAD50 COMPLEX PROMOTES 5' STRAND RESECTION AT A DNA DOUBLE-STRAND BREAK

Portions of this chapter have been published: Hopkins B.B. and Paull T.T. (2008), Cell 135: 250-350.

Introduction

The rapid detection and subsequent repair of DNA double-strand breaks (DSBs) is critical for the survival of all organisms. Breaks in chromosomal DNA occur during replication, oxidative damage, programmed recombination events, including meiosis and V(D)J recombination, and exposure to exogenous agents, such as ionizing radiation (IR) and radiomimetic chemicals. Two distinct pathways exist to repair DSBs: non-homologous end joining (NHEJ) and homologous recombination (HR). NHEJ proteins process and religate the DNA ends, whereas the HR pathway uses a homologous template to repair DNA breaks and is considered a relatively error-free method of DSB repair.

The choice of DSB repair pathway varies by organism as well as by cell cycle stage. In bacteria, the predominant DSB repair pathway is HR (Kowalczykowski et al., 1994). Both NHEJ and HR are used in eukaryotic cells; however HR is preferred in S and G_2 when sister chromatids are present (Sonoda et al., 2006). HR is presumably the preferred method of DSB repair in Archaea as proteins involved in HR have been identified, but NHEJ Ku70/80 homologs are absent in most Archaea (Aravind and Koonin, 2001; Doherty et al., 2001).

HR proceeds in several distinct stages: the earliest step is processing of the DNA end to produce 3' single-stranded DNA (ssDNA). Following or during 5' strand resection, the 3' ssDNA is bound by RecA-family recombinases into a filament that catalyzes homologous pairing and DNA strand exchange. The 3' end then primes DNA synthesis, and resolution of Holliday junctions or strand annealing between newly-synthesized ends results in repair of the initial DSB (Seitz et al., 2001).

Much of our understanding of the initial DSB processing step in HR results from studies of the *E. coli* RecBCD complex (Kowalczykowski et al., 1994; Kuzminov, 1999; Singleton et al., 2004; Smith, 2001). RecBCD exists as a heterotrimeric complex and exhibits DNA helicase, ATPase, and both 5' and 3' exonuclease activities. RecBCD binds with high affinity to DNA ends and translocates along the DNA duplex, usually accompanied by degradation of both strands, until it encounters the cis-element Chi on the 3' strand. Binding of RecBCD to the Chi sequence results in pausing, nicking of the 3' strand at Chi, and 5' DNA strand resection (or further unwinding of the duplex). RecBCD also facilitates the loading of the RecA recombinase onto the 3' ssDNA, which catalyzes strand exchange.

Despite the importance of RecBCD for DSB processing in bacteria, there are no apparent functional homologs of this complex in eukaryotes or Archaea. In eukaryotes, the processing step is a critical decision point in HR and is controlled by cyclin-dependent kinases to occur in the S and G_2 phases of the cell cycle (Aylon et al., 2004; Ira et al., 2004; Jazayeri et al., 2006). Genetic evidence from budding yeast suggests that the Mre11/Rad50/Xrs2 (MRX) complex is involved in the resection process in eukaryotic cells. The *MRE11*, *RAD50*, and *XRS2* genes were identified in *S. cerevisiae* through

mutations that resulted in poor vegetative growth, reduced survival of ionizing radiation (IR), and spore inviability (Symington, 2002). Hypomorphic mutations in Rad50 (and functionally similar mutations later found in Mre11) were also found to specifically block resection of Spo11-induced DSBs during meiosis (Alani et al., 1990; Nairz and Klein, 1997; Tsubouchi and Ogawa, 1998). This evidence, combined with observations that MRX-null mutants exhibit a marked delay in DSB resection in vegetative cells (Ivanov et al., 1994), suggests that the MRX complex plays a direct role in DNA end processing in eukaryotes.

Homologs of Mre11 and Rad50 are present in all organisms studied to date and exist as a stable complex. In eukaryotes, the Mre11/Rad50 (MR) complex also contains Nbs1 (Nibrin) in mammalian cells or Xrs2 in budding yeast to form MRN and MRX, respectively. However, the *E. coli* SbcCD complex and archaebacteria MR do not have an associated third component. Sequence analysis of Mre11/SbcD identified four N-terminal phosphodiesterase and two DNA-binding domains, and biochemical studies demonstrate that Mre11 exhibits manganese-dependent 3'-5' exonuclease and ssDNA endonuclease activities *in vitro* (Connelly et al., 1999; Paull and Gellert, 1998; Trujillo and Sung, 2001). Rad50/SbcC is architecturally related to the Structural Maintenance of Chromosomes (SMC) family of proteins, with N- and C-terminal head domains which contain the Walker A and Walker B motifs, respectively, separated by a long coiled-coil region with a zinc hook. Biochemical characterization of Rad50 indicate that in addition to ATPase activity, it posseses adenylate kinase activity that is involved in DNA tethering (Bhaskara et al., 2007). The MR complex also plays a role in both NHEJ and HR pathways of DSB repair (D'Amours and Jackson, 2002).

Archaea constitute the third kingdom of life and consist of organisms that live in varied and extreme conditions. In all thermophilic Archaea studied to date, the genes encoding Mre11 and Rad50 are found together in an operon, similar to *E. coli* SbcCD. In addition to Mre11 and Rad50, two other genes which encode an ATP-dependent, bidirectional DNA helicase (HerA/MlaA) and a 5'-3' exonuclease (NurA) are found together with Mre11/Rad50 in almost all thermophilic Archaea (Constantinesco et al., 2002; Constantinesco et al., 2004; Manzan et al., 2004). Besides their initial biochemical characterization, little is known about HerA and NurA *in vivo* activities. Based on this strong association and genetic evidence from eukaryotic cells, I hypothesize that Mre11 and Rad50 may function with the HerA and NurA gene products to catalyze DSB resection. To test this idea, I used proteins from the Euryarchaea hyperthermophile *Pyrococcus furiosus* (*Pf*), which grows optimally at 96°C under anaerobic conditions (Allers and Mevarech, 2005). The Archaeal homologs of Mre11 and Rad50 were initially identified in *P. furiosus* (Hopfner et al., 2000a), and the crystal structures of the catalytic domains have been solved for these proteins (Hopfner et al., 2002; Hopfner et al., 2001; Hopfner et al., 2000b).

In this work, I show that purified, recombinant *Pf*HerA and *Pf*NurA interact physically and functionally to carry out helicase and nuclease activities on double-stranded DNA. I also show that at limiting levels of HerA and NurA, *Pf*Mre11/Rad50 is required for 5' end resection and that this process is dependent upon the enzymatic activities of HerA, NurA, and Rad50, but not Mre11. I then demonstrate that all four proteins together with the RecA-homolog RadA catalyze the formation of D-loop recombination intermediates from linear dsDNA and circular dsDNA *in vitro*. Our

findings support a model where the MR complex is involved in the initial processing step required for the loading or activation of HerA-NurA to promote resection of the 5' strand of the DSB and initiation of strand invasion.

Results

HERA AND NURA PHYSICALLY AND FUNCTIONALLY INTERACT

Based on the operon clustering of the Mre11, Rad50, HerA, and NurA genes in thermophilic Archaea, I hypothesized that these gene products may interact physically and/or functionally. To investigate this possibility, I cloned the HerA and NurA genes from the *Pyrococcus furiosus* genomic DNA, expressed each protein separately in *E. coli*, purified the proteins to ≥95% homogeneity, and performed gel filtration, nuclease, and helicase assays. I observed that *P. furiosus* HerA fractionates as a large complex by gel filtration (Fig. 2.1, top panel), consistent with electron microscopy results showing that a homolog of HerA from *P. abyssi* exists in a hexameric ring structure (Manzan et al., 2004). The *P. furiosus* NurA gel filtration profile is consistent with either a monomer or dimer stoichiometry (Fig. 2.1, middle panel). A strong, ATP-independent interaction was observed between HerA and NurA when incubated together (Fig. 2.1, bottom panel), and based on this result I estimate that between 1-3 NurA monomers bind the HerA hexamer. No direct interaction was observed between purified, recombinant *P. furiosus* Mre11/Rad50 (MR) and either HerA or NurA (data not shown).

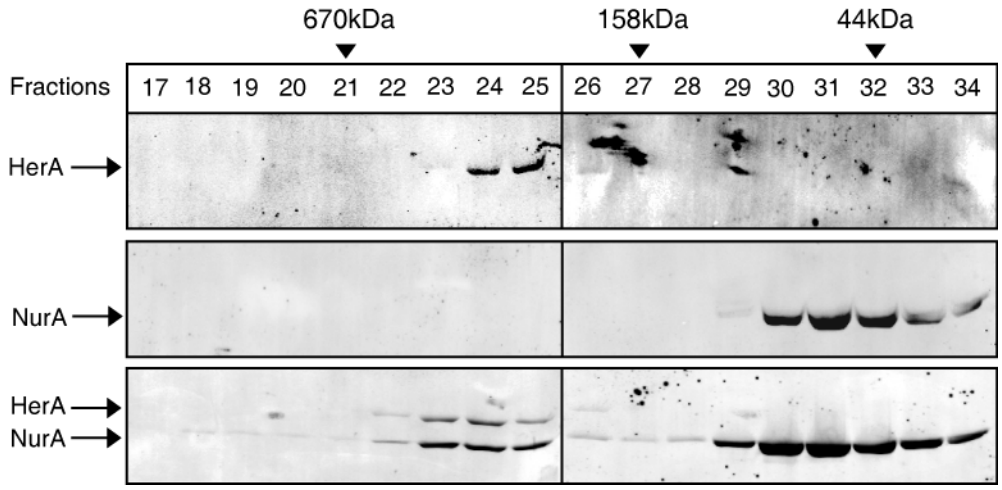

Figure 2.1: *P. furiosus* NurA and HerA interact physically.
Superdex 200 gel filtration of purified HerA and NurA. Purified proteins were incubated alone (HerA: top panel, NurA: middle panel) or in combination (bottom panel) at 55°C for 15 min before gel filtration, as indicated, and fractions were analyzed by SDS-PAGE and α-His Western blot. HerA was used at a concentration of 290 nM (hexamer) and NurA at 7 μM (monomer). HerA is a 62 kDa protein and NurA is a 52 kDa protein. Migration of molecular weight markers are indicated.

Consistent with the physical interaction between HerA and NurA, I found that the catalytic activities of these enzymes were mutually interdependent. The 5' to 3' exonuclease activity of NurA was strictly dependent on manganese when assayed alone, similar to previous results with NurA from *Sulfolobus acidocaldarius* (Constantinesco et al., 2002), but in the presence of HerA, the two enzymes exhibited robust exonuclease and helicase activity in physiological levels of magnesium (Fig. 2.2). Nucleolytic degradation of linear DNA was dependent on the ATP-related functions of HerA and nuclease-activity of NurA (data not shown).

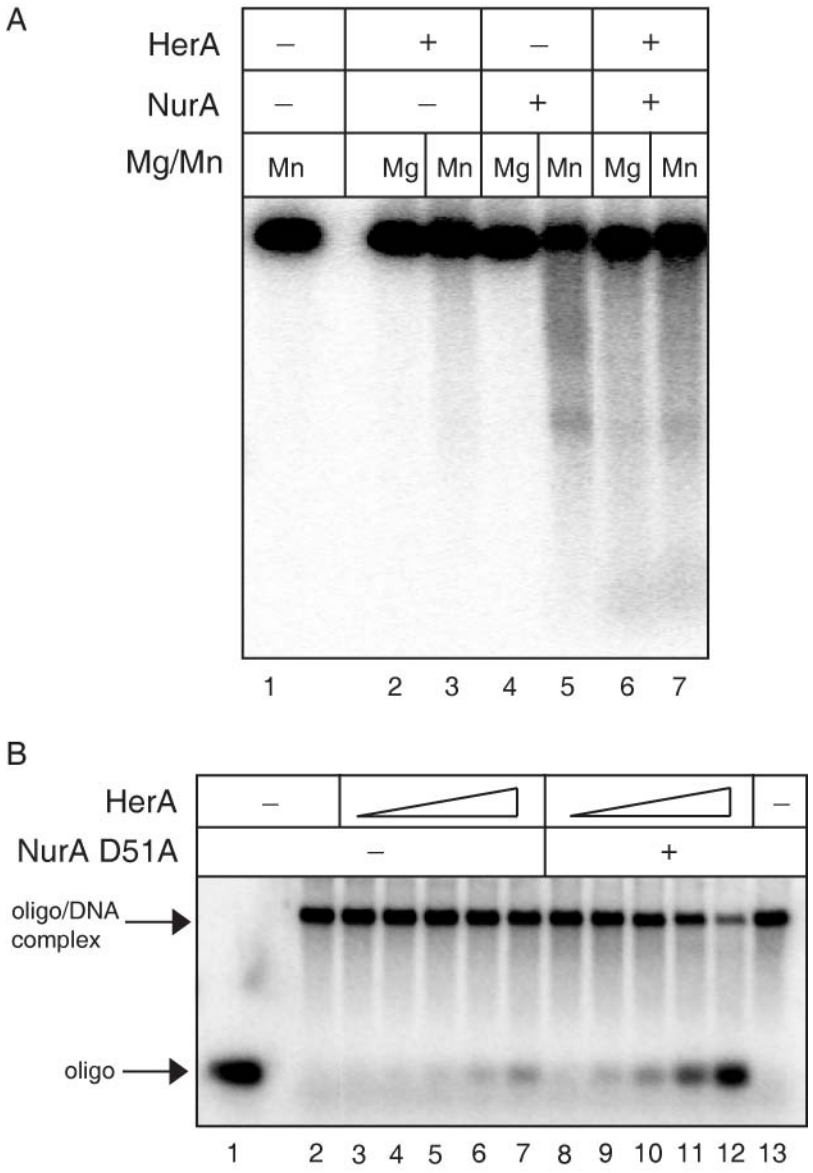

Figure 2.2: HerA and NurA stimulates the nuclease and helicase activities cooperatively. (**A**) Nuclease assays were performed using 2.5 kb internally [^{32}P]-labeled dsDNA. Reactions contained 13.4 nM wild-type HerA, 96.2 nM wild-type NurA, 80 mM NaCl, 1 mM ATP, and 5 mM $MgCl_2$ or $MnCl_2$ as indicated. Reactions were incubated at 65°C for 1 hr before separation on a native agarose gel. (**B**) Wild-type HerA helicase assays were performed with a 5' [^{32}P]-labeled 48 nt oligonucleotide/M13 ssDNA duplex. Reactions contained 0.3, 0.7, 1.3, 2.7, or 6.2 nM wild-type HerA and 9.6 nM NurA D51A (nuclease-deficient NurA) as indicated. Reactions were incubated at 55°C for 1 hr before separation on native 0.8% TAE agarose gels. Lane 1 contains boiled substrate. The positions of the oligonucleotide/ssM13 complex and oligonucleotide are indicated.

THE MRE11/RAD50 COMPLEX STIMULATES DNA DEGRADATION WITH HERA AND NURA

Based on the genomic structure of the operon containing the Mre11, Rad50, HerA, and NurA genes in thermophilic Archaea, I hypothesized that Mre11/Rad50 (MR) may act cooperatively with HerA and NurA. To investigate this possibility, nuclease assays were performed with limiting concentrations of HerA and NurA (2.7 nM HerA hexamer, 19 nM NurA monomer) on a 2.5 kb linear DNA substrate (Fig. 2.3A). When purified MR was titrated into the reaction, I observed a 19-fold stimulation in DNA degradation in the presence of 3.3 nM MR (assuming an M_2R_2 complex) (Fig. 2.3A, lane 2 vs. 4). Under these conditions, 3.3 nM MR demonstrates weak nuclease activity in magnesium in the absence of HerA and NurA (Fig. 2.3A, lane 8). Efficient degradation of dsDNA required all four proteins and ATP (Fig. 2.3B, lanes 1-10).

To investigate the requirements for individual catalytic activities, I used a nuclease-deficient mutant of NurA (D51A), a helicase-deficient mutant of HerA (K164A) (Constantinesco et al., 2004)), a nuclease-deficient mutant of Mre11 (H85L, “Mre11-3”; (Arthur et al., 2004)), and an ATPase- and adenylate kinase-deficient mutant of Rad50 (S793R; (Bhaskara et al., 2007; Hopfner et al., 2000b; Moncalian et al., 2004)). As shown in Figure 2.3B, efficient degradation of the linear DNA substrate required the catalytic activities of all four enzymes. However, the nuclease function(s) of Mre11 appear to be partially dispensable for the cooperative degradation activity, as the reactions containing a nuclease-deficient Mre11 H85L mutant showed DNA degradation

greater than that observed in reactions containing the Rad50 S793R mutant, but still considerably less than with wild-type (WT) Mre11 (Fig. 2.3B, lanes 9, 15-18). Taken together, these results indicate that all four gene products interact functionally to degrade dsDNA.

A

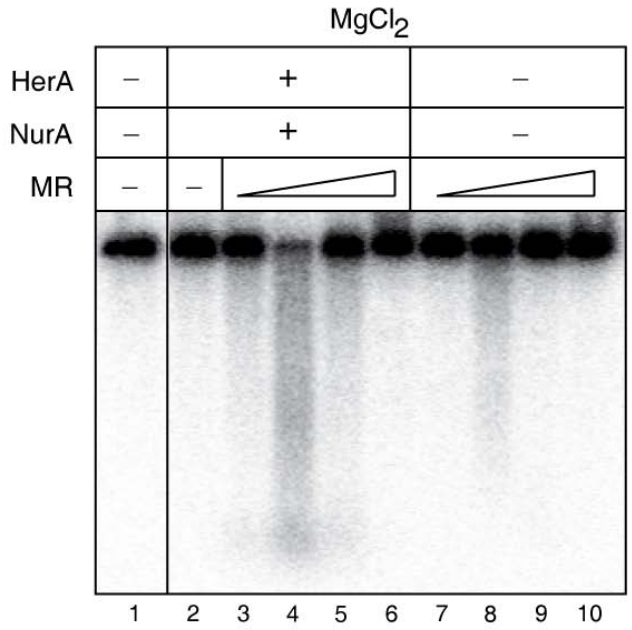
MgCl2
HerA
NurA
MR
–
+
–
1 2 3 4 5 6 7 8 9 10

B

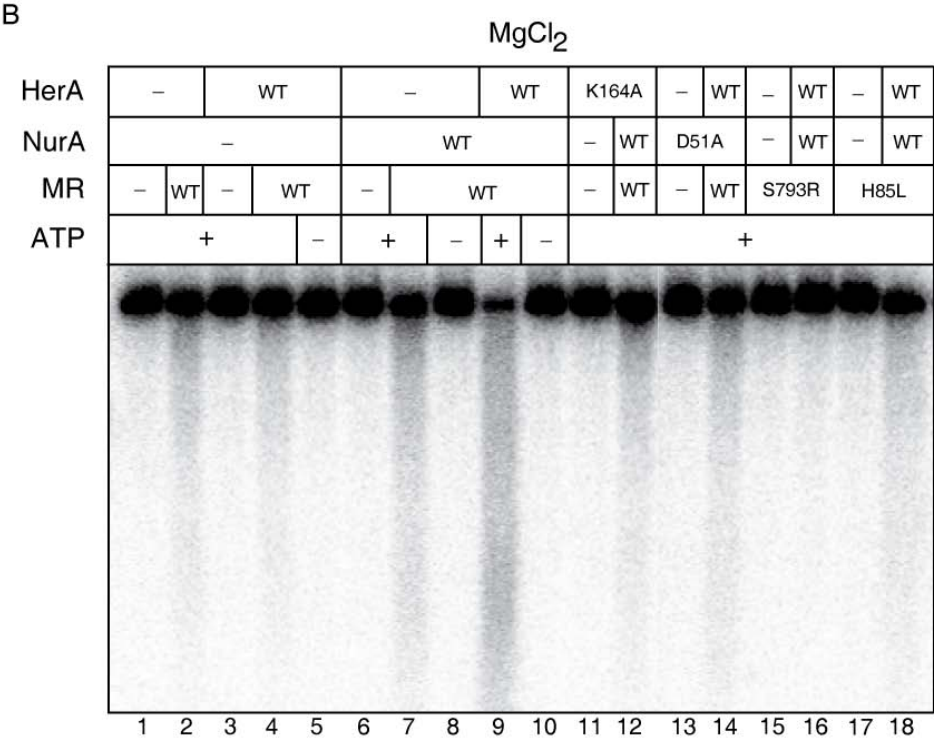
MgCl2
HerA
NurA
MR
ATP
WT
K164A
D51A
S793R
H85L
1 2 3 4 5 6 7 8 9 10 11 12 13 14 15 16 17 18

Figure 2.3: HerA and NurA degrade dsDNA cooperatively with Mre11/Rad50 in magnesium.
(**A**) Nuclease assays were performed using a 2.5 kb internally [^{32}P]-labeled dsDNA. Reactions contained 2.7 nM wild-type HerA and 19.2 nM wild-type NurA, 5 mM $MgCl_2$, 1 mM ATP, and 100 mM NaCl. Wild-type MR complex was included in the reaction at 0.3, 3.3, 33, and 330 nM. HerA molar concentrations are given as a hexamer of 370 kDa, NurA concentrations are given as a monomer of 52 kDa, and MR complex is given as a 2:2 stoichiometric complex of 306 kDa. (**B**) Reactions performed as in (**A**) with HerA wild-type or K164A, NurA wild-type or D51A, and 3.3 nM MR wild-type, M(H85L)R, or MR(S793R) as indicated in 80 mM NaCl.

THE DIRECTIONALITY OF MRE11/RAD50/HERA/NURA RESECTION IS 5' TO 3'

To determine the polarity of the DNA resection catalyzed by Mre11, Rad50, HerA, and NurA (*Pf*MRHN), I used a 6.5 kb linearized plasmid DNA substrate and analyzed the reaction products using non-denaturing Southern hybridization with RNA probes specific for either the 3' or 5' strand of one end of the linear plasmid (Fig. 2.4A). In this reaction with all four proteins present, the 3' strand of the DNA end was exposed as the DNA substrate was degraded (Fig. 2.4B, lanes 2-5, "3' strand"). The resection of the 5' end occurred rapidly as products were observed as early as 2 minutes (Fig. 2.4C, lane 4). I also observed significant levels of 5' ssDNA generated in the reaction, although less efficient than the production of 3' ssDNA (Fig. 2.4B, lanes 14-17, "5' strand"). Southern blot analysis of the resection reactions using HerA, NurA, and MR catalytic mutants demonstrated that the nuclease activity of NurA and the ATP-dependent function of HerA are both required for production of 3' ssDNA (Fig. 2.4D, lanes 3-6). In agreement with the results utilizing labeled DNA substrates, mutation of the Mre11 nuclease domain reduces the efficiency of 5' strand processing, but the ATP-related activities of Rad50 are essential for this process (Fig. 2.4D, lanes 7-10).

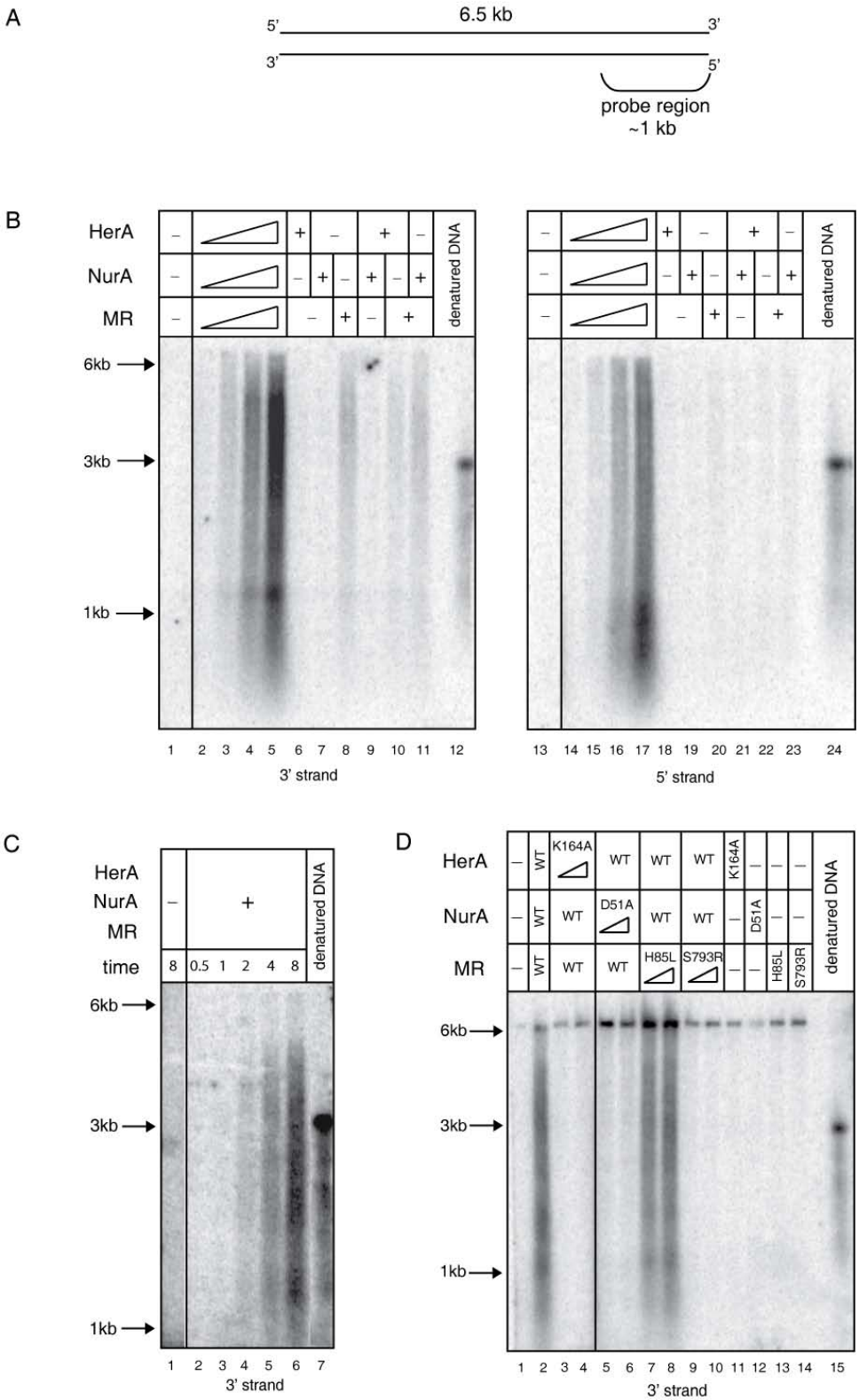
A
6.5 kb
5'
3'
3'
5'
probe region
~1 kb
B
HerA
NurA
MR
denatured DNA
6kb
3kb
1kb
1 2 3 4 5 6 7 8 9 10 11 12
3' strand
13 14 15 16 17 18 19 20 21 22 23 24
5' strand
C
HerA
NurA
MR
time
8 0.5 1 2 4 8
denatured DNA
6kb
3kb
1kb
1 2 3 4 5 6 7
3' strand
D
HerA
NurA
MR
WT
K164A
D51A
H85L
S793R
denatured DNA
6kb
3kb
1kb
1 2 3 4 5 6 7 8 9 10 11 12 13 14 15
3' strand

Figure 2.4: Mre11, Rad50, HerA, and NurA function cooperatively to resect the 5' strand of a DSB.
(**A**) Schematic of the linearized plasmid substrate used in nuclease reactions analyzed by Southern hybridization. The DNA length and location of the probe region are indicated. (**B**) Nuclease assays were performed with a 6.5 kb linearized plasmid DNA substrate and analyzed by non-denaturing Southern hybridization with strand-specific RNA probes. Reactions contained 0.3, 1.4, 2.7, and 5.4 nM wild-type HerA, 1.9, 9.5, 19.2, and 38.4 nM wild-type NurA, and 0.3, 1.7, 3.3, and 6.6 nM wild-type MR in 5 mM $MgCl_2$, 1 mM ATP, and 100 mM NaCl. "+" indicates 5.4 nM HerA, 38.4 nM NurA, and 6.6 nM MR wild-type proteins. Reactions were incubated at 65°C for 15 min and analyzed in native agarose gels. The denatured DNA blot control consists of NaOH-denatured substrate DNA, which runs at a position equivalent to ~3 kb non-denatured dsDNA. DNA molecular weight ladder positions of 6, 3, and 1 kb are indicated. The probe used in the left panel recognizes the 3' strand on one end of the DNA, whereas the probe used in the right panel recognizes the 5' strand. (**C**) Time course reaction as in (**B**) with 5.4 nM HerA, 38.4 nM NurA, and 6.6 nM MR wild-type proteins. Reactions were stopped at 0.5, 1, 2, 4, or 8 mins and analyzed with the 3' strand-specific probe. (**D**) Nuclease assays as in (**B**) but with 5.4 or 10.8 nM HerA K164A, 38.4 or 76.8 nM NurA D51A, and 6.6 or 13.2 nM M(H85L)R and MR(S793R) as indicated. "WT" indicates 5.4 nM HerA, 38.4 nM NurA, and 6.6 nM MR wild-type proteins. Reactions were analyzed with the 3' strand-specific probe.

To determine whether the resection process catalyzed by *Pf*MRHN is a processive reaction, I performed competition experiments and analyzed the products by Southern hybridization. I found that adding up to 50-fold molar excess competitor linear DNA did not decrease the level of 5' strand degradation after resection had been initiated. However, when the same concentration of competitor DNA was added at the beginning of the reaction, resection was completely abolished (data not shown). These results demonstrate that 5' strand resection by *Pf*MRHN occurs through a processive mechanism.

I considered two possibilities for the generation of both 5' and 3' ssDNA in the resection reaction: bidirectional but uncoupled degradation of each DNA end, or resection of the 5' strand from both ends of the DNA. The latter situation would occur if

the enzymes were present at saturating levels in the reaction. Consistent with this hypothesis, I observed that increasing the concentration of DNA in the reactions increased the ratio of 3’ vs. 5’ ssDNA generated (data not shown). To determine more conclusively whether the generation of 5’ ssDNA is the result of degradation from the distal 5’ strand, I constructed a substrate with a biotin attached at the distal 5’ end. The biotinylated DNA was then attached to streptavidin-coated magnetic beads to block access to the distal 5’ strand, and used as a substrate in the resection assay. As shown in Figure 2.5A, the generation of 5’ ssDNA was greatly reduced in comparison to the 3’ ssDNA product. This result strongly supports the conclusion that the cooperative activities of Mre11, Rad50, HerA, and NurA, resect the 5’ strand at a DNA DSB.

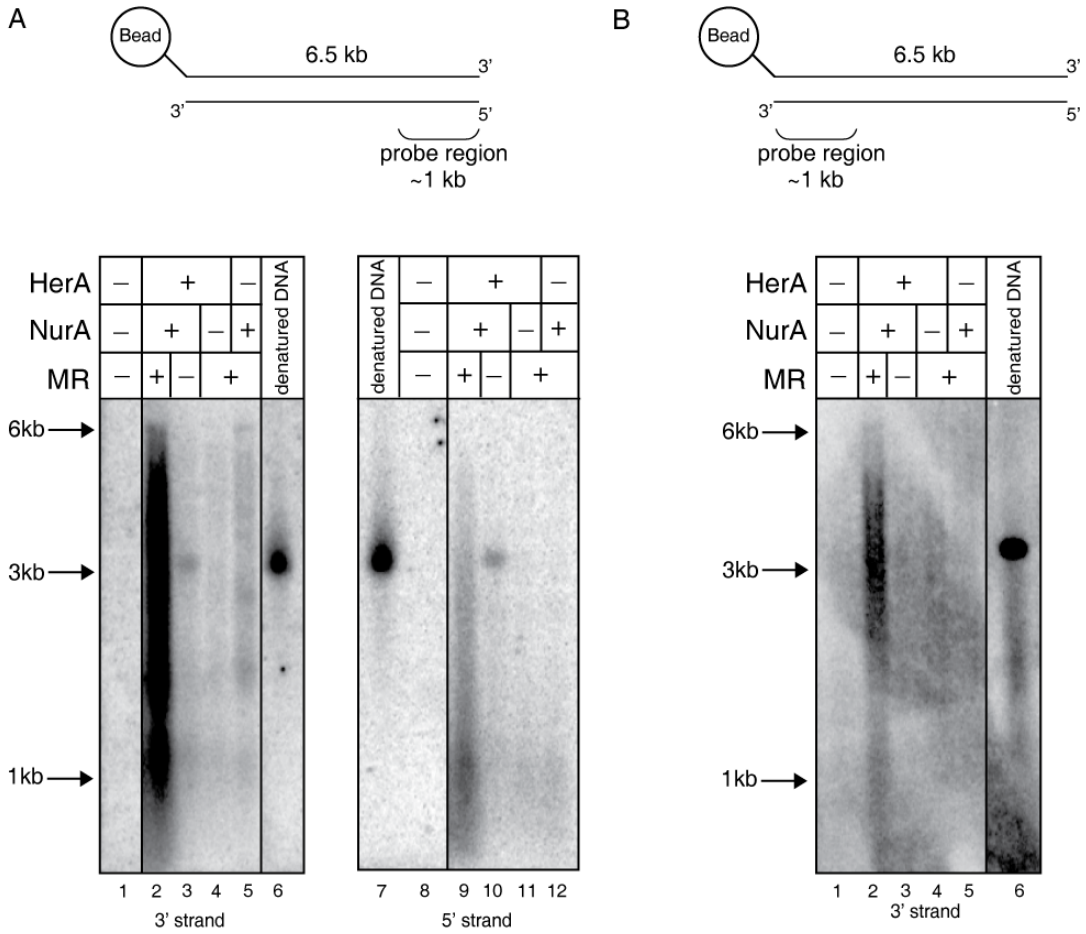

Figure 2.5: Mre11, Rad50, HerA, and NurA resects the 5' strand and not the 3' strand. (**A**) Nuclease assays were performed as in Fig. 2.4 except that the linearized 6.5 kb plasmid substrate was attached to a magnetic bead via a biotin/streptavidin linkage to the 5' strand of the DNA distal to the probe region (see schematic at top). Assays were performed with 5.4 nM wild-type HerA, 38.4 nM wild-type NurA, and 6.6 nM wild-type MR as indicated for 30 min and analyzed in native agarose gels. (**B**) Nuclease assays were performed as in (**A**) but the reaction products were analyzed using a probe specific for the 3' strand adjacent to the 5' biotin/bead (see schematic at top).

The products of the resection reaction shown in Figure 2.5A probed for the 3' strand range in size from nearly full-length (6.5 kb) down to less than 1 kb in the native

agarose gel; however, complete resection of the bottom strand of the substrate should not yield products smaller than ~3 kb (the migration of full-length ssDNA). Two-dimensional gel analysis of these products (first dimension native, second dimension denaturing) indicated that a subset of the products were in fact shorter than full-length (data not shown).

To explain this observation, I hypothesized that the enzymes in the reaction may be removing a subset of the DNA molecules from the bead by cleaving the 5' strand proximal to the biotin-streptavidin linkage. To test this hypothesis, I performed the same reaction and a non-denaturing Southern blot but probed for the 3' strand on the DNA end attached to the bead, a strand which should only be in single-stranded form if the bead is removed. This analysis is shown in Figure 2.5B, clearly indicates that the 5' end of the top strand is resected. This processing is less efficient than the processing of the open 5' strand, but nevertheless provides evidence for 5' strand conjugate removal in this system.

MR GENERATES SHORT 3' OVERHANGS THROUGH 5' STRAND ENDONUCLEOLYTIC ACTIVITY

The role of the MR complex in the resection process is of significant interest since it is conserved in all organisms and has been implicated in the removal of 5' covalent protein complexes during meiotic recombination in eukaryotes. To investigate the role of MR in the resection process, I performed the resection assay with a 6.5 kb DNA substrate in the absence of HerA and NurA, but an increased level of MR to determine whether MR alone has detectable resection activity. Interestingly, 16.5 nM MR complex alone produced a signal on the blot specific for the 3' strand, but the DNA product migrated

close to the size of the 6.5 kb substrate, indicating that the product of the MR reaction contained 3’ ssDNA but was not extensively degraded (Fig. 2.6A, lane 9, 17 and Fig. 2.6B, lane 2, 7). Analysis of this product by primer extension indicated that approximately 15-55 nt of the 5’ strand are removed by MR and were found in three distinct groups ~15 nt apart (Fig. 2.6C, lanes 2, 3). Formation of these products was dependent on both the nuclease activity of Mre11 and the ATP-associated functions of Rad50 (Fig. 2.6B, lanes 3, 4 and Fig. 2.6C, lanes 4, 5). No detectable 5’ ssDNA was observed, which indicates that MR plays a role in producing short 3’ single-stranded overhangs through either an exo- or endo-nucleolytic event. This processing by MR was enhanced by the presence of NurA whereas HerA alone did not affect MR activity (Fig. 2.6A, lanes 5, 6).

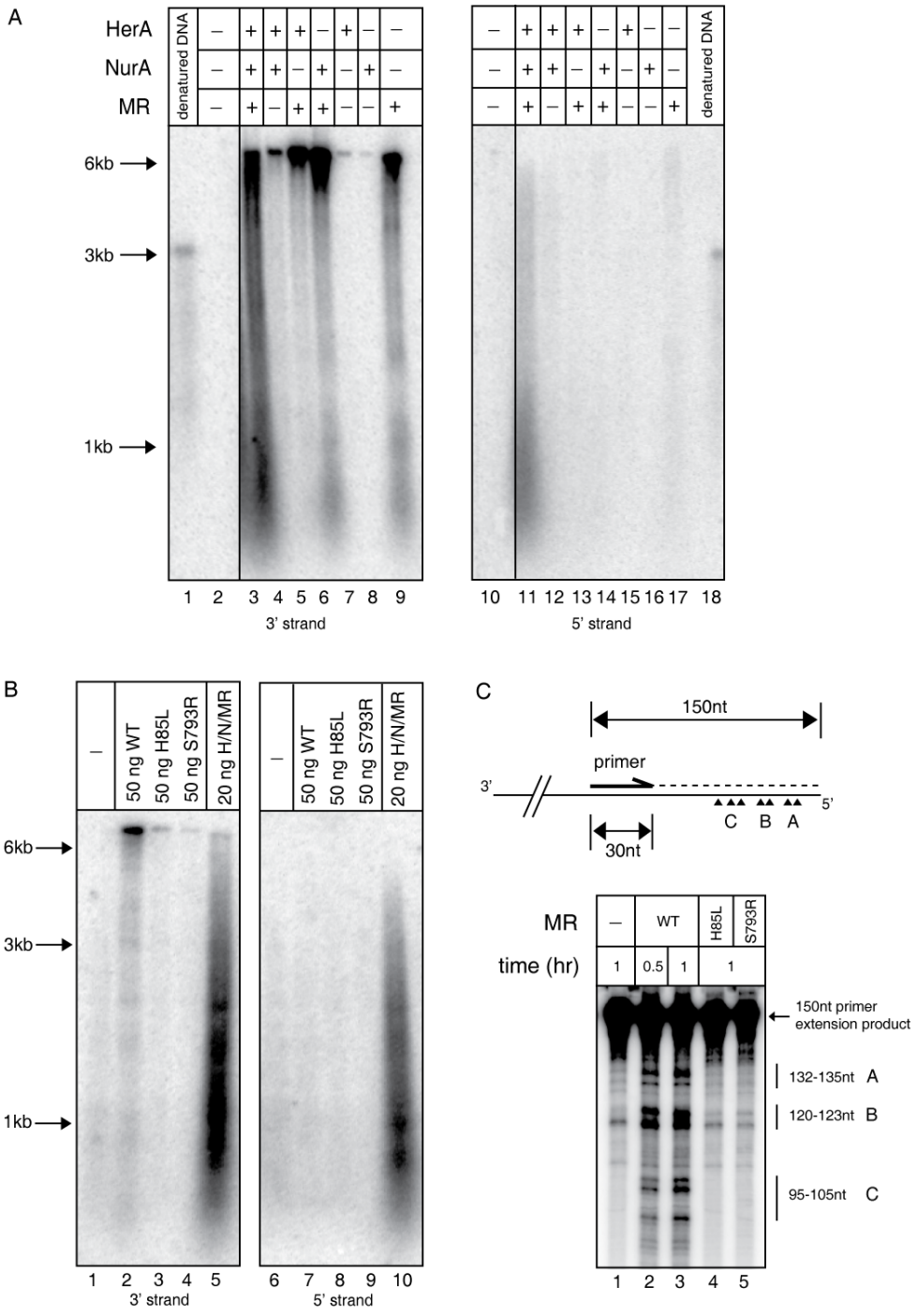

Figure 2.6: Mre11/Rad50 nuclease activity generates short 3' overhangs.
(**A**) Nuclease assays were performed as in Fig. 2.4 but with 13.4 nM wild-type HerA, 96.2 nM wild-type NurA, and 16.5 nM wild-type MR as indicated. Reactions were

incubated at 65°C for 1 hr. (**B**) Reactions performed as in (**A**) but with 16.5 nM MR wild-type, M(H85L)R, or MR(S793R) proteins. Reactions in lanes 5 and 10 contained 5.4 nM HerA, 38.4 nM NurA, and 6.6 nM MR wild-type proteins. Reactions in lanes 1-4 and 6-9 were incubated at 65°C for 1 hr. Reactions in lanes 5 and 10 were incubated at 65°C for 15 min. (**C**) (Top) Schematic of primer extension reaction. For simplicity, only the bottom strand of pTP163 is shown. The lengths of the full-length primer extension product and primer are indicated. The internally labeled primer extension product is indicated by the dashed line. Major MR resection sites are indicated as arrow heads and grouped into A, B, and C subgroups containing 2 or 3 cut sites. (Bottom) *P. furiosus* Mre11/Rad50 resection reactions were performed with 2.3 nM pTP163 linearized with SacI and 165 nM Mre11/Rad50 at 65°C for 30 min or 1 hr as indicated. Reactions were then used in primer extension reactions and the primer extension products were analyzed on 10% polyacrylamide denaturing sequencing gels. The position of the 150 nt primer extension product and the various resected products are indicated. Single-stranded DNA markers are indicated.

These results suggest that the *P. furiosus* MR complex has the ability to cleave the 5' strand of a DNA end under physiological conditions in magnesium. In contrast, previous reports have only observed Mre11 3'-5' exonuclease activity, which was dependent on manganese in the reaction (Hopfner et al., 2000a; Paull and Gellert, 1998; Trujillo et al., 1998; Usui et al., 1998). To examine this issue in greater detail, I used a 5' [^{32}P]-labeled dsDNA oligonucleotide substrates (Fig. 2.7A) and found that MR degraded DNA in a 3'-5' direction on this substrate, as previously reported. At lower temperatures (37°C), MR was active in manganese, but inactive in magnesium (Fig. 2.7B, lanes 7-8). However, at a temperature closer to physiological conditions for *P. furiosus* (55°C), MR demonstrated weak but detectable nuclease activity in magnesium which was dependent on ATP (Fig. 2.7B, lane 10, 11). This activity is Mre11-dependent because the H85L mutant does not generate these products (Fig. 2.7B, lane 12-13).

I observed that Mre11 nuclease products in magnesium differed slightly from manganese nuclease products in that two distinct types of product were generated. The

first type of product was close in size to the original substrate, whereas the second set of products appeared to be much smaller oligonucleotides (~12-25 nt). To determine if any of these products were dependent on the 3'-5' resection of the substrate, I designed an oligonucleotide substrate containing five phosphorothioate bonds at the 3' end of the top strand (Fig. 2.7A, substrate 3). This type of substrate is refractory to human Mre11 3'-5' exonuclease activity *in vitro* (data not shown). As shown in Figure 2.7C, when the 3' end of the labeled strand is blocked, only the smaller type of product is observed after MR incubation (lanes 4-6). The formation of these products is dependent upon the nuclease and ATP-dependent functions of MR as these products are not observed in reactions containing the Mre11 and Rad50 mutants (data not shown). This suggests that the smaller products are not the result of 3' exonuclease activity on the top strand but have to be products of endonuclease activity.

Consistent with endonucleolytic cut sites close to the 5' end, I observed products ranging from 20-30 nt when Substrate 3 was labeled at the 3' end (data not shown). Endonucleolytic cuts proximal to the 5' end would explain the absence of products between 30 and 50 nt. With a substrate containing phosphorothioates at both 3' ends, neither product species were observed (Fig. 2.7C, lanes 7-9). Together these data confirm that the MR complex can cleave DNA in magnesium, and that this cleavage activity consists of both a weak 3'-5' exonuclease activity as well as endonucleolytic cleavage activity on the 5' strand at a break. This result suggests that this novel 5' endonucleolytic activity of Mre11 is responsible for the generation of limited 3' ssDNA on the plasmid substrate in Figure 2.6.

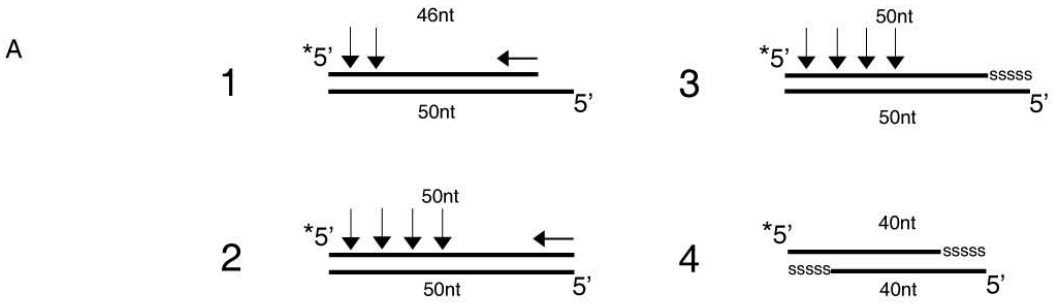
A
1
46nt
*5'
50nt
5'
2
50nt
*5'
50nt
5'
3
50nt
*5'
sssss
50nt
5'
4
40nt
*5'
sssss
sssss
40nt
5'

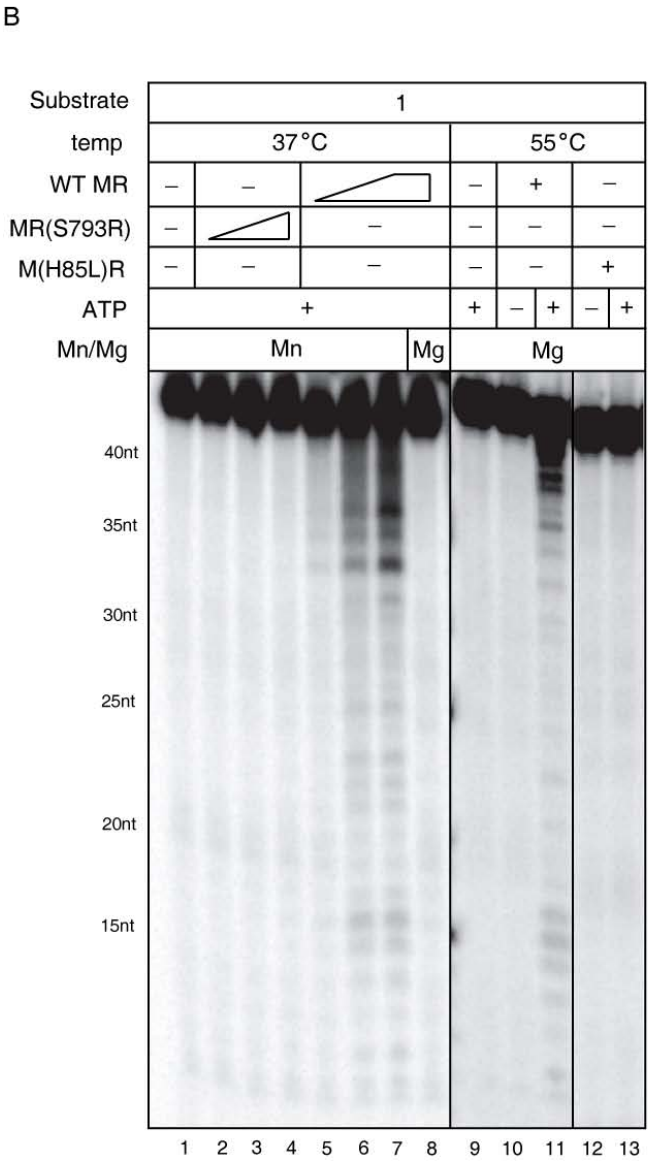
B
Substrate
1
temp
37°C
55°C
WT MR
MR(S793R)
M(H85L)R
ATP
Mn/Mg
Mn
Mg
Mg
40nt
35nt
30nt
25nt
20nt
15nt
1 2 3 4 5 6 7 8 9 10 11 12 13

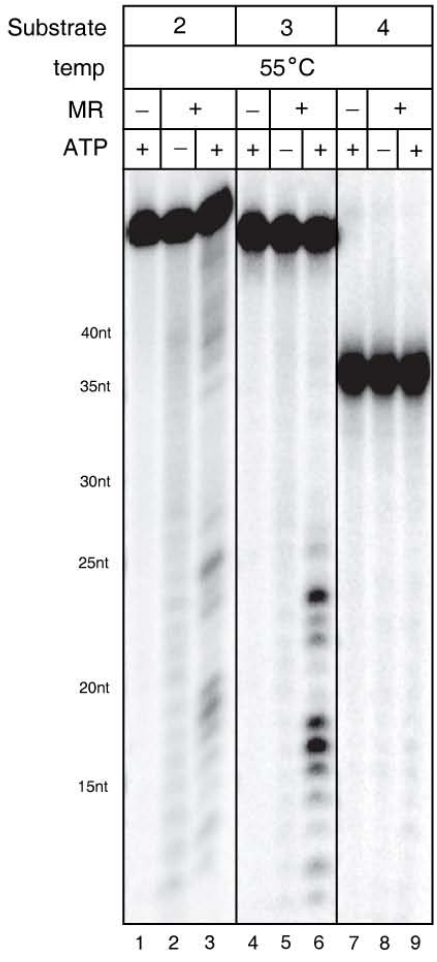
C
Substrate
2
3
4
temp
55°C
MR
ATP
40nt
35nt
30nt
25nt
20nt
15nt
1 2 3 4 5 6 7 8 9

Figure 2.7: Mre11/Rad50 5’ endonucleolytic activity occurs in magnesium and is dependent on 3’-5’ exonuclease activity.
(**A**) Schematic of the oligonucleotide substrates is shown. The 5’ [^{32}P]-label is indicated by an asterisk, and the length of each oligonucleotide is indicated. Phosphorothioate bonds are shown as “sssss.” The positions of the nucleolytic cuts from data shown in (**B**) and (**C**) are indicated by arrows. Vertical arrows indicate major endonuclease cleavage sites and the horizontal arrows denote 3'-5' exonuclease activity. (**B**) Nuclease assays were performed with MR wild-type or MR(S793R) and 2 nM Substrate 1 at 37°C for 30 min (lanes 1-8) or 55°C for 1 hr (lanes 9-13). Reactions at 37°C contained 11, 55, or 275 nM MR protein, 70-80 mM NaCl, 0.5 mM ATP, 1 mM $MnCl_2$, or 5 mM $MgCl_2$ as indicated. Reactions at 55°C were similar except they contained 60 mM NaCl, 2 mM $MgCl_2$, and 11 nM MR proteins as indicated. (**C**) Nuclease assays were performed with 1 nM Substrates 2, 3, or 4 as indicated. Reactions contained 58 nM wild-type MR in 60 mM NaCl and 2 mM $MgCl_2$, and were incubated at 55°C for 1 hr. Reaction products were analyzed on 15% denaturing sequencing gels. Single-stranded DNA markers are indicated.

3’ SSDNA GENERATED BY *PF*MRHN IS USED BY RADA IN STRAND EXCHANGE

Following the initiation and processing events of DNA ends, the 3’ ssDNA is coated with strand-exchange factor(s), which catalyze strand invasion and homologous pairing. To examine whether strand invasion can occur in a concerted way with Archaeal proteins, I cloned the RecA/Rad51-homolog RadA from *P. furiosus* genomic DNA and purified the RadA protein. I then characterized purified RadA strand-exchange activity using a joint-molecule (JM) assay. As shown in Figure 2.8A, RadA catalyzed the formation of joint-molecules with internally-labeled dsDNA and homologous circular single-stranded M13 DNA in an ATP-dependent manner at 50°C (lanes 5-8), similar to previous reports of RadA activity *in vitro* (Komori et al., 2000; Seitz et al., 1998). In comparison, RecA-catalyzed JM reactions performed at 37°C are shown in Figure 2.8A, lanes 1-4.

If Mre11, Rad50, HerA, and NurA work together cooperatively to process DNA for RadA loading and strand invasion, it should be possible to perform a concerted reaction with all of these proteins, starting from a double-stranded linear DNA substrate and producing a D-loop strand invasion product with negatively supercoiled DNA. I performed this reaction with labeled linear dsDNA and found that HerA, NurA, and MR together with RadA catalyzed the formation of joint molecule (D-loop) products in the presence of supercoiled DNA and ATP (Fig. 2.8B and Fig. 2.8C). I observed low levels of D-loop formation (up to 20% of the level seen with all proteins present) in the absence of any one of the three components, suggesting that extensive 5' strand resection is not necessary for initiating strand exchange (Fig. 2.8C). This is consistent with previous findings that short ssDNA (54 nt) is sufficient for RadA-catalyzed strand exchange (Seitz et al., 1998). Therefore the cooperative activities of HerA, NurA, and MR are sufficient to process DNA ends such that RadA is able to bind and initiate homologous pairing and strand exchange.

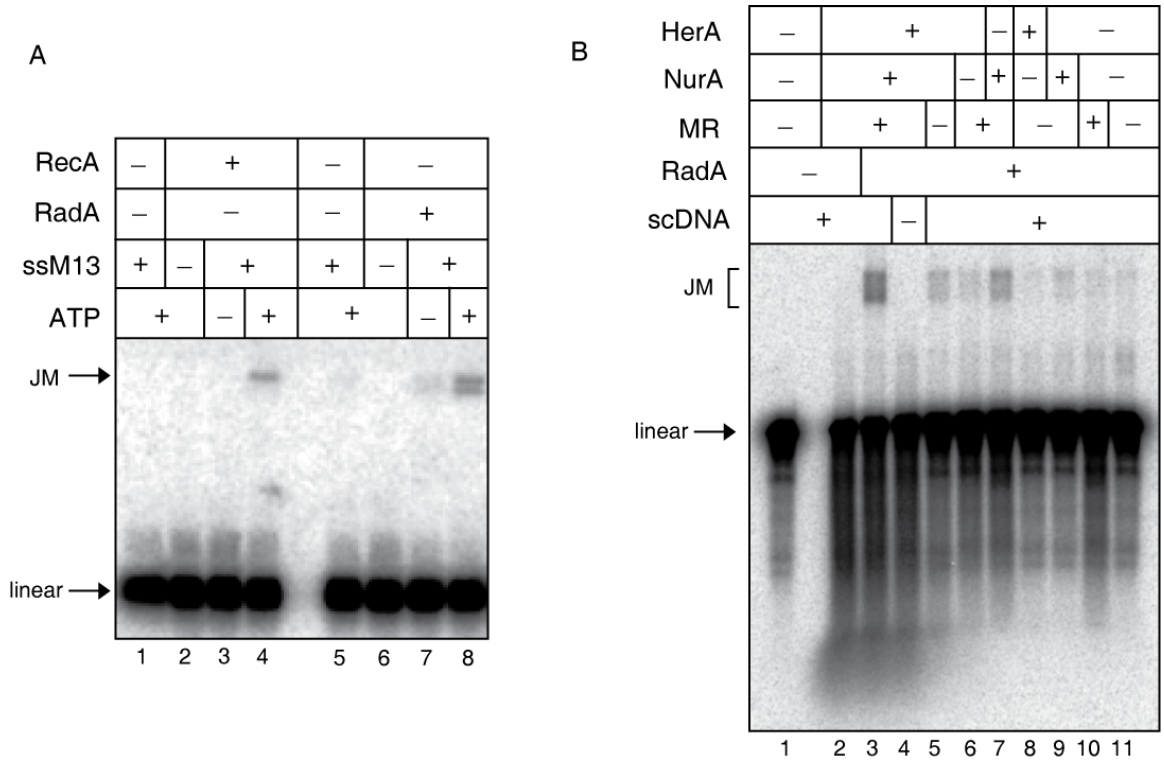
A
RecA
RadA
ssM13
ATP
JM
linear
1 2 3 4 5 6 7 8
B
HerA
NurA
MR
RadA
scDNA
JM
linear
1 2 3 4 5 6 7 8 9 10 11

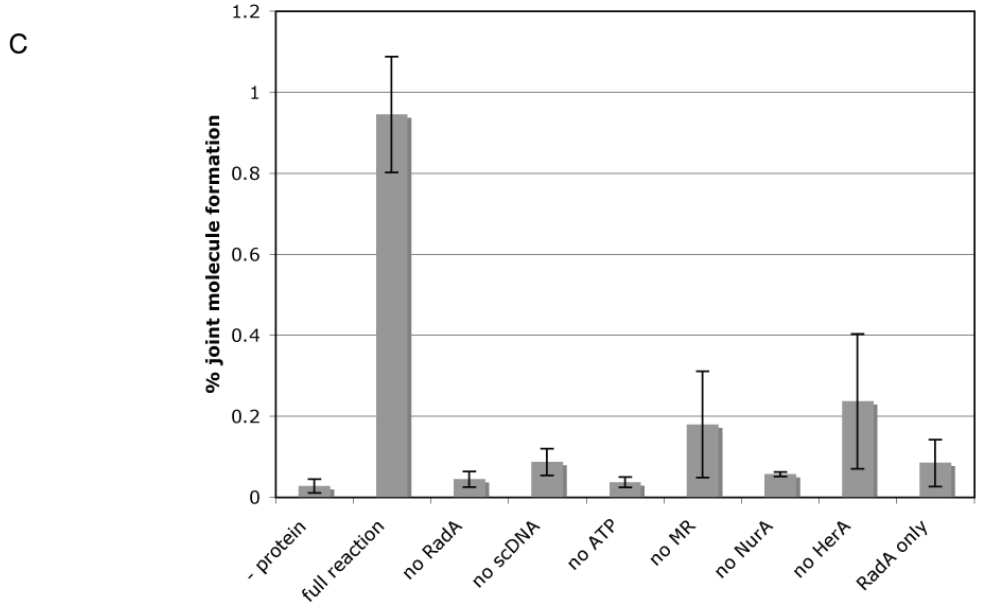
C
% joint molecule formation
1.2
1
0.8
0.6
0.4
0.2
0
- protein
full reaction
no RadA
no scDNA
no ATP
no MR
no NurA
no HerA
RadA only

Figure 2.8: Mre11, Rad50, HerA, and NurA together with RadA catalyze homologous strand exchange.

(**A**) Joint molecule reactions were performed with 100 nM RecA at 37°C (lanes 1-4) and 50 nM RadA at 50°C (lanes 5-8). Reactions contained 1.8 nM linear [^{32}P]-labeled 415 bp DNA, 0.2 nM circular M13 ssDNA, and 2 mM ATP as indicated and were separated by native agarose gel electrophoresis. Positions of the linear dsDNA (linear) and the joint molecule product (JM) are indicated. (**B**) Strand invasion experiments were performed with 13.2 nM MR, 10.8 nM HerA, 76.8 nM NurA, and 52.6 nM RadA as indicated. Reactions contained 0.1 nM [^{32}P]-labeled linear 1.4 kb dsDNA and 1.7 nM supercoiled dsDNA as indicated and were separated by native agarose gel electrophoresis. Positions of the linear DNA and the joint molecule products (JM) are indicated. (**C**) Quantitation of joint molecule formation by *P. furiosus* Mre11/Rad50/HerA/NurA/RadA. Five independent sets of reactions containing the components indicated above were analyzed as described in (**B**) and the percentage of the linear substrate converted into joint molecules (D-loop products) was quantitated using phosphorimager analysis. Bars indicate the average and the error bars are calculated from standard deviation. The full reaction contains *Pf*Mre11/Rad50, HerA, NurA, RadA, [^{32}P]-labeled linear DNA, supercoiled plasmid DNA, ATP, and magnesium chloride.

Discussion

The Mre11/Rad50 (MR) complex is implicated in both non-homologous end joining (NHEJ) and homologous recombination (HR) double-strand break (DSB) repair pathways in eukaryotes and is conserved in all three biological kingdoms. In almost all thermophilic Archaea, the *mre11* and *rad50* genes exist in an operon with the genes encoding the HerA helicase and the NurA nuclease (Constantinesco et al., 2004; Manzan et al., 2004). Based on this genomic organization and the absence of RecBCD homologs, I hypothesize that Mre11, Rad50, HerA, and NurA are involved in DNA end processing for DSB repair through HR.

I show here that purified, recombinant HerA and NurA from *Pyrococcus furiosus* interact physically, and that this association stimulates NurA 5'-3' exonuclease and HerA DNA helicase activities. I also demonstrate that in the presence of low levels of HerA and NurA (2.7 hexamer and 19 nM monomer, respectively), the addition of *Pf*MR (3.3 nM M_2R_2) stimulated the degradation of linear dsDNA up to 19-fold. This highly cooperative reaction occurred at 65°C and generated 3' single-stranded DNA (ssDNA) tails, which could be used by *Pf*RadA *in vitro* to catalyze strand invasion. Taken together, this evidence suggests that Mre11, Rad50, HerA, and NurA function cooperatively in the creation of 3' ssDNA and illustrate how Mre11/Rad50 complexes in higher organisms may also function in DSB resection.

HERA AND NURA

*Pf*HerA and NurA clearly act as a functional unit. The helicase activity of HerA is stimulated approximately 3-fold by NurA, and NurA 5' to 3' exonuclease activity is completely dependent on the presence of HerA when assayed in physiological magnesium conditions (Fig. 2.2). The two proteins interact in the absence of DNA and, based on gel filtration studies, I estimate between 1 and 3 NurA monomers bind HerA (Fig. 2.1), which I infer to be a hexamer based on previously published results with MlaA from *P. abyssi* (Manzan et al., 2004). Two other groups have reported that HerA and Mre11 from *Sulfolobus tokodaii* and *S. acidocaldarius* interact directly whereas HerA and NurA do not (Quaiser et al., 2008; Zhang et al., 2008). However, I did not observe any direct protein-protein interactions between *Pf*MR and either *Pf*HerA or *Pf*NurA (data not shown). Since I observed a strong functional interaction between these four proteins in reactions containing DNA (Fig. 2.3A), it is possible that alternative protein-binding interfaces may be exposed in response to DNA-induced conformational changes. Interestingly, the optimal concentrations of MR and HerA in the reaction were approximately equal (~3 nM), suggesting a potential stoichiometric activation mechanism.

CATALYTIC ACTIVITIES OF MRE11 AND RAD50 IN STRAND RESECTION

The cooperative degradation of linear DNA by 5' strand resection required all four of the proteins in the operon, but only absolutely required the enzymatic activities of HerA, NurA, and Rad50 (Fig. 2.3B and 2.4D). The nuclease function of Mre11 appears to be partially dispensable for this cooperative DNA degradation, which is consistent

with earlier findings that Mre11 nuclease activity is not required for mitotic DSB processing in budding yeast (Moreau et al., 1999). I hypothesize that Mre11 nuclease function may only be absolutely required if the 5' strand at a break is blocked by an adduct or a covalently attached protein. Consistent with this possibility is the observation that Spo11 conjugates persist in yeast strains expressing nuclease-deficient Mre11 mutants (Moreau et al., 1999).

Although I did not test for the removal of proteins conjugates in our assays, I did observe a catalytic activity with the *Pf*MR complex that would explain a conserved requirement for Mre11/Rad50 complexes in 5' conjugate removal. I found that MR alone at higher concentrations catalyzed the formation of a 3' single-stranded tail by removing approximately 15-55 nt from the 5' strand (Fig. 2.6). This product was abolished in reactions containing either the nuclease-deficient Mre11 H85L mutant or the signature motif Rad50 S793R mutant (Fig. 2.6B and Fig. 2.6C). The most likely explanation for this event is the removal of the 5' end through a combined unwinding/endonucleolytic cut which requires both Mre11 nuclease activity and Rad50 ATP-dependent functions. Thus, the role of Mre11 nuclease activity in resection may be to remove the terminal 15-55 nt of the 5' strand at a DSB, but this may only be essential when the 5' strand has an adduct or protein conjugate. A recent study indicates that the structure of a DNA end influences the rate and efficiency of DSB processing in budding yeast (Barlow et al., 2008). Cells expressing an Mre11-nuclease deficient mutant exhibit a delay in the formation of RPA filaments on ssDNA in G_1 phase, which may indicate a requirement for Mre11 nuclease activity to remove conjugates or damaged bases.

METAL ION SPECIFICITY OF MRE11

The ability of MR to cleave DNA using magnesium instead of manganese is a critical observation as the intracellular magnesium concentration is orders of magnitude higher than manganese in most organisms. A recent report analyzing the thermophilic bacteria *Thermus thermophilus* showed that intracellular free magnesium and manganese levels are 1.53 mM and 0.9 μM, respectively (Kondo et al., 2008). Previous to this report, purified Mre11 and Mre11/Rad50 complexes from several species have only been shown to be active in manganese (Connelly et al., 1997; Hopfner et al., 2000a; Paull and Gellert, 1998; Trujillo and Sung, 2001). From our observations I suggest two explanations for this discrepancy. First, it appears that the MR-dependent nuclease activity I have observed in magnesium is more efficient on long DNA substrates such as plasmid DNA compared to oligonucleotide substrates, but most *in vitro* studies on these complexes have been performed with oligonucleotides. Second, when using long DNA substrates, it is technically difficult to document a loss of 15-55 nt on one strand, but the strand-specific Southern assay I use here is capable of identifying these cleavage events. The crystal structure of *Pf*Mre11 shows two metal-binding pockets in the active site, which are involved in catalysis (Hopfner et al., 2001), suggesting that manganese may be bound to one site constitutively, or both sites may bind magnesium in our assays. I do not know if our *Pf*MR contains manganese and contributes to our observed magnesium activity *in vitro*; however, exonuclease assays performed in the absence of divalent cations do not demonstrate detectable nuclease activity (data not shown).

The observed differences of Mre11/Rad50 activity in manganese or magnesium may also be explained by the physical chemistry of these two metal ions. Compared to

magnesium, manganese is better at reducing the activation energy of a reaction, which results in increased enzyme efficiency (Kehres and Maguire, 2003). Additionally, use of manganese instead of magnesium has also been shown to decrease DNA polymerase fidelity, increase endonuclease cutting at noncognate sites, and increase exonuclease activity (Puapaiboon et al., 2001; Sirover and Loeb, 1976; Vermote and Halford, 1992). These observations may explain why Mre11/Rad50 was found to be active only in manganese, but still does not clarify which cation is the physiological cofactor. It is interesting to note that Archaea possess manganese transporters (Kehres and Maguire, 2003). However, it is unclear whether Archaea control manganese transport to regulate intracellular enzymes, and if so, if this plays a role in Mre11/Rad50 activity.

Despite the inefficiency of oligonucleotide cleavage by *Pf*MR in magnesium, I was able to observe endonucleolytic cleavage events on the 5' strand of a short duplex. When the 3' bottom strand was blocked by phosphorothioate nucleotides, this 5' strand cutting was abolished (Fig. 2.7C). Thus, it appears that Mre11 3'-5' degradation of the 3' end is required for the endonucleolytic cutting of the 5' strand.

JOINT MOLECULE FORMATION IN CONCERT WITH RADA

Consistent with the hypothesis that Mre11, Rad50, HerA, and NurA are involved in DSB-end processing during the initial stages of HR, I observed that these proteins together with the RadA recombinase catalyzed the formation of joint molecules starting with linear dsDNA and supercoiled plasmid DNA (Fig. 2.8B). This indicates that the processed ends are suitable for RadA binding and that the nucleoprotein filament formed

is competent for homologous pairing and strand exchange. In the case of RecBCD in *E. coli*, the RecB subunit makes direct protein-protein interactions with RecA that are important for the recruitment of RecA to ssDNA produced by RecBCD (Spies and Kowalczykowski, 2006). With *Pf*MR, HerA, and NurA, I do not currently know if RadA is actively loaded onto the 3' ssDNA and, if so, which component(s) are involved.

DNA topology is regulated by various topoisomerases which are involved in the transient cleavage of the DNA strands. In most bacteria and mesophilic archaea, plasmid DNA is found to be negatively supercoiled through the activity of DNA gyrase. However, in hyperthermophilic archaea and bacteria, the enzyme reverse gyrase introduces positive supercoils into closed circular DNA and catalyzes the relaxation of negatively supercoiled DNA in an ATP-dependent manner (Nadal, 2007). Surprisingly, plasmid DNA isolated from various hyperthermophilic archaea demonstrate a range of topologies, from positively to negatively supercoiled (Lopez-Garcia and Forterre, 1997). DNA isolated from *Pyrococcus abyssi* was found to be relaxed with a slight negative supercoiling density at physiological temperatures despite the presence of reverse gyrase (Charbonnier et al., 1992; Charbonnier and Forterre, 1994; Lopez-Garcia and Forterre, 1997). DNA topology is additionally regulated by DNA-binding proteins, and many archaea possess histones which are involved in DNA organization and compaction (White and Bell, 2002). Thus, it is unclear how the topology of DNA at physiological temperatures will affect DNA repair and strand exchange *in vivo*.

Based on the work described here, I propose a model for the function of Mre11, Rad50, HerA, and NurA in the processing of DNA ends, where the ATP-related functions of Rad50 are necessary for initiating or activating HerA/NurA, and the NurA nuclease

together with HerA helicase activities produce the long 3' single-strand tails necessary for RadA loading (Fig. 2.9). I do not yet know how *Pf*MR activates HerA/NurA and whether this is through a specific DNA structure or protein-protein interactions on the DNA. Our inability to detect physical interactions between *Pf*MR and HerA/NurA suggests that the role of *Pf*MR is to generate a specific DNA structure that is optimal for entry of HerA/NurA. Based on previous observations with human MRN (Paull and Gellert, 1999), I propose that this DNA structure may contain unwound DNA strands. Alternatively, it may be a combination of an unwound DNA structure and a protein surface that is recognized by HerA/NurA. Recent evidence from *S. cerevisiae* suggest that an unwinding event coupled with endonucleolytic cleavage may generate single-stranded DNA in this organism (Zierhut and Diffley, 2008).

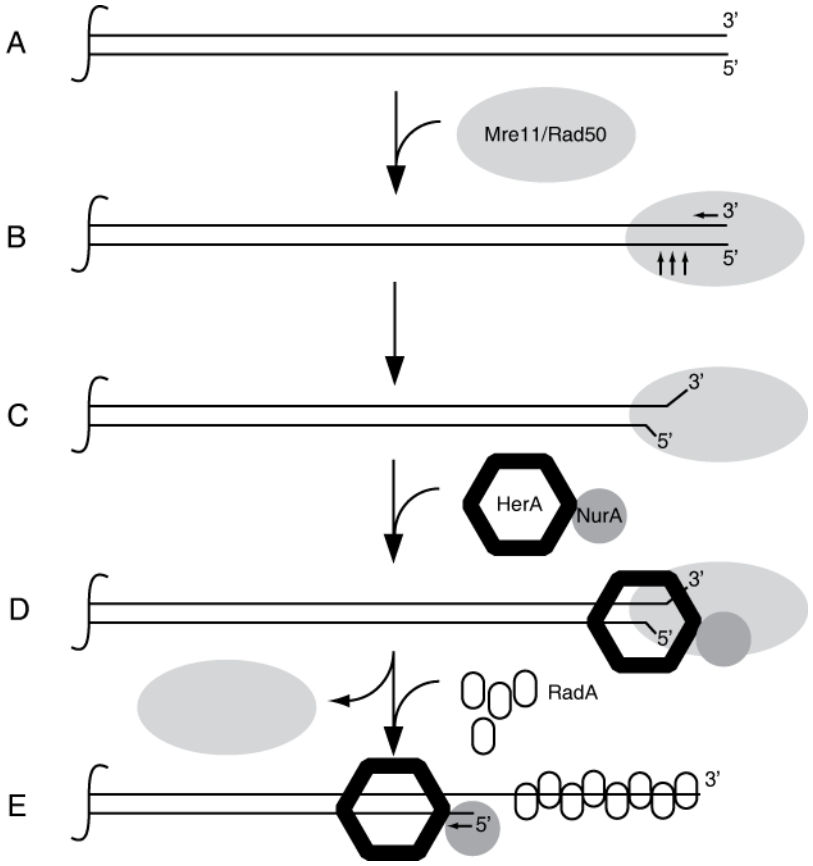

Figure 2.9: Schematic model of *Pf*MRHN resection process.
The Mre11/Rad50 complex binds to DSB ends and processes the 3' and 5' ends (**A** & **B**). MR may also facilitate opening of the processed DNA ends to aid in the recruitment of HerA/NurA (**C** & **D**). The HerA/NurA complex catalyzes 5' strand resection in a processive fashion producing 3' ssDNA for RadA binding (**E**). I do not know the specific structure of the DNA end bound by MR or whether MR leaves the processed DNA end. However, I suggest the dissociation of MR from the DNA ends based on data in yeast demonstrating loss of MRX at resected ends (Lisby et al., 2004). The HerA/NurA complex is shown with one NurA monomer, but may contain up to three NurA monomers per HerA hexamer based on my gel filtration studies.

The RecBCD system in bacteria is unique in its regulation by the Chi sequence in chromosomal DNA (Amundsen et al., 2007; Spies et al., 2003). In Archaea and in eukaryotes, there has been no indication of a Chi-like sequence regulating recombination

frequency. Consistent with this, my studies with *Pf*MR and HerA/NurA on different plasmid substrates have not indicated any preference for specific sequences. The strand specificity of the resection argues that a polarity-switching signal like Chi should not be required in this system.

Archaea are excellent systems for the study of DNA repair due to their relative simplicity compared to eukaryotic organisms. Also, many of the proteins in Archaea involved in DNA repair show higher sequence and structural similarity to their eukaryotic counterparts than to bacterial proteins, including RadA/RecA/Rad51, Mre11/SbcD, and Rad50/SbcC (Allers and Mevarech, 2005; Seitz et al., 2001). HerA and NurA homologs are absent in eukaryotes; however, there are likely functional homologs that may include Sgs1, Exo1, and Dna2 (Mimitou and Symington, 2008; Zhu et al., 2008). Studies in budding yeast suggest that the MRX complex is involved in the initial stages of DNA resection, whereas Sgs1, Exo1, and Dna2 are redundantly necessary for the extensive 5' strand resection (Mimitou and Symington, 2008; Zhu et al., 2008). The model proposed by Ira and Symington is consistent with ours and supports an evolutionarily conserved function for the Mre11/Rad50 complex. Our results with Mre11/Rad50 are consistent with the known activities of the MRX and MRN complexes, and thus provide a conceptual framework for understanding the roles of this enzyme in homologous recombination in higher organisms.

Experimental Procedures

EXPRESSION CONSTRUCTS

Pyrococcus furiosus Mre11/Rad50 was expressed from a bicistronic pET27b vector (gift from J. Carney). The *P. furiosus* HerA and NurA genes were amplified from *P. furiosus* genomic DNA (ATCC). The HerA and NurA genes were cloned separately into pETDuet-1 (Novagen), creating pTP1044 (HerA) and pTP1045 (NurA) expression constructs. The RadA gene was PCR amplified from *P. furiosus* genomic DNA and cloned into pETDuet-1 to create pTP1184. Point mutations were constructed using QuikChange Site-Directed Mutagenesis (Stratagene). Mutations were confirmed by DNA sequencing of the complete open reading frame.

PROTEIN EXPRESSION AND PURIFICATION

The *Pf*MR complex was coexpressed in BL21 DE3 codonplus *E. coli* as previously described (Hopfner et al., 2000a) with minor changes. Briefly, cells were grown to an OD_{600} 0.8-1.0 and induced using 0.5 mM IPTG for 4 to 6 hr at 37°C. Cells were harvested by centrifugation, flash frozen in liquid N_2, and lysed in high salt Nickel A buffer (50 mM KH_2PO_4 pH 7.0, 500 mM KCl, 2.5 mM imidazole, 10% glycerol, 20 mM β-mercaptoethanol (BME)) containing 1 mM phenylmethylsulphonyl fluoride (PMSF) and 0.5% Tween-20. Cells were lysed using a French Press (Thermo Fisher), sonicated, and insoluble material was pelleted by centrifugation at 100,000 × g for 1 hr at 4°C. The supernatant was heated at 70°C for 15 min, and the precipitated protein was

pelleted by centrifugation at 45,000 × g for 15 min at 4°C. The soluble fraction was loaded onto a Ni-NTA column (Qiagen) in low salt Nickel A buffer (50 mM KH_2PO_4 pH 7.0, 50 mM KCl, 2.5 mM imidazole, 10% glycerol, 20 mM BME) and washed with 10% Nickel B (Nickel A buffer containing 250 mM imidazole). Proteins were resolved with a linear gradient from 10 to 100% Nickel B buffer. Fractions containing MR were pooled, loaded onto a HiTrap Q HP column (GE) and washed in Buffer A (25 mM Tris pH 8.0, 100 mM NaCl, 10% glycerol, 1 mM dithiothreitol (DTT)). MR was eluted with 50% Buffer B (25 mM Tris pH 8.0, 1 M NaCl, 10% glycerol, 1 mM DTT). Peak fractions were pooled and mixed with 0.2% Tween-20 before separation on a Superdex 200 10/300 GL column (GE) in Buffer A. Fractions containing the MR complex were aliquoted and flash frozen in liquid N_2. Protein expression and recombinant protein purification for HerA and NurA was performed similar to the MR protocol with the exception that NurA was loaded onto a HiTrap SP HP instead of Q HP. RadA expression and purification was performed as previously described (Komori et al., 2000). Mre11, HerA, and NurA were expressed as N-terminal 6×His fusion proteins, whereas Rad50 and RadA were expressed as untagged proteins. Protein concentrations were quantitated using BSA standards on SDS-PAGE gels.

GEL FILTRATION

Wild-type purified HerA (290 nM hexamer), NurA (7 μM monomer), and Mre11/Rad50 (500 nM M_2R_2) were incubated as indicated in Buffer A at 55°C for 15 min. Tween-20 was added to 0.1% before resolving on a Superdex 200 PC 3.2/30 column

run in Buffer A. Fractions were separated on 10% SDS-PAGE gels, transferred to PVDF membranes (Millipore), and probed with His-specific antibodies conjugated to IRDYE-800 dye (Rockland). Western blots were analyzed on a Licor Odyssey system.

NUCLEASE ASSAYS WITH LABELED DNA SUBSTRATES

Nuclease assays with oligonucleotide substrates contained 25 mM MOPS pH 7.0, 1 mM DTT, and 1 to 2 nM [^{32}P]-labeled oligonucleotide duplex with or without 0.5 mM ATP in 10 µl reactions. Assays were performed at 37°C for 30 min or 55°C for 1 hr as indicated. Reactions were stopped by the addition of 0.2% SDS and 10 mM EDTA and were analyzed on 15% polyacrylamide denaturing sequencing gels. Nuclease reactions with internally-labeled DNA substrates were similar to those described for oligonucleotide assays, except that 0.06 nM 2.5 kb DNA was used. Reactions were analyzed by native electrophoresis in 1.2% Tris-acetate-EDTA (TAE; 40 mM Tris-acetate, 1 mM EDTA) agarose gels for 1.5 hrs at 3.9 V/cm, dried, and scanned on a phosphorimager (Bio-Rad or GE). All DNA concentrations were reported as moles of molecules.

OLIGONUCLEOTIDE DNA SUBSTRATES

The substrates in Fig. 2.7A were constructed as follows: Substrate 1 consisted of 5' [^{32}P]-labeled TP74 (5'-CTGCAGGGTTTTTGTTCCAGTCTGTAGCACTGTGTAAGACAGGCCA-3') annealed to TP124 (5'-

CATCTGGCCTGTCTTACACAGTGCTACAGACTGGAACAAAAACCCTGCAG-3'). Substrate 2 consisted of 5' [^{32}P]-labeled TP124 annealed to TP125 (5'-CTGCAGGGTTTTTGTTCCAGTCTGTAGCACTGTGTAAGACAGGCCAGATG-3'). Substrate 3 consisted of 5' [^{32}P]-labeled TP580 (5'-CTGCAGGGTTTTTGTTCCAGTCTGTAGCACTGTGTAAGACAGGCCsAsGsAsTsG-3') annealed to TP124. Phosphorothioate bonds are indicated by "s" between the nucleotides. Substrate 4 consisted of 5' [^{32}P]-labeled TP694 (5'-AAGTAAATCATTAATCTAACAATGCGCTCATCGTCsAsTsCsCsT-3') annealed to TP695 (5'-AGGATGACGATGAGCGCATTGTTAGATTAATGATTsTsAsCsTsT-3'). The helicase assay substrate in Fig. 2.2B was constructed by annealing 5' [^{32}P]-labeled TP1760 (5'-CCACTACGTGAACCATCACCCAAATCAAGTTTTTTGGGGTCGAGGTGC-3') to M13 single-stranded DNA. 3' or 5' [^{32}P]-labeling was performed as described below.

PREPARATION OF OLIGONUCLEOTIDE AND DNA SUBSTRATES

Oligonucleotide DNA substrates (MWG) were either 3' end-labeled with [α-^{32}P]cordycepin (3' deoxyadenosine) (NEN) and Terminal deoxytransferase (TdT) (Roche) or 5' end-labeled with [γ-^{32}P]ATP (NEN) and T4 Polynucleotide Kinase (PNK) (NEB) and annealed to a molar excess of unlabeled complementary oligonucleotide. The 2.5 kb internally-labeled substrate was generated by PCR using [α-^{32}P]dTTP (NEN) and gel purified by native agarose gel electrophoresis and electroelution. The helicase assay substrate consisted of a 5' [^{32}P]-labeled 48 nt oligonucleotide annealed to M13 single-

stranded DNA (NEB). The 5' Biotin/bead substrate was constructed by ligating an oligonucleotide containing a 5' Biotin-TEG (MWG) to the plasmid DNA substrate and attaching the DNA to streptavidin-coated magnetic beads (Dynal). The beads were washed extensively to remove unbound DNA. Labeled linear dsDNA for the joint-molecule assay was prepared by PCR amplification of a 415 bp region of M13 phage DNA in the presence of [α-^{32}P]dTTP and gel purification by native gel electrophoresis and electroelution. Labeled linear DNA for strand invasion experiments was prepared by PCR amplification of a 2.2 kb region of pTP179 in the presence of [α-^{32}P]dATP (NEN), which was digested at both ends with SphI (NEB) to produce a 1.4 kb linear DNA fragment and gel purified by native gel electrophoresis. Supercoiled 3.6 kb pTP179 plasmid DNA was prepared by sucrose gradient centrifugation.

HELICASE ASSAYS

Helicase reactions contained 0.15 nM [^{32}P]-labeled oligonucleotide/ssM13 DNA complexes in 20 µl reactions containing 20 mM HEPES pH 7.5, 5 mM $MgCl_2$, 1 mM ATP, 50 mM NaCl, 1 mM DTT, and 100 µg/ml BSA. Reactions were incubated at 55°C for 1 hr before separation by native agarose electrophoresis in 0.8% TAE agarose gels for 1 hr at 3.5 V/cm. Reactions were terminated by the addition of 0.2% SDS, 10 mM EDTA, and 0.5 µg/ml ethidium bromide (EtBr). Gels were dried and products were analyzed by phosphorimager (Biorad or GE). Oligonucleotide sequences and preparation of the duplex substrate were reported as described above.

ATPASE ASSAYS

Wild-type or K164A HerA was incubated in 10 µl reactions containing 25 mM MOPS pH 7.0, 5 mM $MgCl_2$, 40 mM NaCl, 2 mM DTT, and 50 µM [γ-^{32}P]ATP (MP Biomedical) at 65°C for 1 hr in the presence or absence of 100 ng linear double-stranded DNA (1 kb ladder, Invitrogen). Reactions were stopped by the addition of 0.2% SDS, 10 mM EDTA, and 0.5 µg/ml EtBr. Reactions were analyzed by thin-layer chromatography (TLC) as described previously (Bhaskara et al., 2007).

NUCLEASE ASSAYS ANALYZED BY NON-DENATURING SOUTHERN HYBRIDIZATION

The unlabeled DNA substrate consisted of a 6.5 kb plasmid (pTP163) linearized at a single site with SacI (NEB). Ten microliter reactions contained 0.2 nM DNA in 25 mM MOPS pH 7.0, 1 mM DTT, 100 mM NaCl, 5 mM $MgCl_2$, and 1 mM ATP and were incubated at 65°C for varying lengths of time as indicated. Reactions were terminated by the addition of 0.2% SDS and 10 mM EDTA, split into two equal volumes (one for the blot with the 3' strand-specific probe and the other for the 5' strand-specific probe), and were separated by native agarose gel electrophoresis in 0.8% TAE agarose gels for 14 hrs at 0.9 V/cm.

Nuclease reactions with the 5' Biotin substrate were performed as above except that proteinase K was also added to 1 µg and incubated for 15 min at 37°C, the beads were then treated with 2% SDS and 10 mM EDTA and incubated for 5 min at 65°C before separation by gel electrophoresis. All DNA concentrations have been reported as moles of molecules.

PROCESSING OF GELS AND MEMBRANES FOR SOUTHERN HYBRIDIZATION

Agarose gels were washed into 20× SSC (3 M NaCl, 0.3 M sodium citrate) and DNA was transferred by capillary action onto nylon membranes (NEN) overnight in 20× SSC. Membranes were probed with RNA complementary to either the 3' or 5' strand of the DNA substrate in a 1 kb region on one end, adjacent to the SacI site. The probes were internally labeled with [α-^{32}P]CTP (NEN) and were made using Riboprobe System T7 (Promega) according to the manufacturer's instructions. The 3' strand-specific probe of a 1 kb region adjacent to the bead attachment site was made by primer extension with [α-^{32}P]dATP (NEN). Denatured DNA controls consisted of substrate DNA denatured with NaOH.

PRIMER EXTENSION

Primer extension reactions were performed in 25 mM MOPS pH 7.0, 1 mM DTT, 1 mM ATP, 5 mM $MgCl_2$, and 100 mM NaCl at 65°C for 30 min or 1 hr as indicated. Reactions contained 2.3 nM pTP163 digested with SacI and 165 nM MR complex as indicated. Reactions were stopped by the addition of 20 mM EDTA and placed on ice. Half of the reaction was used in primer extension reactions containing [α-^{32}P]dATP (NEN). Primer extension products were analyzed on 10% polyacrylamide denaturing sequencing gels.

JOINT MOLECULE AND STRAND INVASION ASSAYS

Joint-molecule reactions contained 1.8 nM 415 bp [^{32}P]-labeled dsDNA in 20 mM Tris pH 7.4, 10 mM $MgCl_2$, 2 mM DTT, 50 mM NaCl, 50 µg/ml BSA, and 2 mM ATP as

indicated in 19 µl reactions. RadA was incubated with the labeled DNA at 50°C for 20 min, then 1 µl ssM13 DNA was added (final 0.2 nM) and incubated an additional hour. RecA reactions were incubated at 37°C for 40 min in the presence of both linear and single-stranded M13 DNA. Reactions were stopped by the addition of 0.2% SDS, 10 mM EDTA, and 0.5 µg/ml EtBr, and were separated by native gel electrophoresis in 1.2% TAE gels for 1.25 hr at 3.5 V/cm.

Strand invasion reactions contained 25 mM MOPS pH 7.0, 2 mM DTT, 2 mM ATP, 10 mM $MgCl_2$, 100 mM NaCl, and 0.1 nM linear [^{32}P]-labeled dsDNA in 9 µl reactions. Reactions were incubated at 65°C for 15 min before the addition of 1 µl of 17 nM supercoiled DNA and incubated for an additional 15 min. Reactions were stopped with 0.2% SDS, 10 mM EDTA, and 0.5 µg/ml EtBr, and separated by native agarose gel electrophoresis in 0.7% Tris-borate EDTA (TBE; 89 mM Tris-borate, 2 mM EDTA) gels for 2 hr at 4.3 V/cm. Preparation of the internally-labeled substrates and supercoiled plasmid DNA are described above.

CHAPTER 3: CHARACTERIZATION OF 5' STRAND RESECTION AND MRE11/RAD50 STIMULATION

Introduction

Protection of genomic DNA from damaging agents is crucial for survival. One of the most cytotoxic forms of damage are DNA double-strand breaks (DSBs), which are caused by external factors such as ionizing radiation (IR) and radiomimetic compounds. DSBs also arise during normal cellular processes, such as immunoglobulin gene rearrangements, DNA replication through single-strand breaks, meiotic recombination, and reactive oxygen species (ROS). In higher eukaryotes, DSBs are predominantly repaired by non-homologous end joining (NHEJ), whereas lower eukaryotes and prokaryotes utilize homologous recombination (HR) (Kowalczykowski et al., 1994; Shrivastav et al., 2008; Takata et al., 1998). One of the earliest steps in repair through the HR pathway is the resection of the 5' strand to produce 3' single-stranded DNA (ssDNA), and resection is a tightly regulated process as it commits the cell to the HR pathway. Cyclin dependent kinases (CDKs) play a role in regulating the repair choice and are involved in promoting HR during the S and G_2 cell cycle phases when sister chromatids are available to serve as the repair template (Aylon et al., 2004; Ira et al., 2004).

The mechanics of 5’ strand resection have been extensively studied in bacteria, where the majority of DSBs are resected by the RecBCD heterotrimeric complex (Kowalczykowski et al., 1994; Kuzminov, 1999; Smith, 2001). This multifunctional complex translocates along dsDNA utilizing both 3’-5’ (RecB) and 5’-3’ (RecD) helicase activities and either degrades both strands asymmetrically or unwinds the two strands until the complex encounters the Chi-sequence on the 3’ strand. At Chi, the enzymatic activity of RecBCD changes so that it either begins degrading the 5’ strand or induces a nick at Chi (Dixon and Kowalczykowski, 1993; Taylor and Smith, 1995). This change in activity is coupled to RecBCD-mediated loading of the RecA recombinase onto the nascent 3’ ssDNA to form the RecA-ssDNA filament necessary for strand invasion (Anderson and Kowalczykowski, 1997; Spies and Kowalczykowski, 2006). Eukaryotes and Archaea lack RecBCD, and the factors involved in end resection in these organisms have been largely unknown until recently.

The Mre11/Rad50 (MR) complex has been implicated in the repair process largely due to null or hypomorphic mutations that result in meiotic recombination defects in budding yeast (Alani et al., 1990; Ivanov et al., 1992; Nairz and Klein, 1997; Tsubouchi and Ogawa, 1998). Additionally, mutations in Mre11/Rad50/Xrs2 (MRX) result in delayed resection of DSBs in vegetatively growing haploid yeast (Clerici et al., 2005; Ivanov et al., 1994; Tsubouchi and Ogawa, 1998). Together with the observation that Mre11 contains several N-terminal phosphodiesterase motifs suggest that Mre11/Rad50 is directly involved in 5’ strand resection. However, MR complexes from humans, yeast, Archaea, and bacteria have been shown to be 3’-5’ exo- and ssDNA endonucleases (Connelly et al., 1997; Hopfner et al., 2000a; Paull and Gellert, 1998;

Trujillo and Sung, 2001), suggesting that additional factors are involved with MR in the resection process.

Recent work in budding yeast identified two 5'-3' exonucleases, Exo1 and Dna2, and a DNA helicase Sgs1 as additional cofactors involved with MRX in resection (Mimitou and Symington, 2008; Zhu et al., 2008). Analogously, I have shown that a 5'-3' exonuclease NurA and a DNA helicase HerA together with MR from *Pyrococcus furiosus* can catalyze resection cooperatively *in vitro* (Hopkins and Paull, 2008). Furthermore, it was proposed that resection occurs in two stages for both yeast and Archaea. First, MR is involved in an initial processing event of the DSB end, which then activates the downstream enzymes (Exo1/Dna2/Sgs1 or HerA/NurA) for long-range resection. Currently, little is known about what this initial processing event by MR is and how the resection enzymes process the 5' strand. In this study, I use recombinant proteins from *P. furiosus* to analyze the products of 5' strand resection and define the role(s) of the Mre11/Rad50 complex in resection.

Results

5' RESECTION BY MRE11/RAD50 AND HERA/NURA RESULT IN DISTINCT OLIGONUCLEOTIDE PRODUCTS

I previously demonstrated that Mre11/Rad50 and HerA/NurA from *Pyrococcus furiosus* (*Pf*) cooperate functionally to resect the 5' strand at a DNA end (Hopkins and

Paull, 2008). I also discovered a novel activity of *Pf* Mre11/Rad50 in short-range resection of the 5' strand, which I hypothesize may be crucial for the removal of 5' adducts. However, the products of the resection reaction catalyzed by Mre11/Rad50 and HerA/NurA are not known. To determine whether these resection products are mononucleotides or oligonucleotides, I used a 5' Cy5-labeled 700 base pair (bp) DNA substrate in reactions with purified proteins *in vitro*. I observed that HerA/NurA cleaves the 5' labeled strand of the substrate at positions ranging from 8-30 nt from the end, producing oligonucleotide products (Fig. 3.1A, lanes 5-7). I did not observe any products smaller than 8 nt, even with internally-labeled substrate DNA (data not shown), indicating that HerA/NurA mediated long-range resection products are oligonucleotides rather than mononucleotides.

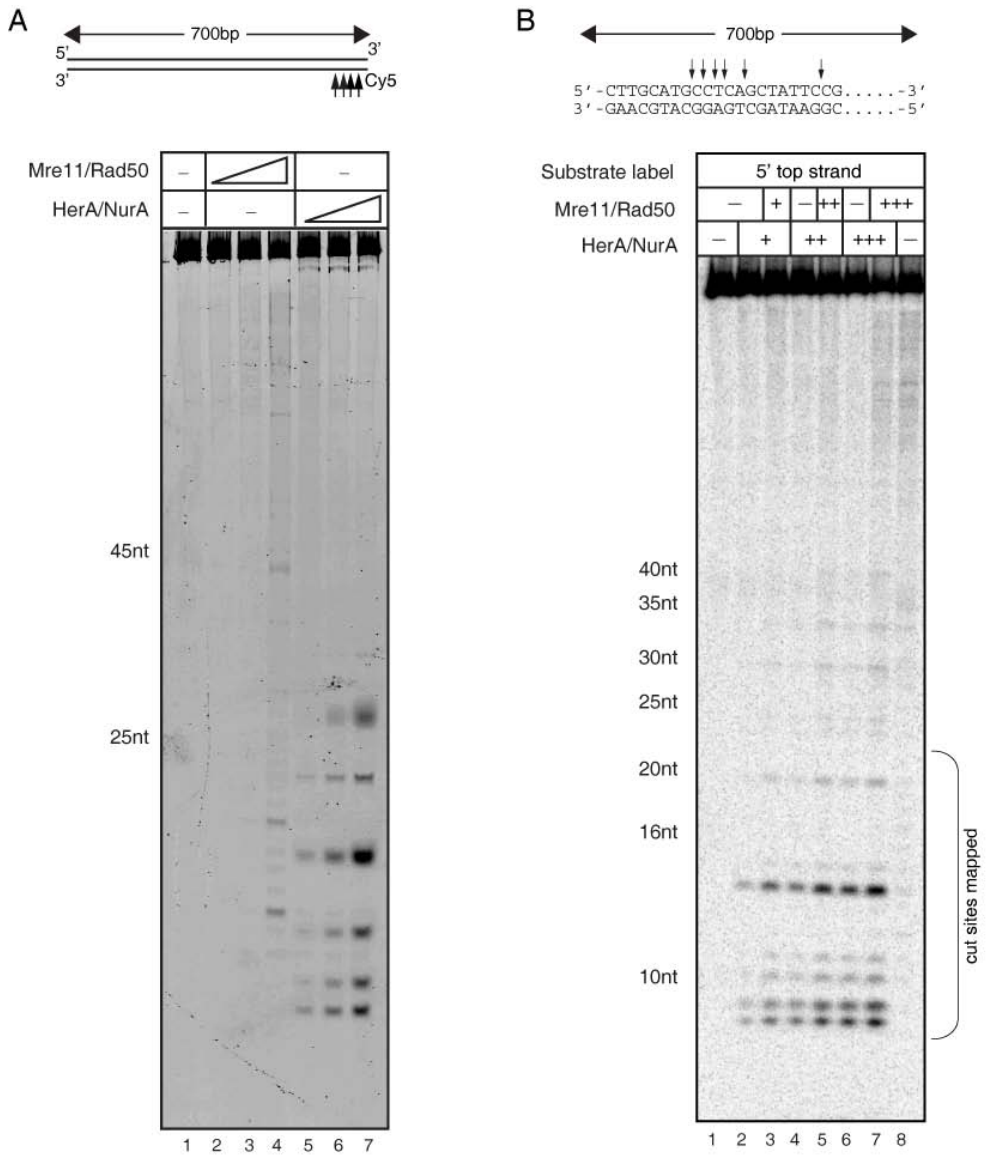

Figure 3.1: Mre11/Rad50 and HerA/NurA catalyze the removal of oligonucleotides from the 5' strand and Mre11/Rad50 stimulates HerA/NurA 5' strand resection. (**A**) Nuclease reactions with 10.8 nM Cy5-labeled 700 bp DNA incubated with either wild-type Mre11/Rad50 (6.5, 32.5, 160 nM) or wild-type HerA (5.4, 10.8, 21.6 nM) and NurA (38.4, 76.8, 153.6 nM) at 65°C for 30 min as indicated. Reaction products were analyzed on a 20% denaturing sequencing gel and scanned for Cy3/Cy5 emission. A schematic of the DNA substrate is shown with the DNA length, position of the Cy5 fluorophore, and the approximate location of cut sites are indicated by vertical arrows.

(**B**) Nuclease reactions with 0.2 nM 700 bp DNA with the top strand 5' [^{32}P] labeled. HerA (+: 1.4, ++: 2.7, +++: 5.4 nM) and NurA (+: 9.5, ++: 19.2, +++: 38.4 nM) were included in the reaction with or without Mre11/Rad50 (+: 1.7, ++: 3.3, +++: 6.6 nM) as indicated. Reaction products were analyzed as in (**A**) but scanned on a phosphorimager. The approximate location of the cut sites ("cut sites mapped") are indicated by vertical arrows on the DNA schematic above. Single-strand markers are shown to the left of the gel.

Mre11/Rad50 complexes from Archaea, bacteria, and eukaryotes have been shown to catalyze manganese-dependent, 3' to 5' exonuclease and endonuclease activity *in vitro* (Connelly et al., 1997; Hopfner et al., 2000a; Paull and Gellert, 1998; Trujillo and Sung, 2001). Yet in our previous study, I found that *Pf* Mre11/Rad50 is also active as a nuclease in magnesium, albeit at a low level (Hopkins and Paull, 2008). Our previous work showed that Mre11/Rad50 is capable of removing 15-55 nt from the 5' end of a linear DNA substrate, and that this activity is abrogated by mutations in the Mre11 nuclease domain (Hopkins and Paull, 2008). To determine whether Mre11/Rad50 acts as an exo- or endonuclease, I tested the *Pf* Mre11/Rad50 complex with the 5' Cy5-labeled DNA at concentrations up to 160 nM. As shown in Figure 3.1A (lane 4), the products of Mre11/Rad50 in magnesium are also oligonucleotide products approximately 10-15 nt long, which are distinct from the HerA/NurA products (compare lane 4 with lane 7). The presence of specific products suggests that Mre11/Rad50 activity may be sequence regulated.

To answer this question, I constructed various fluorophore-labeled DNA substrates shown at the top of Figure 3.2. By analyzing the 5' strand products on different DNA sequences, I can determine whether the sequence near the 5' end affects MR

nuclease activity. Analysis of Cy3-products from the top strand (Fig. 3.2, lanes 5-8) or bottom strand (lanes 9-12) indicates that the DNA sequence alters Mre11/Rad50 nuclease activity (for simplicity, only the ~8-20 nt region of the gel is shown) . I observed that the bottom strand products were identical when the 5' strand was labeled with either Cy5 or Cy3 [Fig. 3.2, compare the red bands in lanes 2-3 to the green bands in lanes 10-11, as well as the individual Cy3 (middle panel) and Cy5 (bottom panel) scans], which indicate that the observed activity is indeed sequence specific and not dependent on the attached fluorophore. These 5' strand products are the result of Mre11 nuclease activity since these products are not observed in reactions containing the Mre11 nuclease-deficient mutant (H85L) (lanes 4, 8, and 12). The 10-15 nt products observed here also confirms our primer extension results, demonstrating that Mre11/Rad50 resects the 5' strand in ~15 nt increments (Hopkins and Paull, 2008). Assays with a 2.4 kb DNA substrate resulted in the same 5' oligonucleotide products, confirming that the endonuclease cleavage activity is the result of cutting proximal to the 5' end (data not shown).

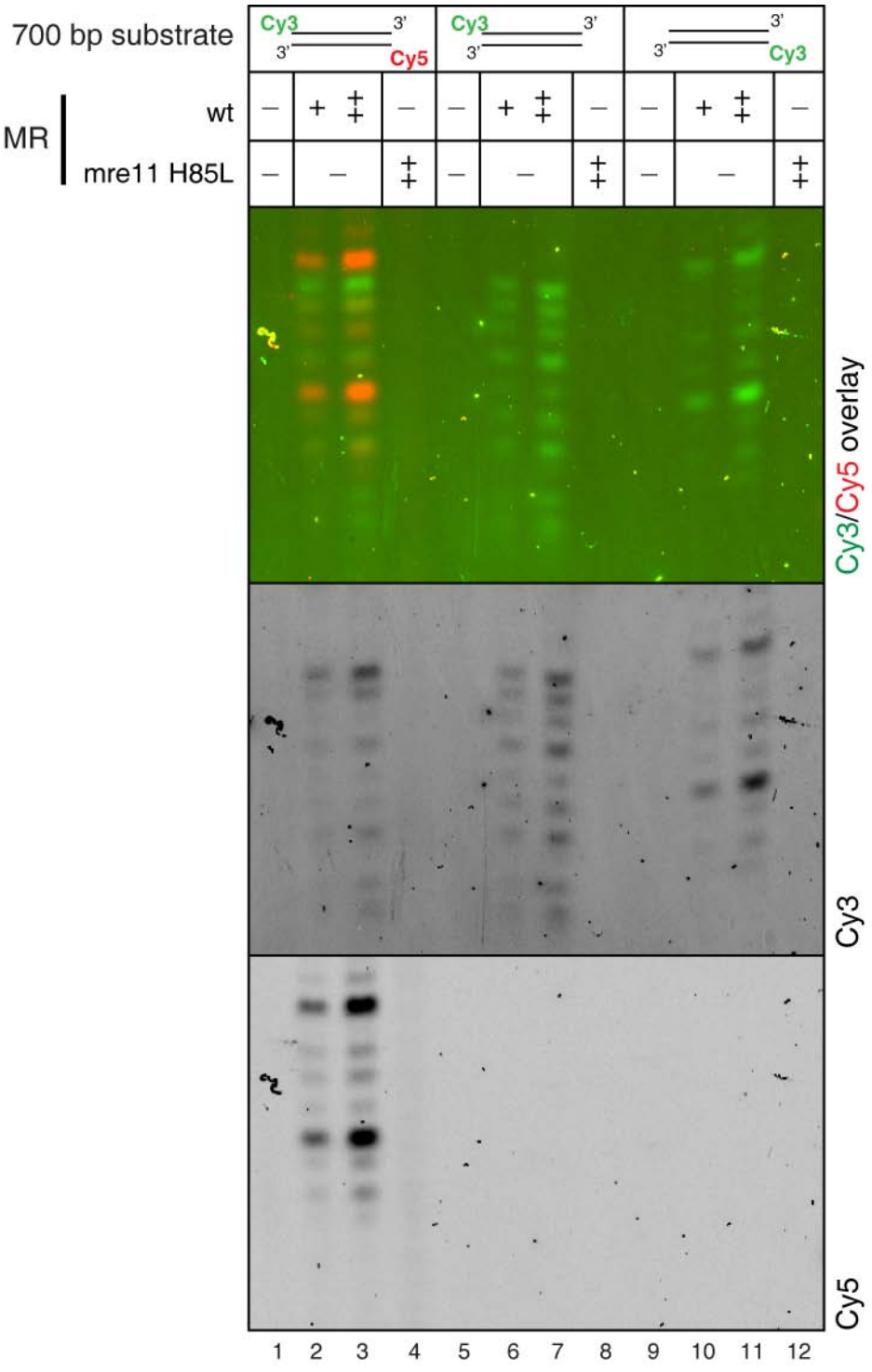
700 bp substrate
Cy3
3'
3'
Cy5
Cy3
3'
3'
Cy3
3'
3'
Cy3
MR
wt
mre11 H85L
Cy3/Cy5 overlay
Cy3
Cy5
1 2 3 4 5 6 7 8 9 10 11 12

Figure 3.2: Mre11/Rad50 demonstrates sequence specificity.
Nuclease reactions with Cy3 (top strand)/Cy5 (bottom strand), Cy3 (top strand) only, or Cy3 (bottom strand) only were performed as in Figure 3.1A except 22 nM DNA was used in each reaction with 0.3 or 0.6 μM wild-type or Mre11(H85L)/Rad50 as indicated at 65°C for 1 hr. Reaction products were analyzed on a 15% sequencing gel. For simplicity, only the 8-20 nt region of the gel is shown. Top panel: overlay of the Cy3 (green) and Cy5 (red) scans. Middle: Cy3 scan alone. Bottom: Cy5 scan alone.

Our previous study showed that *Pf* Mre11/Rad50 markedly stimulated HerA/NurA activity. I also observed this result with a 5' [^{32}P]-labeled substrate using lower levels of *Pf* Mre11/Rad50 (1.7 to 6.6 nM); however, Mre11/Rad50 does not contribute significantly to 5' strand resection at these concentrations (Fig. 3.1B). To confirm that the resection products observed originate from the 5' end closest to the label, I performed nuclease reactions with a 3.4-fold longer DNA substrate (700 bp vs 2.4 kb). I found that the reaction products from both 700 bp and 2.4 kb DNA substrates were identical, which indicates that the 5' resection products are the result of nuclease activity proximal to the dye, similar to Mre11/Rad50 resection activity (Fig. 3.3, compare "Substrate 1" with "Substrate 2"). Reactions performed in the absence of protein did not demonstrate any product formation (data not shown). Surprisingly, I observed different resection products when I assayed a different DNA sequence, which suggests a preference for HerA/NurA to cut at specific DNA sequences (Fig. 3.3, compare "Substrate 2" with "Substrate 3"). Although HerA/NurA activity appears to be sequence-specific, the smallest products observed are ~8-9 nt, which suggests that HerA/NurA resection is regulated by both DNA sequence and distance from the DNA end (Fig. 3.3, lanes 3-6).

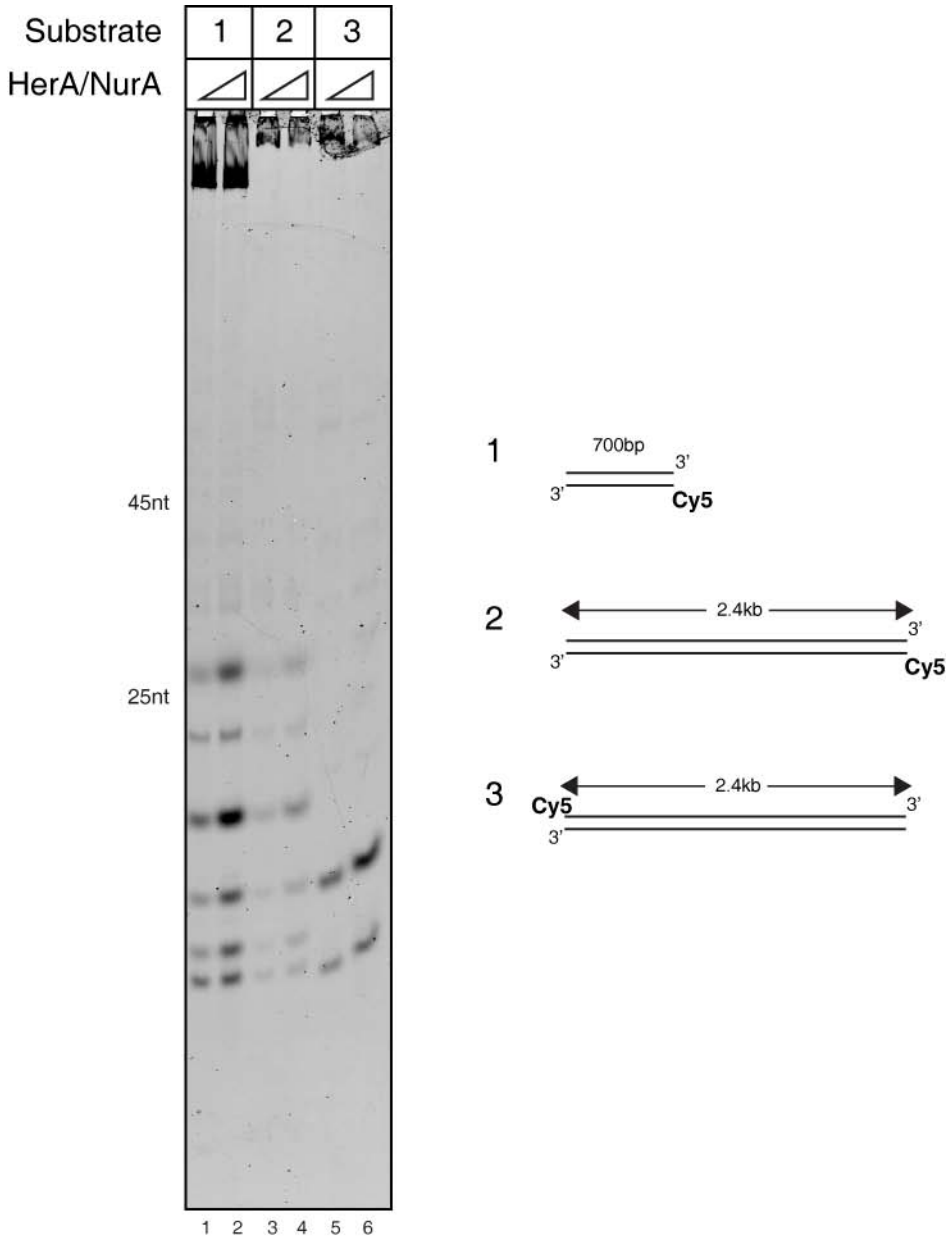

Figure 3.3: HerA/NurA resection demonstrates sequence specificity as well as distance-dependent activity.

Reactions were performed as described in Figure 3.1A with 10.8 nM (700 bp) or 3.2 nM (2.4 kb) DNA and 10.8 nM HerA/78.6 nM NurA or 21.6 nM HerA/153.6 nM NurA as indicated at 65°C for 30 min. Reaction products were analyzed on a 20% denaturing

sequencing gel. A schematic of the three substrates used are shown to the right with the DNA length and position of Cy5 indicated. Single-stranded markers are shown.

STRUCTURE-SPECIFIC CLEAVAGE BY MRE11/RAD50 AND HERA/NURA

The ability of *Pf* Mre11/Rad50 complexes to cleave 5' strands of linear DNA as an endonuclease is consistent with the idea that Mre11/Rad50 complexes open DNA ends into a branched structure prior to cleavage (Paull and Gellert, 1999). These data also suggest the possibility that the DNA sequence at an end may affect the structure in a way that affects unwinding and cleavage efficiency. To investigate this question, I generated a number of oligonucleotide substrates that would be predicted to form unusual structures, including short inverted repeats, direct repeats, and mixed sequences within a poly(T) backbone sequence. *Pf* Mre11/Rad50 cleaved all three oligonucleotide substrate similarly, but preferentially cleaves at a homopolymeric run/mixed sequence junction (Fig. 3.4A, also indicated by a vertical arrow in the top DNA schematic). Mre11/Rad50 makes an endonucleolytic cut 3' of a poly$(T)_{25}$ run, resulting in a 40 nt product when the top strand oligonucleotide is labeled at the 5' end (Fig. 3.4A, left panel "5' top"). Closer inspection of the 40 nt band suggested a distribution of products and when the reaction products were separated further, several minor products which were the result of endonucleolytic cuts within the poly$(T)_{25}$ sequence were observed and almost none were detected within the random DNA sequence (Fig. 3.4B, only the ~34-46 nt region of the gel is shown).

Because the cut at the poly(T)/mixed DNA junction appears to be the predominant cut site, I expect the corresponding 35 nt product when the top strand oligonucleotide is labeled on the 3' strand. As shown in Figure 3.4A (right panel "3' top"), Mre11/Rad50 endonuclease activity results in a predominant 35 nt product when the top strand oligonucleotide is 3' labeled. Further validation of Mre11/Rad50 endonucleolytic activity was performed with oligonucleotide substrates and an endo^{+}/exo^{-} Mre11 His52→Ser (H52S) nuclease mutant (Williams et al., 2008). Both wild-type (wt) and H52S Mre11/Rad50 were able to make endonucleolytic cuts, whereas Mre11/Rad50 complexes containing either the Mre11 exo- and endo-nuclease dead mutant (H85L) or Rad50 signature-motif mutant (S793R) were defective (Fig. 3.5).

The HerA helicase facilitates Mre11/Rad50 cutting at the poly(T)/regular DNA junction (Fig. 3.4B, lanes 2-5 & 8-9), but the NurA nuclease had no effect on Mre11/Rad50 activity (Fig. 3.4B, lanes 10-11). When HerA/NurA were assayed on this DNA substrate, I observed robust activity with a preference to cut in regions of mixed-sequence DNA (Fig. 3.4B, lanes 12-13).

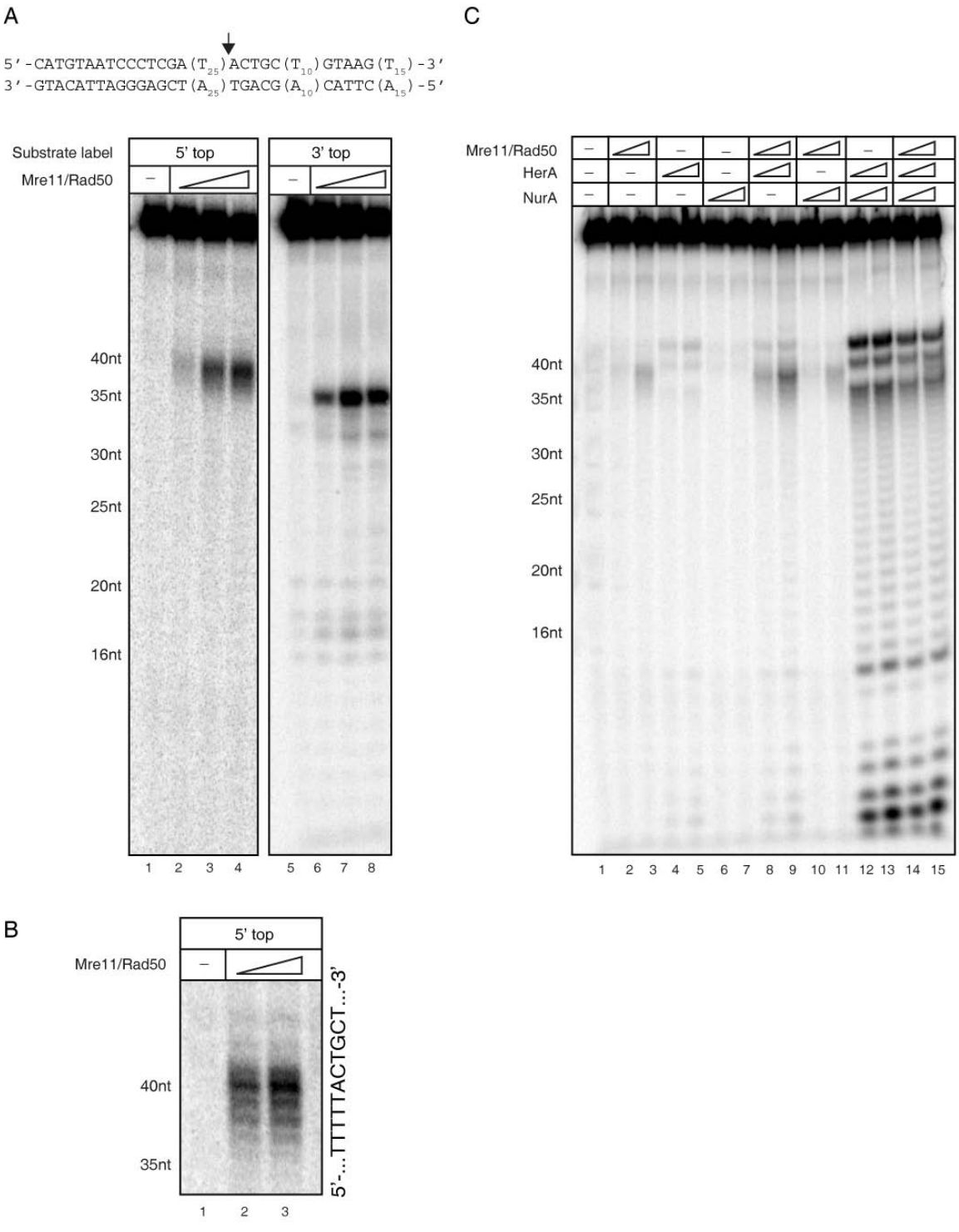
A
5′-CATGTAATCCCTCGA(T25)ACTGC(T10)GTAAG(T15)-3′
3′-GTACATTAGGGAGCT(A25)TGACG(A10)CATTC(A15)-5′
Substrate label
Mre11/Rad50
5' top
3' top
40nt
35nt
30nt
25nt
20nt
16nt
1 2 3 4 5 6 7 8
B
Mre11/Rad50
5' top
40nt
35nt
5'-...TTTTTACTGCT...-3'
1 2 3
C
Mre11/Rad50
HerA
NurA
40nt
35nt
30nt
25nt
20nt
16nt
1 2 3 4 5 6 7 8 9 10 11 12 13 14 15

Figure 3.4: Mre11/Rad50 makes an endonucleolytic cut 3’ to a poly(T) sequence and is stimulated by HerA.
(**A**) Nuclease assays with 1 nM oligonucleotide duplexes labeled at either the 5’ (“5’ top”) or 3’ (“3’ top”) ends. Mre11/Rad50 was incubated with this substrate at 20.4, 40.8, or 81.7 nM as indicated at 65°C for 30 min. The reaction products were analyzed as in Figure 3.1B. The cut site is shown as a vertical arrow in the DNA schematic at the top. (**B**) Reactions were performed as in (**A**) with 40.8 or 81.7 nM Mre11/Rad50 as indicated but separated further. For simplicity, only the 34-46 nt region is shown. The result of DNA sequencing reactions of the substrate is shown on the right. (**C**) Nuclease reactions were performed with the 5’ top substrate as in (**A**) but with Mre11/Rad50 (8.2 or 16.3 nM), HerA (6.7 or 13.4 nM), and NurA (48.1 or 96.2 nM) as indicated. Single-stranded markers are shown.

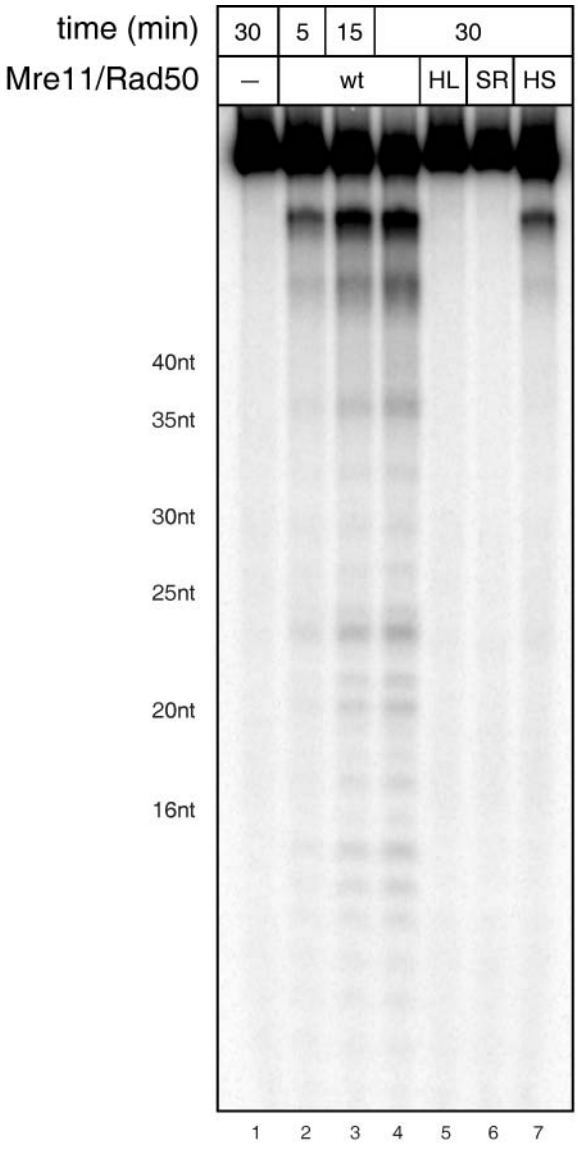

Figure 3.5: Mre11/Rad50 cleavage near a 5' end occurs through endonuclease, not exonuclease activity.

Nuclease reactions with a 5' [^{32}P] labeled-oligonucleotide substrate were performed with 2 nM duplexes and 81.7 nM wild-type and mutant Mre11/Rad50 complexes for the indicated times at 65°C. The reaction products were analyzed as in Figure 3.1B. "HL" is the Mre11(H85L)/Rad50 exo- and endonuclease-deficient mutant. "SR" is the Mre11/Rad50(S793R) ATPase-deficient mutant. "HS" is the Mre11(H52S)/Rad50 exo-deficient, but endonuclease proficient mutant. Single-stranded markers are shown.

MRE11/RAD50 FACILITATES HERA/NURA RESECTION THROUGH A COMBINATION OF END-PROCESSING AND RECRUITMENT MECHANISMS

The results shown here as well as my previous work have shown that Mre11/Rad50 strongly stimulate 5' strand resection by HerA/NurA. However, it is not clear how *Pf* Mre11/Rad50 contributes to the efficiency of HerA/NurA catalyzed resection. To define Mre11/Rad50's function in the resection process, *in vitro* resection assays were performed in two-stages. In the first stage, the DNA substrate was incubated in the presence or absence of wild-type or mutant Mre11/Rad50. The reactions were terminated with SDS, and the SDS was removed using a size-exclusion spin column. The reaction products from the first reaction were then used in a second reaction containing HerA/NurA. I found that the DNA that had been incubated with wild-type Mre11/Rad50 in the first stage was much more efficiently resected by HerA/NurA in the second stage reaction (Fig. 3.6, compare lanes 2-3 with 5-6). This result suggests that the DNA products of Mre11/Rad50 short-range resection are more efficiently resected by HerA/NurA in comparison to the original DNA substrate. When nuclease-deficient (H85L) or ATPase-deficient (S793R) versions of the Mre11/Rad50 complex were used in the initial stage of the reaction, no increase in the level of resection by HerA/NurA in the second stage was observed (Fig. 3.6, lanes 7-12), indicating that the catalytic activities of both proteins are required for this effect.

The sequential reaction with wild-type Mre11/Rad50 in stage 1 and HerA/NurA in stage 2 produces a high level of resection products; however, these are not resected as extensively as the combined reaction in which Mre11/Rad50 and HerA/NurA are all present (Fig. 3.6, compare lane 5 to 14). In addition, as I showed previously, when the combined reaction was performed with the nuclease-deficient Mre11(H85L)/Rad50 and

HerA/NurA, resection levels were similar to wild-type reactions (Fig. 3.6, lanes 14-15). These data suggest that Mre11/Rad50 contributes to HerA/NurA-mediated resection via a protein-independent mechanism (most likely via short-range resection of 5' strands) as well as a protein-dependent mechanism (via a putative DNA recruitment event), and that Mre11-nuclease activity is only essential for the protein-independent pathway.

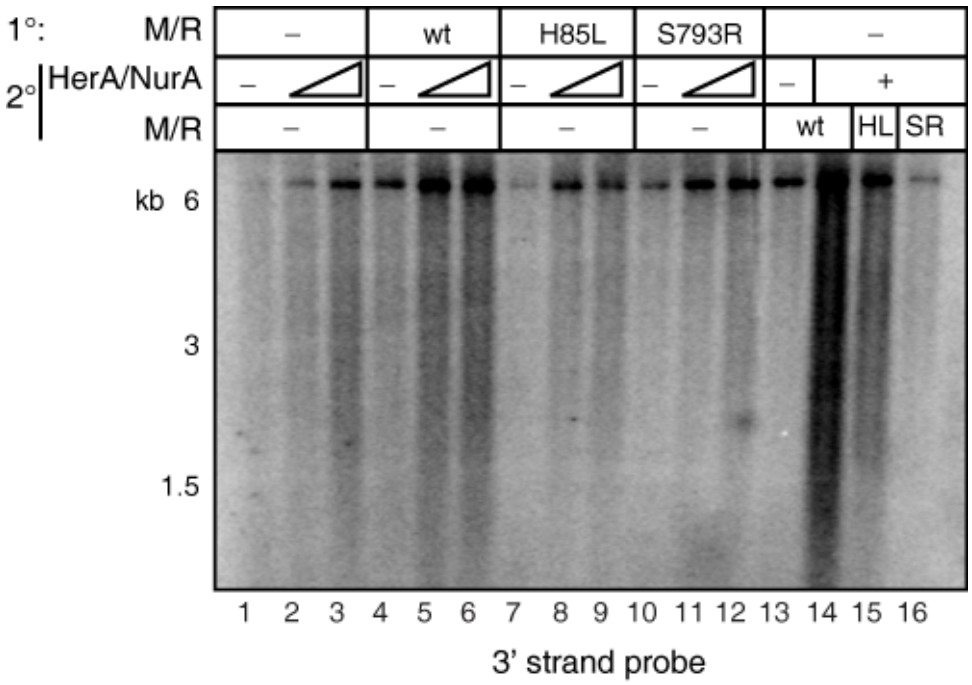

Figure 3.6: Mre11 nucleolytic processing facilitates resection by HerA/NurA.
In vitro resection reactions were performed in two-stages. In the first stage (1°), the DNA substrate was incubated with 16.5 nM wild-type or mutant Mre11/Rad50 as indicated. Reactions were terminated with SDS, and DNA was collected in the flow-through of a Micro-Biospin6 size exclusion column. The second stage reaction (2°), included 7.2 nM HerA/51.3 nM NurA or 14.3 nM HerA/102.6 nM NurA as indicated. Reactions with Mre11/Rad50 contained 4.4 nM MR and 7.2 nM HerA/51.3 nM NurA as indicated. Reaction products were analyzed by non-denaturing Southern hybridization using an RNA probe specific for the 3' strand. Double-stranded DNA markers are shown to the left in kilobase pairs (kb).

To further characterize the resection reaction, we have developed a quantitative PCR method to determine the relative amount of ssDNA at various distances from the DNA end, similar to a method based on the sensitivity of resection enzymes for cleaving at dsDNA vs ssDNA developed to analyze yeast resection *in vivo* (Zierhut and Diffley, 2008). Using two sets of primers and probes located 29 bp and 1025 bp from the DNA end, we quantitated the amount of ssDNA produced by resection (Fig. 3.7A). At the highest HerA/NurA concentrations tested, approximately 31% and 23% ssDNA was formed at 29 nt and ~1 kb, respectively over background levels, during the resection reactions when Mre11/Rad50 and HerA/NurA were incubated together (Fig. 3.7B, column 9). In similar reactions performed at lower HerA/NurA concentrations, approximately 19% and 12% ssDNA was formed at 29 and ~1 kb, respectively (Fig. 3.7B, column 8). However, when Mre11/Rad50 and HerA/NurA reactions were performed as separate incubations, only 16% and 15% ssDNA were formed at 29 nt and ~1 kb, respectively, at the highest HerA/NurA concentrations (Fig. 3.7B, column 6). At the lower HerA/NurA concentrations, only 8% ssDNA was formed at both 29 nt and ~1 kb from the DNA end (Fig. 3.7B, column 5). Thus, the presence of Mre11/Rad50 together with HerA/NurA in the reaction increases resection efficiency and suggests that the protein-dependent mechanism is a more efficient resection pathway.

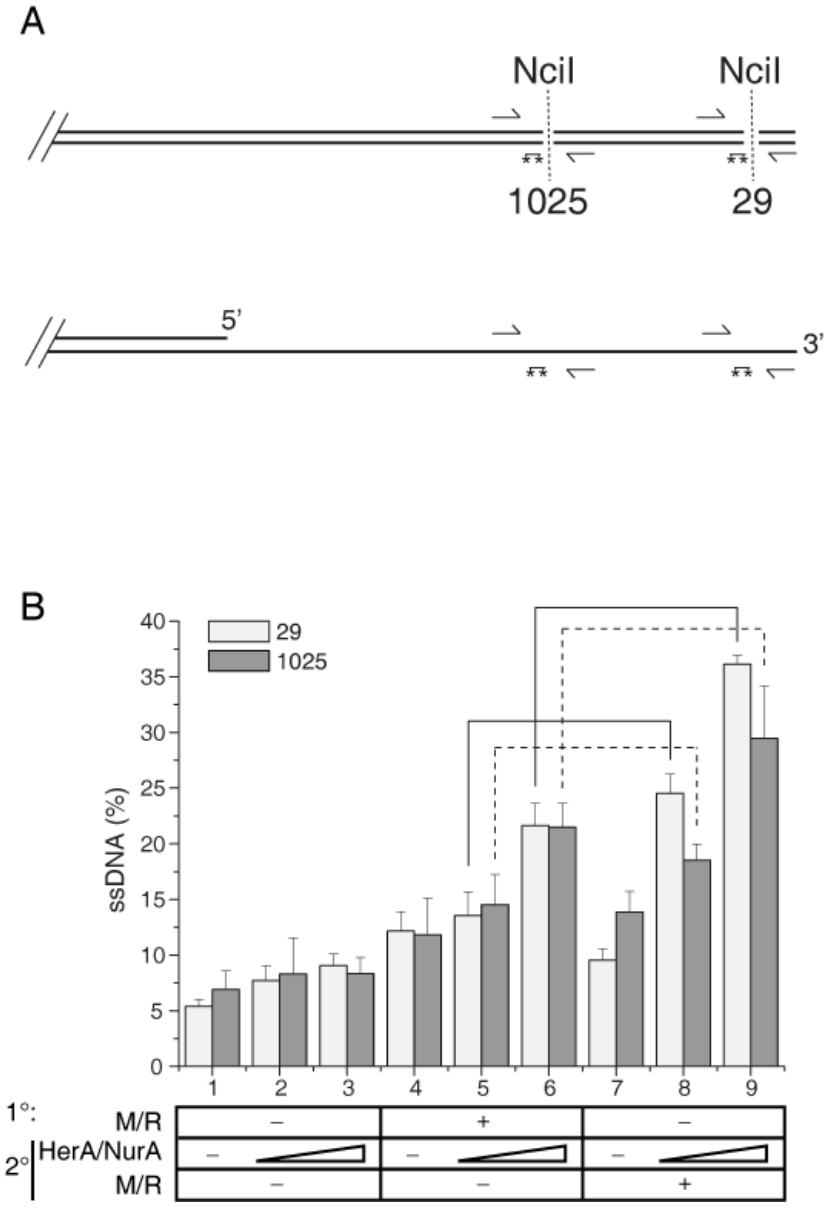

Figure 3.7: Quantitation by qPCR of single-stranded DNA produced by resection. (**A**) Schematic of the location of NciI sites and primer/probe pairs used to measure ssDNA levels produced during resection. (**B**) Levels of ssDNA at 29 and 1025 bp from the DNA end are shown from two-stage resection reactions. Reactions were performed similar to Figure 3.6 using pNO1 as a substrate. First stage reactions (1°) were incubated with 16.5 nM wild-type or mutant Mre11/Rad50 as indicated. Second stage reactions (2°) contained 9 nM HerA/64 nM NurA or 18 nM HerA/128 nM NurA with or without 6.5

nM Mre11/Rad50 as indicated. Shown is the mean percent ssDNA from three independent qPCR runs. Error bars indicate standard error of the mean (SEM) (n=3). Solid lines indicate statistically significant differences ($p < 0.05$), whereas dotted lines indicate no significance differences ($p > 0.05$) according to Student's T-test, two-sample assuming unequal variance. I acknowledge Dr. Zhi Guo for his help in performing these experiments and preparation of this figure.

Despite being a less efficient reaction, the protein-independent pathway provides a viable repair mechanism when Mre11/Rad50 is absent from the DNA end. Here the prerequisite for repair is an initial processing event of the DNA end by Mre11 nuclease activity, which provides a suitable substrate for HerA/NurA resection. Based on the direct removal of 10 to 15 nt of the 5' strand by Mre11 (Fig. 3.1A & Fig. 3.2), I hypothesized that Mre11/Rad50 activity results in the formation of a 3' ssDNA region of approximately 15 nt. To test whether the HerA/NurA enzymes bind preferentially to a 3' ssDNA overhang, I performed gel shift assays with oligonucleotide substrates. I found that NurA demonstrated a preference for an oligonucleotide substrate containing 12 nt 3' overhangs as compared to 4 nt 3' overhangs (Fig. 3.8). Quantitation of the NurA-DNA complex indicates that NurA binds the 12 nt 3' overhang 4 to 6-fold better compared to the 4 nt 3' overhang substrate (Fig. 3.8, "% complex"). Based on the binding affinity of NurA for longer 3' overhang substrates, I conclude that Mre11/Rad50 processing of DNA produces a substrate containing a 3' overhang end, which is recognized and resected by HerA/NurA.

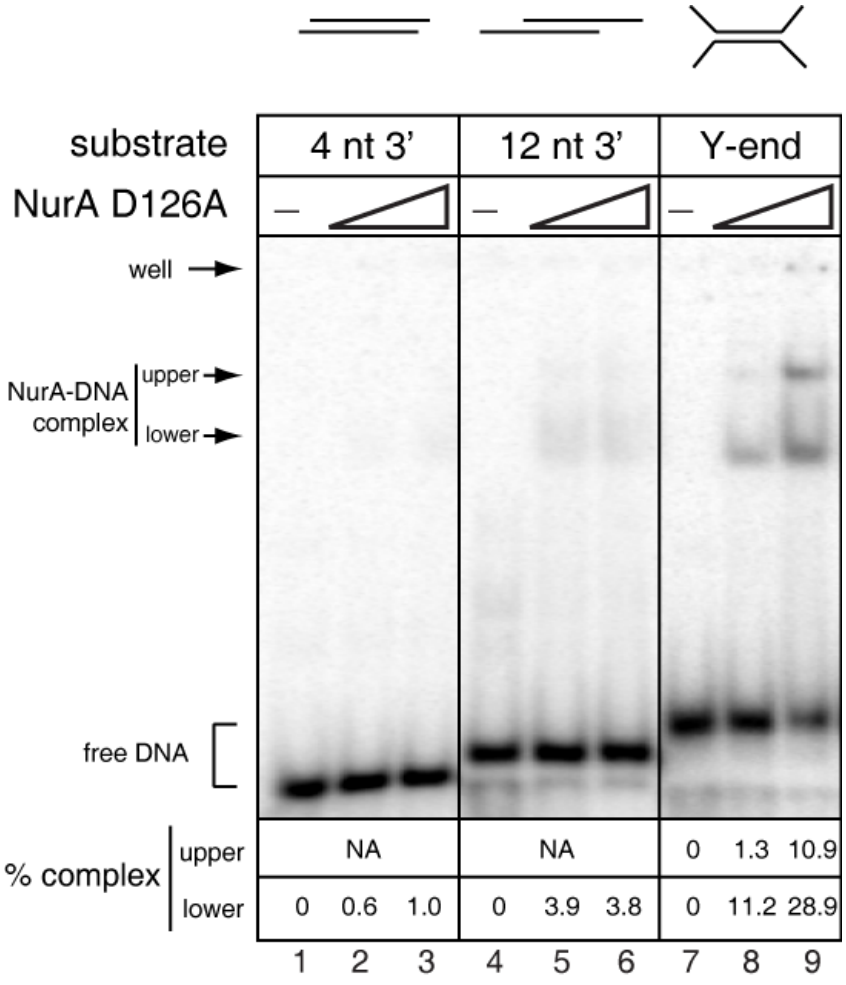

Figure 3.8: NurA binds preferentially to DNA with long 3' overhangs or unwound strands.

Gel mobility shift assays were performed with oligonucleotide duplexes containing either 4 nt 3' overhangs ("4 nt 3' "), 12 nt 3' overhangs ("12 nt 3' "), or 11 and 13 unpaired nucleotides at each end ("Y-end") at each end. Nuclease-deficient NurA (D126A) was included in the binding reaction at 19 or 38 nM as indicated before analysis in a native 6% 0.5× TBE polyacrylamide gel. Quantitation of the NurA-DNA complex bands (upper and lower) are shown below ("% complex", upper and lower). A schematic of the oligonucleotide substrates are indicated above each panel. NA, not applicable.

In the combined Mre11/Rad50/HerA/NurA reaction, the Mre11(H85L)/Rad50 nuclease-deficient mutant is proficient in stimulating HerA/NurA-mediated resection, but the Mre11/Rad50(S793R) ATPase-deficient mutant is not. Based on previous results from our laboratory, I hypothesize that the ATPase activity of Rad50 helps to partially unwind DNA ends and that this branched structure is an optimal HerA/NurA resection substrate. To test whether HerA/NurA binds preferentially to unwound ends, I performed gel-shift assays using double-Y structured oligonucleotide substrates containing 11 and 13 nt single-stranded ends. As shown in Figure 3.8, NurA alone preferentially binds this branched DNA over the substrates containing either 4 nt or 12 nt 3' (compare lanes 7-9 to 1-6). At the highest concentrations assayed, almost 40% of the Y-substrate DNA was bound by NurA compared to 1-4% with the 3' overhang substrates (Fig. 3.8, "% complex"). I found two NurA-DNA complex species with the Y-substrate which I hypothesize is formed by NurA binding to one or both unwound regions on one DNA molecule (Fig. 3.8, lanes 9). This preference for NurA binding to an unwound DNA structure, suggests that one function of Mre11/Rad50 is to unwind the DNA end to facilitate resection by HerA/NurA. In addition, the observation that NurA binds the unwound DNA with higher affinity over the 12 nt 3' overhang substrate supports the idea that the protein-dependent pathway is the more efficient resection mechanism.

To test whether Mre11/Rad50 recruits NurA to DNA we developed an assay to analyze the relative amounts of NurA crosslinked to DNA in the presence and absence of MR, based on a previous study to observe specific protein-DNA interactions (Yang and Nash, 1994). My preliminary data demonstrates that approximately 2-fold more NurA is found associated with DNA in the presence of MR relative to NurA levels in the absence

of MR (data not shown). Based on the preferential binding of NurA to unwound DNA ends and the active recruitment of NurA to DNA by Mre11/Rad50, my data supports the model that Mre11/Rad50 facilitates resection through recruitment of the resection enzymes and local unwinding of DNA ends.

Discussion

Homologous recombination is initiated by the detection of DNA breaks followed by extensive 5' strand resection to produce recombinogenic 3' single-strand DNA, which can range from hundreds of nucleotides to tens of kb in yeast. Genetic evidence suggested that the Mre11/Rad50 complex is involved in the resection process, but the biochemical activities of Mre11/Rad50 are inconsistent with *in vivo* resection. To investigate this discrepancy, I previously tested the activities of *Pyrococcus furiosus* Mre11/Rad50 and HerA/NurA enzymes *in vitro* and found that these enzymes cooperatively resect DSBs *in vitro* (Hopkins and Paull, 2008). However, the precise roles of Mre11/Rad50 and HerA/NurA and products of the resection process have not been directly studied. In the current work, I examined the 5' strand resection products directly using end-labeled DNA substrates. In addition, I elucidated the role of Mre11/Rad50 complex in resection by demonstrating that it promotes resection through multiple mechanisms, including initial nucleolytic DNA end processing and a putative unwinding event, both of which facilitate resection by HerA/NurA.

HERA/NURA RESECTION IS REGULATED BY BOTH SEQUENCE AND DISTANCE FROM THE DNA END

Based on earlier genetic evidence in *S. cerevisiae* and *in vitro* data, it is believed that the Mre11 nuclease is not involved in long-range resection and other factors are necessary for this process (Hopkins and Paull, 2008; Llorente and Symington, 2004). The identity of these putative resection factors were unknown until recently when the Symington and Ira labs independently discovered Sgs1, Exo1, and Dna2 in yeast (Mimitou and Symington, 2008; Zhu et al., 2008). I also identified HerA/NurA in *P. furiosus* as the long-range resection enzymes (Hopkins and Paull, 2008). Since little is known about the enzymatic properties of the resection enzymes, I characterized the 5' strand products using end-labeled DNA substrates *in vitro*. The majority of the long-range resection products catalyzed by HerA/NurA were short oligonucleotide products, and this cleavage activity showed sequence specificity (Fig. 3.1A & Fig. 3.3). HerA/NurA makes the initial nucleolytic cut approximately 8-9 nucleotides (nt) from the 5' end independent of the DNA sequence, suggesting that this complex makes the first cut in a length-dependent manner (Fig. 3.3). A similar phenomenon was observed with the mycobacterial AdnAB helicase/nuclease complex, where AdnAB makes an initial cleavage ~5 nt from the 5' end (Sinha et al., 2009). Also in *E. coli*, the RecB subunit of the RecBCD complex makes the initial cut several nucleotides in from the 5' strand end (Yu et al., 1998). Thus, it appears that resection in prokaryotic organisms begins with an endonucleolytic cleavage event several nucleotides from the 5' strand end.

MRE11/RAD50 ENDONUCLEOLYTIC ACTIVITY IS CONSISTENT WITH 5' CONJUGATE REMOVAL *IN VIVO* AND PREFERENTIALLY CUTS AT SEQUENCES WITH UNUSUAL STRUCTURE

Despite the fact that the coupled resection reaction is independent of the Mre11 nuclease activity, I found that Mre11/Rad50 removed 15-55 nucleotides of the 5' strand by primer extension (Hopkins and Paull, 2008) and is consistent with *in vivo* evidence demonstrating MRX-dependent removal of short DNA fragments from the 5' strand close to a DSB (Zhu et al., 2008). Mre11/Rad50 accomplishes this reaction through a novel endonucleolytic activity by removing oligonucleotides approximately 10 to 15 nt long, which were distinct from HerA/NurA 5' products (Fig. 3.1A). Our observation that Mre11/Rad50 endonuclease activity results in short oligonucleotide products may provide an explanation for the observation from yeast studies in which Spo11/Rec12-conjugates are removed in a Mre11-nuclease dependent manner attached to oligonucleotides approximately 12-34 nt long (Milman et al., 2009; Neale et al., 2005; Rothenberg et al., 2009).

Mre11/Rad50 also demonstrated a preferred endonucleolytic activity for cleaving immediately 3' to a poly$(T)_{25}$ sequence (Fig. 3.4). The absence of products resulting from endonuclease cutting 3' to the poly$(T)_{10}$ sequence indicates that Mre11/Rad50 preferentially recognizes and cuts at polyT sequences >10 nt. Further support that Mre11/Rad50 recognizes and binds poly(T) sequences comes from the observation that MR also makes several cuts within the poly(T) region and not in the mixed sequence adjacent to the poly(T) run (Fig. 3.4B). Cleavage at the poly(T)/mixed DNA junction by Mre11/Rad50 was stimulated by HerA, which suggests that unwinding of the DNA facilitates MR junction cleavage activity (Fig. 3.4C). Poly(T) • poly(A) sequences are

known to alter DNA structure by bending due to base pair tilt and appear to be rigid sequences due to the higher propeller twist of A:T base pairs. Regions between these poly(T)/poly(A) sequences with an adjacent mixed DNA sequence introduces a local DNA junction (McConnell and Beveridge, 2001; Nadeau and Crothers, 1989). Furthermore, A/T-rich sequences were shown to be sensitive to endonucleolytic nicking, and stable unwinding at these sequences enhanced nicking activity (Kowalski et al., 1988).

Given that these polynucleotide sequences adopt unusual structures, it is likely that Mre11/Rad50 recognizes a specific DNA structure and not a particular sequence *per se*. The retrotransposon L1 endonuclease was shown to nick at a poly(T)/poly(A) junction *in vitro* (Cost and Boeke, 1998), providing additional support that nuclease activity may be regulated by DNA structure. However, the physiological role of Mre11/Rad50 junction cleavage activity is unknown, but may be related to cutting DNA substrates with aberrant secondary structure.

MRE11/RAD50 CONTRIBUTES TO RESECTION THROUGH INITIAL NUCLEOLYTIC PROCESSING, PARTIAL UNWINDING OF THE DNA END, AND RECRUITMENT OF NURA TO DNA

The precise involvement of Mre11/Rad50 during the resection reaction has been an enigmatic question for many years. My results and results from others have shown that Mre11/Rad50 is involved in short-range 5' strand resection on the order of 15-100 nt. It was hypothesized that this limited resection was a critical function of Mre11/Rad50 in the removal of 5' conjugates (i.e., Spo11 and "dirty ends") prior to extensive resection, but

the precise role has yet to be elucidated. However, preliminary data demonstrates that Mre11 nuclease as well as HerA/NurA activities are required for removal of 5' protein adducts from synthetic DNA substrates (data not shown). I speculated that Mre11/Rad50 may be necessary to minimally process a DNA end such that the extensive-resection enzymes can bind to the end and initiate resection. I also hypothesized that Mre11/Rad50 bound to a DNA end may serve to recruit the resection machinery to DNA.

To more definitively determine the role of Mre11/Rad50, I developed an *in vitro* resection reaction which was performed in two separate stages. In the first stage, linear DNA was incubated with wild-type or mutant Mre11/Rad50 and then treated with SDS to inactivate the enzymes. The pre-treated DNA was then used as the substrate in a second reaction with HerA/NurA before analysis by Southern hybridization. The DNA that had been processed by wild-type Mre11/Rad50 in the first reaction, was resected by HerA/NurA in the second stage reaction (Fig. 3.6, lanes 1-6). However, reactions performed with either nuclease- or ATPase-deficient Mre11/Rad50 complexes were not efficiently resected by HerA/NurA in the second reaction (Fig. 3.6, lanes 7-12). This combined data suggests that Mre11/Rad50 nuclease activity is involved in minimally processing a DNA end into a structure, which is bound and subsequently resected by the HerA/NurA complex.

I propose that the structure formed by MR nuclease activity contains a short 3' overhang approximately 10 to 15 nt long (Fig. 3.1A) and found that NurA bound an oligonucleotide substrate containing 12 nt 3' overhangs approximately 4-6-fold better than a similar substrate containing only 4 nt 3' overhangs (Fig. 3.8), suggesting that the HerA/NurA complex binds DNA ends only after processing by MR. This pathway

requires an initial processing event by Mre11/Rad50, but does not require Mre11/Rad50 to be present concomitantly with HerA/NurA during resection. Thus, these two stages (Mre11/Rad50 initial processing and HerA/NurA extensive resection) are distinct and can occur independently.

Despite the observation that Mre11/Rad50 and HerA/NurA enzymatic activities can function as separate events, I have shown that robust resection is observed with nuclease deficient Mre11(H85L)/Rad50 when the complex is incubated together with HerA/NurA in a coupled reaction (Hopkins and Paull, 2008). To reconcile the differences with the nuclease-deficient MR complex in the resection reaction, I hypothesize that Mre11/Rad50 promotes resection by recruiting HerA/NurA to DNA ends, as ATM and yeast Exo1 were found to be DNA associated only in the presence of MRN or MRX, respectively (Lee and Paull, 2005; Nicolette and Paull, unpublished data). Consistent with the MR-dependent localization of proteins to DNA, preliminary data demonstrates that MR recruits NurA to DNA (data not shown). Experiments to more rigorously test this are currently underway.

In contrast to wild-type and nuclease-deficient Mre11/Rad50, I found that a mutation in the Rad50 signature motif (S793R) results in a complete block to resection *in vitro* (Hopkins and Paull, 2008). This mutation disrupts ATP binding and the ATP-dependent functions of *P. furiosus,* yeast, and human Mre11/Rad50 complexes (Moncalian et al., 2004). Based on the ability of human MRN to unwind short DNA duplexes (Paull and Gellert, 1999) and the requirement for open DNA ends in the ATM activation pathway (Lee and Paull, 2005), I hypothesize that a core function of Mre11/Rad50 complexes is to locally unwind a DNA end to facilitate downstream

events. Consistent with this hypothesis, I found that NurA preferentially binds to a partially unwound Y- end oligonucleotide compared to a fully complementary substrate (Fig. 3.8). These results suggest that a crucial role of Mre11/Rad50 is the ATP-dependent opening of a DSB end to facilitate HerA/NurA binding and subsequent resection. This pathway requires Mre11/Rad50 to be present to unwind and recruit HerA/NurA to DSB ends. I found that NurA demonstrated a higher affinity for an unwound DNA substrate compared to the 3' overhang substrates (Fig. 3.8). This binding preference may provide a molecular explanation for the observation that the protein-dependent resection is more efficient than the protein-independent pathway when ssDNA levels were measured by quantitative PCR (Fig. 3.7B). However, it should be noted that similar binding experiments with HerA indicate that HerA preferentially binds the 4 nt 3' overhang substrate over the 12 nt 3' overhang (data not shown). HerA also demonstrates the weakest affinity for the Y-end substrate (data not shown), which is consistent with earlier observations that HerA preferentially binds dsDNA over ssDNA (Manzan et al., 2004). Attempts to determine the preferred DNA binding substrate for the HerA/NurA complex have been unsuccessful, but I speculate that the complex will demonstrate the highest affinity for either the 12 nt 3' overhang or Y-end substrates.

Based on my current work, I propose a model of the resection process involving Mre11/Rad50 and HerA/NurA (Fig. 3.9). In the first step, a DNA end is recognized by Mre11/Rad50 and the ends are minimally processed (Fig. 3.9A, B). I also hypothesize that the Mre11/Rad50 complex partially unwinds the DNA end, and that the Mre11/Rad50-bound DNA end is the preferred resection pathway for HerA/NurA (indicated by the thick arrow, Fig. 3.9C-D). However, if Mre11/Rad50 dissociates from

the DNA after the end has been processed, HerA/NurA is still able to bind an Mre11/Rad50-free DNA end (thin arrow, Fig. 3.9C-D). Once the HerA/NurA complex is localized to the DNA end, it is able to processively resect the 5’ strand, producing long recombinogenic 3’ single-strand DNA for RadA recombinase loading (Fig. 3.9E).

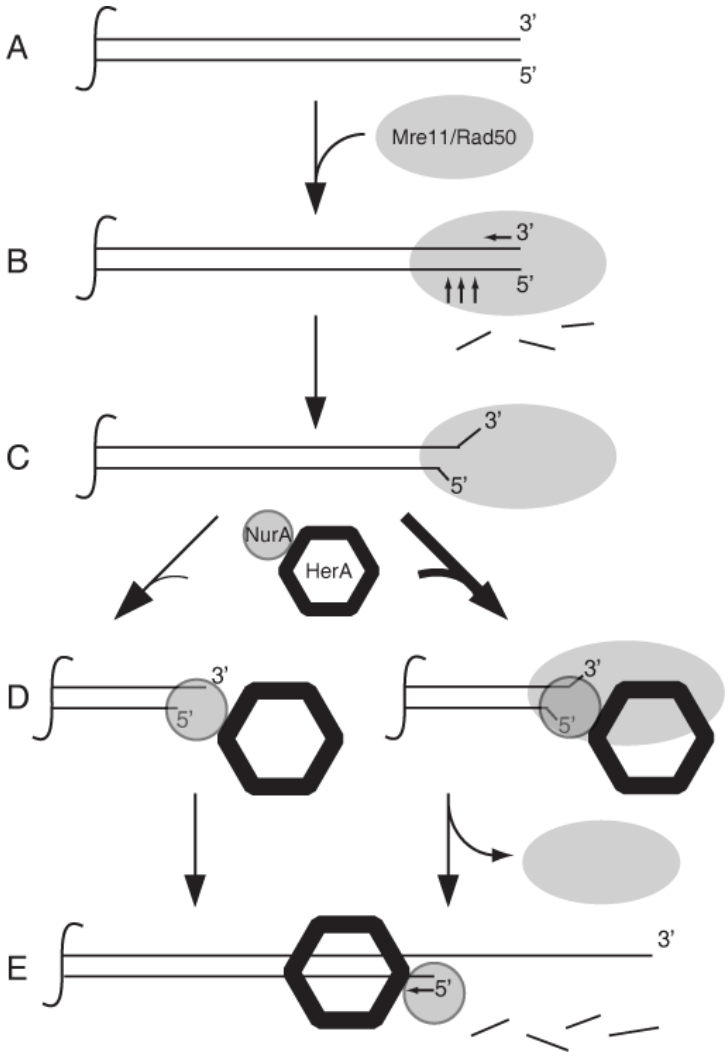

Figure 3.9: Model of 5’ strand resection catalyzed by *P. furiosus* Mre11/Rad50, HerA, and NurA.

Mre11/Rad50 first binds to the DSB end (**A-B**) and is able to perform some initial processing of the end (**B**). This initial processing is not essential when the DNA end does not contain a protein adduct but may increase the efficiency of the subsequent resection event. Mre11/Rad50 partially unwinds the end (**C**) which helps HerA/NurA resection complex binding to the end (**D**, dark arrow). NurA likely binds directly to the unwound DNA end based on our gel shift data with oligonucleotide substrates containing unpaired ends. The Mre11/Rad50-dependent pathway is likely the dominant pathway as inclusion of MR in the *in vitro* resection reactions produces ssDNA more efficiently (dark arrow). An additional Mre11/Rad50-protein independent pathway is also predicted based on HerA/NurA-mediated resection with DNA that had been previously processed by Mre11/Rad50 (**D**, thin arrow). Initial nucleolytic processing by MR results in DNA ends containing short (~10-15 nt) 3' overhangs, which NurA can bind based on gel shift data. This appears to be a minor pathway (thin arrow) based on the observation that resection in the absence of Mre11/Rad50 is less efficient and NurA demonstrates a lower affinity for 12 nt 3' overhang DNA compared to unwound DNA substrates. Once HerA/NurA is localized to the DSB end through either pathway, it begins to extensively resect the 5' strand (**E**). The nascent 3' ssDNA is bound by RadA and the RadA-ssDNA filament catalyzes strand exchange (not shown).

In our earlier work (Hopkins and Paull, 2008) and in the work described here, I reconstituted the resection reaction using magnesium as the metal ion. I reasoned that magnesium was the physiological divalent ion as the intracellular concentration *in vivo* is often several fold higher than manganese (Kondo et al., 2008). However, purified Mre11/Rad50 complexes from several organisms have been characterized to be manganese-dependent enzymes and normally inactive in magnesium when assayed *in vitro*. As discussed in our previous work, I mention several possibilities why I observe magnesium-dependent activity. However, one possibility that I was unable to directly test was the co-purification of metal ions with Mre11/Rad50. To determine whether the purified Mre11/Rad50 was bound to manganese or magnesium, we performed trace metal analysis by inductively coupled plasma mass spectrometry (ICP-MS). In a purified Mre11/Rad50 preparation containing 20.2 μM Mre11 (monomer concentration), we

detected magnesium at 6.8 µM and manganese at 1 µM, which suggests that purified Mre11/Rad50 is unlikely to have manganese bound in the active site. In addition, I have found that *Pf* MR is not active *in vitro* without the addition of magnesium (data not shown). Thus, the measured activity of Mre11/Rad50 in my experiments likely represents magnesium-dependent function.

The results described here demonstrate the multi-faceted role of Mre11/Rad50 in end processing. I show that Mre11/Rad50 has a unique ability to cleave immediately 3' to poly(T) sequences larger than 10 nt and that both the Mre11/Rad50 and HerA/NurA complexes exhibit nuclease sequence specificity. Based on this work and the conservation of Mre11/Rad50 in other organisms, I hypothesize that Mre11/Rad50 in eukaryotes may function similarly. I also speculate that the functional orthologs in yeast and humans of HerA/NurA (Sgs1/BLM, Exo1/hExo1, Dna2) may behave similarly in their dependence on MRX(N) function. An advantage to studying enzymes from Archaea is that they serve as simplified models for the more complex eukaryotic systems. Our ability to study these enzymes biochemically and the tools I have developed will allow us to understand and characterize the homologous enzymes from yeast to humans.

Experimental Procedures

PROTEIN EXPRESSION AND PURIFICATION

Expression and purification of *P. furiosus* Mre11/Rad50, HerA, and NurA was described previously (Hopkins and Paull, 2008).

NUCLEASE ASSAYS WITH LABELED DNA SUBSTRATES

Nuclease assays with 700 bp fluorophore-labeled DNA contained 25 mM MOPS pH 7.0, 1 mM DTT, 100 mM NaCl, 5 mM $MgCl_2$, and 1 mM ATP. DNA concentrations are indicated in the figure legend. Ten microliter reactions were incubated at 65°C for 30 min or 1 hr before reactions were terminated by 0.2% SDS and 10 mM EDTA. Products were analyzed on 15% or 20% polyacrylamide denaturing sequencing gels and scanned for Cy3 and Cy5 emission on a Typhoon imager (GE). The fluorophore-labeled 700 bp DNA substrates were constructed by PCR amplification of pTP466 with TP2108 (5'-Cy3-CTTGCATGCCTCAGCTATTCCGGATTATTCATACCGTCCCA-3') and TP2199 (5'- Cy5-AACCTCTACAAATGTGGTATGGCTG-3') to make the Cy3 (top strand)/Cy5 (bottom strand) substrate. To make the single Cy3 labeled 700 bp DNA substrates, PCR reactions with pTP466 were performed with TP2108 and TP1621 (5'-CCTCTACAAATGTGGTATGGCTG-3') to make Cy3 (top strand) and TP2151 (5'-CTTGCATGCCTCAGCTATTCCGGATTATTCATACCGTCCCA-3') and TP2238 (5'-Cy3-AACCTCTACAAATGTGGTATGGCTG-3') to make Cy3 (bottom strand). The fluorophore-labeled 2.4 kb DNA substrates were constructed by PCR amplification of

pTP36 with TP2108 and TP2199 to make the Cy3 (top strand)/Cy5 (bottom strand) and TP2283 (5'-Cy5-CTTGCATGCCTCAGCTATTCCGGATTATTCATACCGTCCCA-3') and TP2238 to make Cy5 (top strand)/Cy3 (bottom strand). Nuclease reactions with 5' [^{32}P]-700 bp DNA were performed similarly as fluorophore-labeled DNA except 0.2 nM DNA was used. 5' end labeled DNA was constructed by 5' labeling oligonucleotides prior to PCR amplification. The "5' top strand" substrate was constructed by 5' labeling TP2151 and performing PCR with unlabeled TP1621 on pTP466. The "5' bottom strand" substrate was constructed by 5' labeling TP1621 and performing PCR with unlabeled TP2151. Reaction products were analyzed on 20% sequencing gels and phosphorimaging. Nuclease assays with [^{32}P]-labeled oligonucleotide substrates were performed as described above except 1-2 nM oligonucleotide duplex was used in each reaction as indicated in the figure legends. The poly(T) duplex in Figure 3.4 was constructed by annealing either 5' ("5' top") or 3' labeled ("3' top") TP2389 (5'-CATGTAATCCCTCGATTTTTTTTTTTTTTTTTTTTTTTTACTGCTTTTTTTTTTG TAAGTTTTTTTTTTTTTTT-3') to TP2390 (5'-AAAAAAAAAAAAAAACTTACAAAAAAAAAAGCAGTAAAAAAAAAAAAAAA AAAAAAAAAATCGAGGGATTACATG-3'). The duplex in Figure 3.5 was constructed by annealing 5' labeled TP577 (5'-TCCCTCGATGAGGTCTAGAACTGCAGTGGCTGCACATCTGGCCTGTCTTACAC AGTGCTACAGACTGGAACAAAAAC-3') to TP578 (5'-GTTTTTGTTCCAGTCTGTAGCACTGTGTAAGACAGGCCAGATGTGCAGCCACT GCAGTTCTAGACCTCATCGAGGGA-3'). 5' and 3' labeling was performed as described previously (Hopkins and Paull, 2008).

TWO-STAGE *IN VITRO* RESECTION ASSAYS

In vitro resection assays were performed as described previously (Hopkins and Paull, 2008), with minor modifications. In the first stage, the DNA substrate (pTP163 cut at a unique site with SacI) was incubated at 65°C for 1 hr. Reactions were terminated with the addition of 0.01% SDS. I found that 0.01% SDS is sufficient to inactivate Mre11/Rad50 when it is added to the reaction before incubation at 65°C (not shown). Samples were diluted with water to 20 µl before being applied to Micro Bio-spin 6 columns (Biorad). The second stage reactions were performed in 30 µl and were incubated at 65°C for 30 min. Reactions were terminated with the addition of 0.2% SDS and 10 mM EDTA. Samples were analyzed on an agarose gel and analyzed by Southern hybridization as described previously (Hopkins and Paull, 2008).

QUANTITATIVE PCR

Resection products were analyzed by qPCR after performing two-stage reactions described above with some modifications. The DNA substrate consisted of a 4.4 kb plasmid (pNO1, Topogen) linearized at a unique site with SphI (NEB). First stage reactions were performed in a 10 µl volume containing 0.3 nM DNA in 25 mM MOPS pH 7.0, 1 mM DTT, 100 mM NaCl, 5 mM $MgCl_2$, and 1 mM ATP. Reactions were performed, terminated, and run through Micro-Biospin 6 columns as described above. Second stage reactions were performed as described above and terminated with the addition of 0.01% SDS. Five microliters of the reaction were diluted 20-fold into 1× NEB buffer 4. One-half of the mixture was digested with 2 units NciI (NEB) overnight at

37°C, and the other half was incubated under the same conditions but without the enzyme. Two microliters of digested or undigested DNA sample, 1 μl of each primer (25 μM) and probe (25 μM) were added to 50 μl reaction together with 25 μl 2x Taqman universal master mix (ABI). qPCR was performed on 7900HT Fast Real-Time PCR System (ABI) under standard thermal cycling conditions. Results were analyzed with SDS2.3 (ABI) and Microcal Origin 6.0. For each sample, a ΔC_T was calculated by subtracting the C_T value of the NciI-undigested from the C_T value of the digested sample. The percentage of ssDNA was determined using the equation: ssDNA % = (1/(2^(ΔC_T-1)+0.5) × 100. Primers and probes used for the analysis of the 29 nt site were: TP2493 (5'-GAGATGGCGCCCAACAGT-3'), TP2494 (5'-AAGATCGGGCTCGCCACT-3'), and TP2495 (5'-6FAM-ACGCCGAAACAAGCGCTCATGAG-TAMRA-3'). Primers and probes used for the analysis of the 1025 nt site were: TP2516 (5'-TGCTATGTGGCGCGGTATTAT-3'), TP2517 (5'-CTGTCATGCCATCCGTAAGATG), and TP2518 (5'-6FAM-CAAGAGCAACTCGGTCGCCGCATA-TAMRA-3'). I performed the two-stage resection reactions and preparation of DNA samples for qPCR. Dr. Zhi Guo performed qPCR and data analysis. I performed statistical analysis of the data using Student's T-test, two-sample assuming unequal variance in Microsoft Excel 2007. Statistically significant differences are based on $p < 0.05$ (two-tail p value).

GEL SHIFT BINDING ASSAYS

Binding reactions were performed in 25 mM MOPS pH 7.0, 1 mM DTT, 50 mM NaCl, 5 mM $MgCl_2$, and 1 nM oligonucleotide duplex. The 4 nt 3' overhang substrate was constructed by annealing TP74 (Paull and Gellert, 2000) (5'-CTGCAGGGTTTTTGTTCCAGTCTGTAGCACTGTGTAAGACAGGCCA-3') to TP2680 (5'-CTGTCTTACACAGTGCTACAGACTGGAACAAAAACCCTGCAGTACA-3'). The double-Y end substrate was constructed by annealing TP74 to TP2681 (5'-CTAGCTACTTGACACAGTGCTACAGACTGGAACTGACTTCATGCTA-3'). The 12 nt 3' overhang substrate was constructed by annealing TP74 to TP2682 (5'-CACAGTGCTACAGACTGGAACAAAAACCCTGCAGACTGACTTCATG-3'). All duplexes consisted of TP74 labeled at the 3' end. Binding was performed in 10 µl reactions at room temperature for 20 min before adding glycerol (5% final) and analyzed on native 6% 0.5× Tris-borate EDTA (TBE; 44.5 mM Tris-borate, 1 mM EDTA) polyacrylamide gels. Gels were dried and products were analyzed by phosphorimager (GE).

CHAPTER 4: CONCLUSIONS AND FUTURE DIRECTIONS

Repair of DNA double-strand breaks (DSB) by the homologous recombination (HR) pathway is the preferred method of repair for yeast and prokaryotes and is essential for development in vertebrates. By utilizing a non-broken homologous chromosome or sister chromatid as a template, HR results in accurate repair of the break. The earliest stage of HR repair is the generation of 3' single-stranded DNA (ssDNA) by degradation of the 5' strand in a process termed resection. In bacteria, the majority of DSBs are repaired by the RecBCD complex; however, no homologs of RecBCD have been found outside of bacteria. Based on genetic evidence in yeast, the Mre11/Rad50/Xrs2 (MRX) complex is implicated in the repair pathway, but a mechanistic understanding of how the Mre11/Rad50 complex and what other enzymes are involved is currently unknown. The purpose of this work was to biochemically characterize the role Mre11/Rad50 and other repair enzymes *in vitro* using recombinant proteins.

MRE11/RAD50 IN DSB REPAIR

The organization of prokaryotic genes into operons often suggests that the gene products functionally interact in a common biochemical pathway. This operon structure is also observed in genes necessary for DNA repair as the *recB* and *recD* genes are found in an operon in bacteria. These two gene products interact with RecC to form the RecBCD complex, which is involved in DNA double-strand break (DSB) repair. No orthologs for

RecBCD have been identified outside of prokaryotes and much research has been done to try and identify the enzymes involved in DSB repair in other organisms. Genetic screens in *S. cerevisiae* demonstrated that the *MRE11*, *RAD50*, and *XRS2* genes appear to be involved in break repair, but the biochemical activities of the Mre11/Rad50/Xrs2 (Mre11/Rad50/Nbs1 in humans and *S. pombe*) complex are inconsistent with the necessary repair steps observed *in vivo*. It was proposed that the MRX/N complex may modulate its activity in response to damage or other repair factors may be involved. The recent identification of the *mre11-rad50-herA-nurA* operon in thermophilic Archaea provided the first evidence that other cellular repair factors may collaborate with Mre11/Rad50 in the repair pathway (Constantinesco et al., 2002; Constantinesco et al., 2004; Manzan et al., 2004).

MRE11/RAD50 AND HERA/NURA COOPERATE TO RESECT THE 5' STRAND

The work described here characterized the roles of Mre11/Rad50 and HerA/NurA in DNA resection *in vitro*. My work demonstrated that Mre11/Rad50 is not involved in extensive 5' strand resection, but is critical for the activation and recruitment of HerA/NurA to DNA ends. Once HerA/NurA is localized to DNA ends in a process dependent on Rad50 ATP-dependent activities, HerA/NurA catalyzes 5' strand resection. Thus, resection of DSBs occurs in two distinct stages, which provides for multiple mechanisms of regulation.

COMBINED HELICASE/NUCLEASE ACTIVITY IN DNA REPAIR

The involvement of a DNA helicase and 5'-3' exonuclease in the repair of DSBs is important to the repair of DSBs in bacteria. The best characterized complex is the RecBCD heterotrimeric enzyme, which is the primary pathway for processing DSBs in *E. coli*. However, at least two other systems are involved in repair which also consists of combined helicase/nuclease functions: AddAB and AdnAB (Kooistra et al., 1997; Sinha et al., 2009). Considering that mutliple helicase/nuclease enzymes are involved in repair in bacteria, it is also likely that similar systems function to repair breaks in other prokaryotic organisms such as Archaea.

The observation that HerA and NurA interact directly in the absence of DNA suggests that HerA and NurA are found as a complex under normal conditions. Formation of a complex also explains why the helicase and nuclease activities of HerA and NurA, respectively, are enhanced in the presence of the other interacting partner. Cooperation between a DNA helicase and 5'-3' exonuclease in DNA resection is also observed in humans, where the BLM helicase physically interacts with hExo1 which promotes extensive DNA resection (Nimonkar et al., 2008), but may also play redundant roles (Gravel et al., 2008). Yeast orthologs to BLM and hExo1 also appear to participate in resection as Sgs1 (BLM homolog) and yExo1 play redundant roles in the repair pathway (Gravel et al., 2008; Mimitou and Symington, 2008; Zhu et al., 2008). Sgs1 and a second 5'-3' exonuclease Dna2 may cooperate in a common pathway (Budd and Campbell, 2009; Zhu et al., 2008). Based on these studies in humans, yeast, Archaea, and bacteria, resection of DSB ends by a helicase/nuclease complex appears to be a universal mechanism to repair DNA breaks.

Hexameric helicases are found in all kingdoms and catalyze the unwinding of DNA and RNA duplexes in a process dependent on nucleotide triphosphate hydrolysis. These enzymes are involved in multiple cellular functions, including DNA replication, recombination, and transcription (Patel and Picha, 2000). The RecQ-family helicase BLM was shown to form hexamers by gel filtration and electron microscopy and is involved in maintaining genomic stability by stimulating recombination repair through enhancement of Exo1-mediated resection (Gravel et al., 2008; Karow et al., 1999; Nimonkar et al., 2008).

The functional ortholog of BLM in *P. furiosus*, HerA, was also shown to form hexameric rings (Manzan et al., 2004), and both HerA and BLM have a central pore ranging is diameter from 20-35 Å, which is large enough to accommodate the DNA helix (~20 Å). HerA is related to FtsK and TrwB bacterial hexameric helicases (Iyer et al., 2004). Based on the crystal structure of FtsK and TrwB, the monomers form a ring by burying a large fraction of the protein surface with the neighboring monomer (~50% in the case of TrwB), and ATP is bound at the interface between monomers (Gomis-Ruth et al., 2001; Massey et al., 2006). The requirements for oligomerization vary as FtsK is normally monomeric but forms hexamers in the presence of DNA; however, oligomerization was independent of nucleotide (Massey et al., 2006). TrwB and HerA readily form hexamers in the absence of DNA and ATP (Gomis-Ruth et al., 2001; Manzan et al., 2004). The observation that ATP binding is found in the monomer-monomer interface suggests that nucleotide hydrolysis results in a conformational change, which allows the enzymes to translocate along the DNA helix and unwind one strand.

Several models for hexameric helicases have been proposed to explain the mechanism by which they unwind the two strands, including the wedge, torsion, and helix-destabilizing models (Patel and Picha, 2000). It is currently unknown which mechanism applies to helicases involved in DNA repair and is an active area of research for many groups.

The coupling of a 5'-3' exonuclease to a helicase during repair suggests a model for how the 5' strand is preferentially degraded during DSB repair. A physical or functional interaction between a helicase and 5'-3' exonuclease is observed in both yeast and human DNA repair systems. In yeast, the Sgs1 helicase and Dna2 exonuclease appear to function in a common pathway *in vivo*, and the human BLM helicase and Exo1 physically interact *in vitro* (Budd and Campbell, 2009; Nimonkar et al., 2008; Zhu et al., 2008). Similarly, a physical interaction between the *P. furiosus* HerA and NurA proteins is observed, and this interaction promotes both helicase and 5'-3' exonuclease activities *in vitro* (Hopkins and Paull, 2008).

Stimulation of a nuclease by a DNA helicase has been observed in several systems, ranging from bacteria to humans. The nuclease activity of RecB is stimulated when the RecD 5'-3' helicase is present (Yu et al., 1998), and human BLM activates hExo1 resection *in vitro* (Nimonkar et al., 2008). *P. furiosus* NurA functions as a 5'-3' exonuclease in manganese, but is inactive in magnesium. However, NurA is active as a nuclease in magnesium when functional HerA is present, suggesting that the activity of HerA results in a substrate for the NurA exonuclease. Together with earlier results demonstrating NurA substrate preference for ssDNA (Constantinesco et al., 2002), I hypothesize that the HerA helicase produces ssDNA available for NurA degradation and

explains how NurA may be active in magnesium. An alternative model is that binding to HerA results in a change in NurA conformation into a more active nuclease structure.

Although several examples of helicases stimulating nuclease activity exist, few examples of stimulation of helicase activity by nucleases have been reported. Work from Douglas Julin's laboratory demonstrated that the helicase activity of RecBC was abolished when the C-terminal nuclease domain of RecB was removed (Yu et al., 1998). HerA from *P. furiosus* is a weak DNA helicase when assayed alone *in vitro,* but the helicase activity is greatly increased in the presence of a nuclease-deficient NurA (Hopkins and Paull, 2008). The molecular mechanism underlying HerA helicase activation by NurA is currently unclear, but I hypothesize that the presence of an additional DNA-binding protein in a complex will result in an increased number of DNA contacts and these increase DNA interactions result in a higher affinity for DNA. This higher affinity for DNA makes the HerA/NurA complex more processive in DNA unwinding. Alternatively, binding of NurA to an allosteric site on HerA may alter its conformation into a more active helicase structure.

This close functional relationship between HerA and NurA is further supported by the observation that HerA and NurA physically interact. However, the interaction domains on HerA and NurA are currently unknown, but the association would presumably place NurA close to the 5' strand. Thus, depending on the unwinding mechanism of HerA and how the DNA strand is displaced, will determine the positioning of NurA. One caveat is that the translocation direction of HerA on DNA is also unknown and so it is impossible to determine a helicase mechanism based on the location of NurA.

Similar questions also apply to the yeast Sgs1/Dna2 system, where it is still unknown if and how these two enzymes interact.

FUNCTIONAL ROLE OF MRE11/RAD50

The evolutionarily conserved Mre11/Rad50 complex plays multiple roles involving DNA. It plays critical roles in the detection of DSB ends and the activation of the ATM signaling pathway, meiotic recombination, telomere maintenance, and in various repair pathways. The work discussed here has focused on the role of Mre11/Rad50 in repair by homologous recombination.

I found that the Mre11/Rad50 complex promotes DNA end resection by HerA and NurA *in vitro*, and that this stimulatory effect requires Rad50 ATP-dependent activity. The observation that Mre11 nuclease-deficient mutants do not completely impair resection is consistent with *in vivo* data demonstrating that the Mre11 nuclease activity is not essential for processing mitotic breaks in yeast (Moreau et al., 1999). There is a slight defect in long-range resection when the nuclease domain of Mre11 is mutated. Although the nuclease activity is not strictly required, it may play a currently unknown, subtle role in the resection process. Conversely, resection is completely dependent on Rad50 activity which may be related to Mre11/Rad50 catalyzed unwinding of the DNA end. Previous work has shown that human MRN is able to unwind short (17 bp) DNA duplexes in an ATP-dependent manner and that unwinding of DNA ends by MRN is critical for ATM activation (Lee and Paull, 2005; Paull and Gellert, 1999). Thus, I hypothesized that local melting of the duplex end by the Mre11/Rad50 complex is involved in the recruitment

and activation of downstream factors, and in this case the HerA/NurA resection machinery. Supporting the model that local unwinding of a DNA end is involved in activation of these resection enzymes is the observation that NurA preferentially binds to an oligonucleotide substrate containing partially unwound ends.

MRE11 NUCLEASE ROLE IN RESECTION

In vitro reactions with the Mre11 nuclease-deficient complex demonstrated a slight defect in HerA/NurA-mediated resection. Several possibilities exist to explain this effect, including weaker unwinding capability of the complex, impaired dissociation from DNA ends, or an Mre11 nuclease-dependent pathway in resection. To test the possibility that Mre11 nuclease activity may play a role in the resection process, I performed *in vitro* resection experiments, which were performed in two stages. DNA processed by wild-type Mre11/Rad50 in the first stage was resected by HerA/NurA more efficiently in the second stage compared to DNA that was not first incubated with MR. In this two-stage experiment, resection was ablated when the Mre11 nuclease mutant complex was used in the first reaction, suggesting that the nuclease activity of Mre11 plays a role in processing DNA prior to resection. Based on my Southern and end-labeled DNA substrate experiments which demonstrate that Mre11/Rad50 is capable of removing ~10-15 nt from the 5' strand to produce short 3' ssDNA regions, I hypothesize that the formation of DNA substrates with short 3' ssDNA regions at the ends is a preferred substrate for HerA/NurA resection. This is consistent with the fact that NurA demonstrates a

preference for binding oligonucleotide substrates containing 12 nt 3' ssDNA overhangs and is more efficient at degrading ssDNA (Constantinesco et al., 2002).

Theoretically, under conditions where Mre11/Rad50 may be limiting ([DSBs] > [Mre11/Rad50]), the Mre11/Rad50 complex may perform some initial nucleolytic processing of the ends before dissociating and localizing to another break end. After Mre11/Rad50 has dissociated from the end, the resection machinery HerA/NurA can bind and perform the necessary resection to facilitate repair. This may indeed be the case as MRX nuclease mutants demonstrate similar ionizing radiation (IR) survival under low doses as compared to wild-type *S. cerevisiae* strains, but have decreased survival at higher IR exposure (Lewis et al., 2004; Moreau et al., 1999). Other members of the Paull laboratory have also observed a slight defect in resection with a Mre11 nuclease mutant in a reconstituted reaction containing yeast MRX, Sae2, and yExo1 (Nicolette and Paull, unpublished data). This effect of Mre11 nuclease activity correlates with preferential binding of Exo1 to DNA substrates containing long (12 nt) 3' overhangs (unpublished results).

In addition to playing a role in resection of mitotic breaks, Mre11 nuclease activity is essential for the processing of meiotic DSBs in all organisms that undergo sexual reproduction (Furuse et al., 1998; Moreau et al., 1999; Tsubouchi and Ogawa, 1998; Usui et al., 1998). In *S. cerevisiae* and *S. pombe*, Sae2/Ctp1 is also required to remove Spo11/Rec12 5' conjugates (Hartsuiker et al., 2009; Milman et al., 2009; Neale et al., 2005; Rothenberg et al., 2009). I have shown that Mre11 removes 10-15 nt from the 5' strand by an endonucleolytic cleavage event, which is similar to the length of oligonucleotide attached to Spo11/Rec12 removed *in vivo* (~12-34 nt) (Milman et al.,

2009; Neale et al., 2005; Rothenberg et al., 2009). This biochemical activity of Mre11/Rad50 is consistent with the observed removal of 5' Spo11 conjugates *in vivo* and may explain why Rec12/Spo11 is found conjugated to short oligonucleotides when removed from meiotic hotspots.

I also tested the ability of Mre11/Rad50 complexes to remove 5' adducts by constructing a DNA substrate containing biotin on the end of both 5' strands. After conjugation to streptavidin, I performed reactions with either wild-type or nuclease-deficient Mre11/Rad50 complexes. I found that the Mre11 nuclease activity was required in addition to the helicase and nuclease activities of HerA/NurA for the removal of 5' conjugates (discussed in Chapter 3). The observation that the Mre11/Rad50 functions cooperatively with other cofactors to remove 5' protein adducts is not surprising considering yeast require Sae2/Ctp1 in addition to MR to remove Spo11/Rec12 adducts *in vivo*.

RAD50 ATP-DEPENDENT ACTIVITIES IN REPAIR

Early genetic evidence suggested that non-null mutations in Rad50 (*rad50S*) imparted a meiotic recombination defect in *S. cerevisiae* (Alani et al., 1990) due to the presence of unprocessed Spo11-induced DSBs at meiotic hotspots (Cao et al., 1990; Johzuka and Ogawa, 1995; Keeney et al., 1997). The *rad50S* mutations map to the Walker A domain, which suggests that the ATP-dependent activities of Rad50 are important for processing of meiotic breaks *in vivo*. However, these Rad50 mutations

result in a weak mitotic damage phenotype, which correlates with a slight defect of resection *in vitro* (Alani et al., 1990; Nicolette and Paull, unpublished data).

To better understand the role of Rad50 function in repair, a mutation in the conserved LSGG signature motif was constructed based on the Ser549→Arg mutation in the cystic fibrosis transmembrane conductance regulator (CFTR), which results in cystic fibrosis (Moncalian et al., 2004). The Ser793→Arg mutation in *P. furiosus* Rad50 blocks ATP binding and the MR(S1202R)N complex exhibits loss of ATP-dependent activities (Moncalian et al., 2004). The analogous mutation in *S. cerevisiae* Rad50 (S1205R) fails to complement a *rad50*Δ strain when exposed to DNA damaging agents and results in a significant delay in mating-type switching in mitotic cells (Moncalian et al., 2004). Budding yeast strains expressing MR(S1205R)X are also deficient in repair of both cohesive and noncohesive ends by nonhomologous end joining and defective meiosis (Bhaskara et al., 2007; Zhang and Paull, 2005). I found that Mre11/Rad50(S793R) complexes were completely deficient in resection *in vitro* (Hopkins and Paull, 2008). I speculated that mutation of the Rad50 signature motif results in defective DNA unwinding at the end, which is necessary for activation of downstream enzymes, such as ATM (Lee and Paull, 2005).

To test whether Mre11/Rad50 may locally unwind a DNA end to facilitate recruitment of the resection enzymes, an oligonucleotide substrate containing 11 and 13 unpaired nucleotides at both ends was constructed. NurA bound to this Y-end substrate preferentially over a fully closed substrate, suggesting that Mre11/Rad50 unwinding at a DNA end promotes binding of HerA/NurA to initiate resection. Binding to an unwound end may be a universal initiating resection mechanism as yeast Exo1 also binds

preferentially to a branched DNA end structure (Nicolette and Paull, unpublished data). The binding of HerA/NurA to an unwound DNA end defines an Mre11/Rad50 protein dependent repair pathway, and is distinct from the Mre11 nuclease dependent processing of ends as a prerequisite for resection described above. Based on quantitative measurements of resected ssDNA generated, the protein-dependent pathway is more efficient and likely the dominant repair pathway. I found that Mre11/Rad50 mediates recruitment of NurA to DNA, which likely forms the basis for the protein-dependent pathway (data not shown). Similar results were observed with yeast Exo1 and MRX *in vitro* (Nicolette and Paull, unpublished data).

Unfortunately, we do not yet know which component of Mre11/Rad50 is involved with the recruitment of NurA to DNA or which region on NurA forms contacts with the Mre11/Rad50 complex. The precise structure of the putatively unwound end is also currently unknown, but I estimate that approximately 15 nt are unwound. Attempts to determine the number of unwound nucleotides by potassium permanganate cleavage ($KMnO_4$) were unsuccessful, but similar chemical sensitivity techniques were used to determine that at least 5 nt were unwound by the RecBCD complex in a sequence-independent manner *in vitro* (Farah and Smith, 1997). The unwinding of DNA ends may be a common initiating mechanism and may serve a regulatory role such that only DSBs bound and unwound by Mre11/Rad50 are processed.

STRAND EXCHANGE BY THE RADA RECOMBINASE

The 3' ssDNA generated by resection is bound by the RecA-family of recombinases, and the RecA-filament catalyzes homologous pairing and strand exchange into an intact DNA template. The RecA ortholog in Archaea is RadA and is important for damage repair *in vivo* (Woods and Dyall-Smith, 1997) and catalyzes ATP-dependent strand exchange *in vitro* (Hopkins and Paull, 2008; Komori et al., 2000; Seitz et al., 1998). When *in vitro* resection assays were performed with Mre11/Rad50, HerA/NurA, RadA, and a supercoiled homologous plasmid, I observed formation of a joint-molecule product that corresponds to strand exchange of the resected linear DNA with the supercoiled DNA. The formation of the joint-molecule product was dependent on all of the enzymes, ATP, and the supercoiled DNA. The coordinated efforts of resection and strand exchange enzymes to produce a joint molecule demonstrate reconstitution of the first stage of HR repair *in vitro*. However, I still do not know if resection and RadA-filament formation occur simultaneously or as two separate events.

In the case of RecBCD, the RecB C-terminal nuclease domain makes direct contact with RecA and facilitates its loading onto ssDNA (Spies and Kowalczykowski, 2006). Of the 23 amino acids of RecA predicted to interact with RecB, 11 of them are conserved in RadA (48%) between aa 172-226, suggesting that RadA may be recruited to ssDNA through a similar domain. However, preliminary analysis of the putative interaction sequence of RecB was not found in Mre11/Rad50, HerA, or NurA.

In eukaryotes, Brca2 is involved in loading of Rad51 into ssDNA (Yuan et al., 1999) and the crystal structure of Brca2 bound to Rad51 demonstrates intimate contacts between the BRC domain 4 of Brca2 and Rad51 (Pellegrini et al., 2002). Interestingly,

sequence analysis demonstrates that a region between BRC 4 and BRC 5 shares sequence similarity to a region on HerA (aa 267-374), and the interacting region of Rad51 shares similarity to RadA. This putative interaction motif of RadA also overlaps with the RecA-RecB interaction region on RadA described earlier. Therefore, I hypothesize that HerA actively recruits RadA to the nascent ssDNA during HerA/NurA resection. To test this model, mutants of the HerA-RadA interaction motif need to be assayed in the combined resection/strand exchange experiment. Also, two-stage experiments described earlier where RadA is added after resection has been terminated will determine whether the loading of RadA occurs concurrently with or after resection is complete.

FUTURE WORK

To fully comprehend *in vivo* processes, it is desirable to reconstitute the necessary reactions *in vitro*. To study homologous recombination repair, I have reconstituted the first few steps in homologous recombination from 5' strand resection to strand exchange using purified proteins from *P. furiosus*. However, many other factors that may mediate or regulate these processes have yet to be studied. For example, the RadA paralog RadB in Archaea interacts with RadA and promotes RadA-catalyzed recombination (Komori et al., 2000). RadB was also shown to interact with the Holliday-junction resolvase Hjc and regulate Holliday-junction cleavage (Komori et al., 2000). Thus, the interaction between recombinase paralogs and Holliday-junction resolution enzymes connects these two processes.

Single-stranded DNA and ssDNA binding proteins play an important role in the repair process. Recent work has shown that activation of the ATM or ATR signaling pathway is a function of ssDNA length (Shiotani and Zou, 2009), and that human SSB1 and SSB2 complexes are involved in genome stability (Huang et al., 2009; Li et al., 2009; Richard et al., 2008). Archaea possess either SSB or RPA complexes, and *P. furiosus* RPA was shown to interact with RadA and Hjc *in vivo* and stimulate RadA activity *in vitro* (Komori and Ishino, 2001).

Based on these observations, it is clear that recombinase enzymes and ssDNA-binding proteins play a key role in both the recombination and resolution steps of HR repair. However, their role in resection has yet to be elucidated. I have purified *P. furiosus* RadB and the heterotrimeric RPA complex, but have yet to perform extensive *in vitro* experiments with these proteins. It is highly likely that inclusion of RadA paralogs and ssDNA binding proteins may increase the efficiency of resection and enhance the rate of strand exchange. Considering the interaction of these proteins with Holliday-junction resolvase (HJR), it appears that including the necessary DNA polymerases and HJRs that reconstitution of the repair process from resection to resolution of the repair products should be possible.

In addition to multiple factors involved in the repair process, posttranslational modification also has a role in regulating repair enzymes. Many enzymes involved in repair have been shown to be phosphorylated, including Mdc1, 53BP1, Nbs1, Mre11, CtIP/Ctp1/Sae2, Rad51, RPA, histone H2AX, and Exo1. It is unclear whether the repair enzymes in Archaea are phosphorylated *in vivo* and if this serves to regulate their activities; however, proteins involved in nucleotide metabolism have been shown to be

phosphorylated in the archaeon *H. salinarum* on serine or threonine residues (Aivaliotis et al., 2009), which suggests that DNA repair proteins may indeed be posttranslationally modified.

Additionally, the *in vivo* role of Mre11/Rad50, HerA, and NurA in *P. furiosus* has yet to be studied. Further insight into the physiological repair roles of these enzymes has been hindered by the lack of a tractable genetic system for *P. furiosus*. Development of an *in vivo* system to study Mre11/Rad50, HerA, and NurA will provide important *in vivo* evidence to support our *in vitro* work.

CONCLUDING REMARKS

I have reconstituted the first steps of homologous recombination repair with recombinant proteins from *P. furiosus*, and have shown that 5' strand resection is dependent upon the Mre11/Rad50 and HerA/NurA complexes. I have also shown that the newly resected DNA is sufficient for RadA loading and the RadA filament catalyzes strand exchange into an unbroken DNA template. By successfully reconstituting the repair process *in vitro*, I have identified the necessary core enzymatic activities required for HR *in vivo*. This has also been demonstrated in the yeast system, where the rate of resection *in vitro* closely mimics the *in vivo* rate (Nicolette and Paull, unpublished data; Zhu et al., 2008). Unfortunately, I do not know if my *in vitro* resection rate is similar to the rate *in vivo*. For both eukaryotes and Archaea, it is still unknown what controls the extent of resection. In bacteria, RecBCD catalyzed resection is mitigated by the Chi sequence. It is unknown whether any "Chi-like" sequences exist in either eukaryotes or

Archaea but it is possible that initiation of strand exchange or chromatin-bound proteins may attenuate resection. Alternatively, modification of the resection enzymes may modulate their activity, such as phosphorylation of Exo1 (Bolderson et al., 2009).

The work described here helps to understand the proteins and factors involved in DNA resection and strand exchange. It lays the framework for studies of both yeast and human repair mechanisms as well as for the understanding of other mediator factors, such as recombinase paralogs and ssDNA binding proteins. This work can be extended to include DNA extension of the joint molecule intermediate to Holliday junction (HJ) formation and the subsequent resolution of the HJ. This work hopefully is a model for understanding the repair system in other organisms and serves as an initiating point for future projects.

References

Aivaliotis, M., Macek, B., Gnad, F., Reichelt, P., Mann, M., and Oesterhelt, D. (2009). Ser/Thr/Tyr protein phosphorylation in the archaeon Halobacterium salinarum--a representative of the third domain of life. PLoS One *4*, e4777.

Ajimura, M., Leem, S.H., and Ogawa, H. (1993). Identification of new genes required for meiotic recombination in *Saccharomyces cerevisiae*. Genetics *133*, 51-66.

Alani, E., Padmore, R., and Kleckner, N. (1990). Analysis of wild-type and rad50 mutants of yeast suggests an intimate relationship between meiotic chromosome synapsis and recombination. Cell *61*, 419-436.

Allers, T., and Mevarech, M. (2005). Archaeal genetics—the third way. Nat Rev Genet *6*, 58-73.

Amundsen, S.K., Taylor, A.F., Reddy, M., and Smith, G.R. (2007). Intersubunit signaling in RecBCD enzyme, a complex protein machine regulated by Chi hot spots. Genes Dev *21*, 3296-3307.

Anderson, D.G., and Kowalczykowski, S.C. (1997). The translocating RecBCD enzyme stimulates recombination by directing RecA protein onto ssDNA in a chi-regulated manner. Cell *90*, 77-86.

Aravind, L., and Koonin, E.V. (2001). Prokaryotic homologs of the eukaryotic DNA-end-binding protein Ku, novel domains in the Ku protein and prediction of a prokaryotic double-strand break repair system. Genome Res *11*, 1365-1374.

Arthur, L.M., Gustausson, K., Hopfner, K.-P., Carson, C.T., Stracker, T.H., Karcher, A., Felton, D., Weitzman, M.D., Tainer, J., and Carney, J.P. (2004). Structural and functional analysis of Mre11-3. Nucl Acids Res *32*, 1886-1893.

Aylon, Y., Liefshitz, B., and Kupiec, M. (2004). The CDK regulates repair of double-strand breaks by homologous recombination during the cell cycle. EMBO J *23*, 4868-4875.

Barlow, J.H., Lisby, M., and Rothstein, R. (2008). Differential regulation of the cellular response to DNA double-strand breaks in G1. Mol Cell *30*, 73-85.

Baroni, E., Viscardi, V., Cartagena-Lirola, H., Lucchini, G., and Longhese, M.P. (2004). The functions of budding yeast Sae2 in the DNA damage response require Mec1- and Tel1-dependent phosphorylation. Mol Cell Biol *24*, 4151-4165.

Bergerat, A., de Massy, B., Gadelle, D., Varoutas, P.C., Nicolas, A., and Forterre, P. (1997). An atypical topoisomerase II from Archaea with implications for meiotic recombination. Nature *386*, 414-417.

Bhaskara, V., Dupre, A., Lengsfeld, B., Hopkins, B.B., Chan, A., Lee, J.H., Zhang, X., Gautier, J., Zakian, V., and Paull, T.T. (2007). Rad50 adenylate kinase activity regulates DNA tethering by Mre11/Rad50 complexes. Mol Cell *25*, 647-661.

Boehmer, P.E., and Emmerson, P.T. (1992). The RecB subunit of the Escherichia coli RecBCD enzyme couples ATP hydrolysis to DNA unwinding. J Biol Chem *267*, 4981-4987.

Bolderson, E., Tomimatsu, N., Richard, D.J., Boucher, D., Kumar, R., Pandita, T.K., Burma, S., and Khanna, K.K. (2009). Phosphorylation of Exo1 modulates homologous recombination repair of DNA double-strand breaks. Nucleic Acids Res.

Borde, V., Lin, W., Novikov, E., Petrini, J.H., Lichten, M., and Nicolas, A. (2004). Association of Mre11p with double-strand break sites during yeast meiosis. Mol Cell *13*, 389-401.

Budd, M.E., and Campbell, J.L. (2009). Interplay of Mre11 nuclease with Dna2 plus Sgs1 in Rad51-dependent recombinational repair. PLoS One *4*, e4267.

Cann, K.L., and Hicks, G.G. (2007). Regulation of the cellular DNA double-strand break response. Biochem Cell Biol *85*, 663-674.

Cao, L., Alani, E., and Kleckner, N. (1990). A pathway for generation and processing of double-strand breaks during meiotic recombination in *S. cerevisiae*. Cell *61*, 1089-1101.

Chapman, J.R., and Jackson, S.P. (2008). Phospho-dependent interactions between NBS1 and MDC1 mediate chromatin retention of the MRN complex at sites of DNA damage. EMBO Rep *9*, 795-801.

Charbonnier, F., Erauso, G., Barbeyron, T., Prieur, D., and Forterre, P. (1992). Evidence that a plasmid from a hyperthermophilic archaebacterium is relaxed at physiological temperatures. J Bacteriol *174*, 6103-6108.

Charbonnier, F., and Forterre, P. (1994). Comparison of plasmid DNA topology among mesophilic and thermophilic eubacteria and archaebacteria. J Bacteriol *176*, 1251-1259.

Clerici, M., Mantiero, D., Lucchini, G., and Longhese, M.P. (2005). The Saccharomyces cerevisiae Sae2 protein promotes resection and bridging of double strand break ends. J Biol Chem *280*, 38631-38638.

Connelly, J.C., de Leau, E.S., and Leach, D.R.F. (1999). DNA cleavage and degradation by the SbcCD protein complex from Escherichia coli. Nucleic Acids Res *27*, 1039-1046.

Connelly, J.C., de Leau, E.S., Okely, E.A., and Leach, D.R. (1997). Overexpression, purification, and characterization of the SbcCD protein from *Escherichia coli*. J Biol Chem *272*, 19819-19826.

Connelly, J.C., and Leach, D.R. (1996). The sbcC and sbcD genes of *Escherichia coli* encode a nuclease involved in palindrome inviability and genetic recombination. Genes Cells *1*, 285-291.

Constantinesco, F., Forterre, P., and Elie, C. (2002). NurA, a novel 5'-3' nuclease gene linked to rad50 and mre11 homologs of thermophilic Archaea. EMBO Rep *3*, 537-542.

Constantinesco, F., Forterre, P., Koonin, E.V., Aravind, L., and Elie, C. (2004). A bipolar DNA helicase gene, herA, clusters with rad50, mre11 and nurA genes in thermophilic archaea. Nucleic Acids Res *32*, 1439-1447.

Cost, G.J., and Boeke, J.D. (1998). Targeting of human retrotransposon integration is directed by the specificity of the L1 endonuclease for regions of unusual DNA structure. Biochemistry (Mosc) *37*, 18081-18093.

D'Amours, D., and Jackson, S.P. (2002). The Mre11 complex: at the crossroads of dna repair and checkpoint signalling. Nat Rev Mol Cell Biol *3*, 317-327.

de Jager, M., van Noort, J., van Gent, D.C., Dekker, C., Kanaar, R., and Wyman, C. (2001). Human Rad50/Mre11 is a flexible complex that can tether DNA ends. Mol Cell *8*, 1129-1135.

Delacote, F., Han, M., Stamato, T.D., Jasin, M., and Lopez, B.S. (2002). An xrcc4 defect or Wortmannin stimulates homologous recombination specifically induced by double-strand breaks in mammalian cells. Nucleic Acids Res *30*, 3454-3463.

Desai-Mehta, A., Cerosaletti, K.M., and Concannon, P. (2001). Distinct functional domains of nibrin mediate Mre11 binding, focus formation, and nuclear localization. Mol Cell Biol *21*, 2184-2191.

Dillingham, M.S., and Kowalczykowski, S.C. (2008). RecBCD enzyme and the repair of double-stranded DNA breaks. Microbiol Mol Biol Rev *72*, 642-671, Table of Contents.

Dillingham, M.S., Spies, M., and Kowalczykowski, S.C. (2003). RecBCD enzyme is a bipolar DNA helicase. Nature *423*, 893-897.

DiRuggiero, J., Santangelo, N., Nackerdien, Z., Ravel, J., and Robb, F.T. (1997). Repair of extensive ionizing-radiation DNA damage at 95 degrees C in the hyperthermophilic archaeon Pyrococcus furiosus. J Bacteriol *179*, 4643-4645.

Dixon, D.A., and Kowalczykowski, S.C. (1993). The recombination hotspot chi is a regulatory sequence that acts by attenuating the nuclease activity of the E. coli RecBCD enzyme. Cell *73*, 87-96.

Doherty, A.J., Jackson, S.P., and Weller, G.R. (2001). Identification of bacterial homologues of the Ku DNA repair proteins. FEBS Lett *500*, 186-188.

Dolganov, G.M., Maser, R.S., Novikov, A., Tosto, L., Chong, S., Bressan, D.A., and Petrini, J.H. (1996). Human Rad50 is physically associated with human Mre11: identification of a conserved multiprotein complex implicated in recombinational DNA repair. Mol Cell Biol *16*, 4832-4841.

Falck, J., Coates, J., and Jackson, S.P. (2005). Conserved modes of recruitment of ATM, ATR and DNA-PKcs to sites of DNA damage. Nature *434*, 605-611.

Farah, J.A., and Smith, G.R. (1997). The RecBCD enzyme initiation complex for DNA unwinding: enzyme positioning and DNA opening. J Mol Biol *272*, 699-715.

Furuse, M., Nagase, Y., Tsubouchi, H., Murakami-Murofushi, K., Shibata, T., and Ohta, K. (1998). Distinct roles of two separable in vitro activities of yeast Mre11 in mitotic and meiotic recombination. EMBO J *17*, 6412-6425.

Game, J.C., and Mortimer, R.K. (1974). A genetic study of x-ray sensitive mutants in yeast. Mutat Res *24*, 281-292.

Gerard, E., Jolivet, E., Prieur, D., and Forterre, P. (2001). DNA protection mechanisms are not involved in the radioresistance of the hyperthermophilic archaea Pyrococcus abyssi and P. furiosus. Mol Genet Genomics *266*, 72-78.

Gomis-Ruth, F.X., Moncalian, G., Perez-Luque, R., Gonzalez, A., Cabezon, E., de la Cruz, F., and Coll, M. (2001). The bacterial conjugation protein TrwB resembles ring helicases and F1-ATPase. Nature *409*, 637-641.

Gravel, S., Chapman, J.R., Magill, C., and Jackson, S.P. (2008). DNA helicases Sgs1 and BLM promote DNA double-strand break resection. Genes Dev *22*, 2767-2772.

Handa, N., Bianco, P.R., Baskin, R.J., and Kowalczykowski, S.C. (2005). Direct visualization of RecBCD movement reveals cotranslocation of the RecD motor after chi recognition. Mol Cell *17*, 745-750.

Hartsuiker, E., Mizuno, K., Molnar, M., Kohli, J., Ohta, K., and Carr, A.M. (2009). Ctp1CtIP and Rad32Mre11 nuclease activity are required for Rec12Spo11 removal, but Rec12Spo11 removal is dispensable for other MRN-dependent meiotic functions. Mol Cell Biol *29*, 1671-1681.

Hopfner, K.P., Craig, L., Moncalian, G., Zinkel, R.A., Usui, T., Owen, B.A., Karcher, A., Henderson, B., Bodmer, J.L., McMurray, C.T., *et al.* (2002). The Rad50 zinc-hook is a structure joining Mre11 complexes in DNA recombination and repair. Nature *418*, 562-566.

Hopfner, K.P., Karcher, A., Craig, L., Woo, T.T., Carney, J.P., and Tainer, J.A. (2001). Structural biochemistry and interaction architecture of the DNA double-strand break repair Mre11 nuclease and Rad50-ATPase. Cell *105*, 473-485.

Hopfner, K.P., Karcher, A., Shin, D., Fairley, C., Tainer, J.A., and Carney, J.P. (2000a). Mre11 and Rad50 from Pyrococcus furiosus: cloning and biochemical characterization reveal an evolutionarily conserved multiprotein machine. J Bacteriol *182*, 6036-6041.

Hopfner, K.P., Karcher, A., Shin, D.S., Craig, L., Arthur, L.M., Carney, J.P., and Tainer, J.A. (2000b). Structural biology of Rad50 ATPase: ATP-driven conformational control in DNA double-strand break repair and the ABC-ATPase superfamily. Cell *101*, 789-800.

Hopkins, B.B., and Paull, T.T. (2008). The P. furiosus Mre11/Rad50 complex promotes 5' strand resection at a DNA double-strand break. Cell *135*, 250-260.

Huang, J., Gong, Z., Ghosal, G., and Chen, J. (2009). SOSS complexes participate in the maintenance of genomic stability. Mol Cell *35*, 384-393.

Huertas, P., Cortes-Ledesma, F., Sartori, A.A., Aguilera, A., and Jackson, S.P. (2008). CDK targets Sae2 to control DNA-end resection and homologous recombination. Nature *455*, 689-692.

Huertas, P., and Jackson, S.P. (2009). Human CtIP mediates cell cycle control of DNA end resection and double strand break repair. J Biol Chem *284*, 9558-9565.

Ira, G., Pellicioli, A., Balijja, A., Wang, X., Fiorani, S., Carotenuto, W., Liberi, G., Bressan, D., Wan, L., Hollingsworth, N.M., *et al.* (2004). DNA end resection, homologous recombination and DNA damage checkpoint activation require CDK1. Nature *431*, 1011-1017.

Ivanov, E.L., Korolev, V.G., and Fabre, F. (1992). XRS2, a DNA repair gene of *Saccharomyces cerevisiae*, is needed for meiotic recombination. Genetics *132*, 651-664.

Ivanov, E.L., Sugawara, N., White, C.I., Fabre, F., and Haber, J.E. (1994). Mutations in XRS2 and RAD50 delay but do not prevent mating-type switching in Saccharomyces cerevisiae. Mol Cell Biol *14*, 3414-3425.

Iyer, L.M., Makarova, K.S., Koonin, E.V., and Aravind, L. (2004). Comparative genomics of the FtsK-HerA superfamily of pumping ATPases: implications for the origins of chromosome segregation, cell division and viral capsid packaging. Nucleic Acids Res *32*, 5260-5279.

Jazayeri, A., Falck, J., Lukas, C., Bartek, J., Smith, G.C.M., Lukas, J., and Jackson, S.P. (2006). ATM- and cell cycle-dependent regulation of ATR in response to DNA double-strand breaks. Nat Cell Biol *8*, 37-45.

Johzuka, K., and Ogawa, H. (1995). Interaction of Mre11 and Rad50: two proteins required for DNA repair and meiosis-specific double-strand break formation in *Saccharomyces cerevisiae*. Genetics *139*, 1521-1532.

Karow, J.K., Newman, R.H., Freemont, P.S., and Hickson, I.D. (1999). Oligomeric ring structure of the Bloom's syndrome helicase. Curr Biol *9*, 597-600.

Keeney, S. (2001). Mechanism and control of meiotic recombination initiation. Curr Top Dev Biol *52*, 1-53.

Keeney, S., Giroux, C.N., and Kleckner, N. (1997). Meiosis-specific DNA double-strand breaks are catalyzed by Spo11, a member of a widely conserved protein family. Cell *88*, 375-384.

Keeney, S., and Kleckner, N. (1995). Covalent protein-DNA complexes at the 5' strand termini of meiosis- specific double-strand breaks in yeast. Proc Natl Acad Sci *92*, 11274-11278.

Kehres, D.G., and Maguire, M.E. (2003). Emerging themes in manganese transport, biochemistry and pathogenesis in bacteria. FEMS Microbiol Rev *27*, 263-290.

Komori, K., and Ishino, Y. (2001). Replication Protein A in Pyrococcus furiosus Is Involved in Homologous DNA Recombination. J Biol Chem *276*, 25654-25660.

Komori, K., Miyata, T., DiRuggiero, J., Holley-Shanks, R., Hayashi, I., Cann, I.K., Mayanagi, K., Shinagawa, H., and Ishino, Y. (2000). Both RadA and RadB are involved in homologous recombination in Pyrococcus furiosus. J Biol Chem *275*, 33782-33790.

Kondo, N., Nishikubo, T., Wakamatsu, T., Ishikawa, H., Nakagawa, N., Kuramitsu, S., and Masui, R. (2008). Insights into different dependence of dNTP triphosphohydrolase on metal ion species from intracellular ion concentrations in Thermus thermophilus. Extremophiles *12*, 217-223.

Kooistra, J., Haijema, B.J., Hesseling-Meinders, A., and Venema, G. (1997). A conserved helicase motif of the AddA subunit of the Bacillus subtilis ATP-dependent nuclease (AddAB) is essential for DNA repair and recombination. Mol Microbiol *23*, 137-149.

Kowalczykowski, S.C., Dixon, D.A., Eggleston, A.K., Lauder, S.D., and Rehrauer, W.M. (1994). Biochemistry of homologous recombination in Escherichia coli. Microbiol Rev *58*, 401-465.

Kowalski, D., Natale, D.A., and Eddy, M.J. (1988). Stable DNA unwinding, not "breathing," accounts for single-strand-specific nuclease hypersensitivity of specific A+T-rich sequences. Proc Natl Acad Sci U S A *85*, 9464-9468.

Kuzminov, A. (1999). Recombinational repair of DNA damage in Escherichia coli and bacteriophage lambda. Microbiol Mol Biol Rev *63*, 751-813, table of contents.

Lee, J.-H., Ghirlando, R., Bhaskara, V., Hoffmeyer, M.R., Gu, J., and Paull, T.T. (2003). Regulation of Mre11/Rad50 by Nbs1: effects on nucleotide-dependent DNA binding and association with ATLD mutant complexes. J Biol Chem *278*, 45171-45181.

Lee, J.H., and Paull, T.T. (2005). ATM activation by DNA double-strand breaks through the Mre11-Rad50-Nbs1 complex. Science *308*, 551-554.

Lengsfeld, B.M., Rattray, A.J., Bhaskara, V., Ghirlando, R., and Paull, T.T. (2007). Sae2 Is an Endonuclease that Processes Hairpin DNA Cooperatively with the Mre11/Rad50/Xrs2 Complex. Mol Cell *28*, 638-651.

Lewis, L.K., Storici, F., Van Komen, S., Calero, S., Sung, P., and Resnick, M.A. (2004). Role of the nuclease activity of Saccharomyces cerevisiae Mre11 in repair of DNA double-strand breaks in mitotic cells. Genetics *166*, 1701-1713.

Li, S., Ting, N.S., Zheng, L., Chen, P.L., Ziv, Y., Shiloh, Y., Lee, E.Y., and Lee, W.H. (2000). Functional link of BRCA1 and ataxia telangiectasia gene product in DNA damage response. Nature *406*, 210-215.

Li, Y., Bolderson, E., Kumar, R., Muniandy, P.A., Xue, Y., Richard, D.J., Seidman, M., Pandita, T.K., Khanna, K.K., and Wang, W. (2009). HSSB1 and hSSB2 form similar multiprotein complexes that participate in DNA damage response. J Biol Chem *284*, 23525-23531.

Limbo, O., Chahwan, C., Yamada, Y., de Bruin, R.A., Wittenberg, C., and Russell, P. (2007). Ctp1 is a cell-cycle-regulated protein that functions with Mre11 complex to control double-strand break repair by homologous recombination. Mol Cell *28*, 134-146.

Lisby, M., Barlow, J.H., Burgess, R.C., and Rothstein, R. (2004). Choreography of the DNA damage response: spatiotemporal relationships among checkpoint and repair proteins. Cell *118*, 699-713.

Llorente, B., and Symington, L.S. (2004). The Mre11 nuclease is not required for 5' to 3' resection at multiple HO-induced double-strand breaks. Mol Cell Biol *24*, 9682-9694.

Lloyd, J., Chapman, J.R., Clapperton, J.A., Haire, L.F., Hartsuiker, E., Li, J., Carr, A.M., Jackson, S.P., and Smerdon, S.J. (2009). A supramodular FHA/BRCT-repeat architecture mediates Nbs1 adaptor function in response to DNA damage. Cell *139*, 100-111.

Lobachev, K., Vitriol, E., Stemple, J., Resnick, M.A., and Bloom, K. (2004). Chromosome fragmentation after induction of a double-strand break is an active process prevented by the RMX repair complex. Curr Biol *14*, 2107-2112.

Lobachev, K.S., Gordenin, D.A., and Resnick, M.A. (2002). The Mre11 complex is required for repair of hairpin-capped double-strand breaks and prevention of chromosome rearrangements. Cell *108*, 183-193.

Lopez-Garcia, P., and Forterre, P. (1997). DNA topology in hyperthermophilic archaea: reference states and their variation with growth phase, growth temperature, and temperature stresses. Mol Microbiol *23*, 1267-1279.

Luo, G., Yao, M.S., Bender, C.F., Mills, M., Bladl, A.R., Bradley, A., and Petrini, J.H. (1999). Disruption of mRad50 causes embryonic stem cell lethality, abnormal embryonic development, and sensitivity to ionizing radiation. Proc Natl Acad Sci U S A *96*, 7376-7381.

Manzan, A., Pfeiffer, G., Hefferin, M.L., Lang, C.E., Carney, J.P., and Hopfner, K.P. (2004). MlaA, a hexameric ATPase linked to the Mre11 complex in archaeal genomes. EMBO Rep *5*, 54-59.

Massey, T.H., Mercogliano, C.P., Yates, J., Sherratt, D.J., and Lowe, J. (2006). Double-stranded DNA translocation: structure and mechanism of hexameric FtsK. Mol Cell *23*, 457-469.

McConnell, K.J., and Beveridge, D.L. (2001). Molecular dynamics simulations of B '-DNA: sequence effects on A-tract-induced bending and flexibility. J Mol Biol *314*, 23-40.
McKee, A.H., and Kleckner, N. (1997). A general method for identifying recessive diploid-specific mutations in Saccharomyces cerevisiae, its application to the isolation of mutants blocked at intermediate stages of meiotic prophase and characterization of a new gene SAE2. Genetics *146*, 797-816.
Melander, F., Bekker-Jensen, S., Falck, J., Bartek, J., Mailand, N., and Lukas, J. (2008). Phosphorylation of SDT repeats in the MDC1 N terminus triggers retention of NBS1 at the DNA damage-modified chromatin. J Cell Biol *181*, 213-226.
Milman, N., Higuchi, E., and Smith, G.R. (2009). Meiotic DNA double-strand break repair requires two nucleases, MRN and Ctp1, to produce a single size class of Rec12 (Spo11)-oligonucleotide complexes. Mol Cell Biol *29*, 5998-6005.
Mimitou, E.P., and Symington, L.S. (2008). Sae2, Exo1 and Sgs1 collaborate in DNA double-strand break processing. Nature *455*, 770-774.
Moncalian, G., Lengsfeld, B., Bhaskara, V., Hopfner, K.P., Karcher, A., Alden, E., Tainer, J.A., and Paull, T.T. (2004). The Rad50 signature motif: essential to ATP binding and biological function. J Mol Biol *335*, 937-951.
Moreau, S., Ferguson, J.R., and Symington, L.S. (1999). The nuclease activity of Mre11 is required for meiosis but not for mating type switching, end joining, or telomere maintenance. Mol Cell Biol *19*, 556-566.
Nadal, M. (2007). Reverse gyrase: an insight into the role of DNA-topoisomerases. Biochimie *89*, 447-455.
Nadeau, J.G., and Crothers, D.M. (1989). Structural basis for DNA bending. Proc Natl Acad Sci U S A *86*, 2622-2626.
Nairz, K., and Klein, F. (1997). mre11S--a yeast mutation that blocks double-strand-break processing and permits nonhomologous synapsis in meiosis. Genes & Dev *11*, 2272-2290.
Neale, M.J., Pan, J., and Keeney, S. (2005). Endonucleolytic processing of covalent protein-linked DNA double-strand breaks. Nature *436*, 1053-1057.
Nicolette, M.L., and Paull, T.T. (unpublished data).
Nimonkar, A.V., Ozsoy, A.Z., Genschel, J., Modrich, P., and Kowalczykowski, S.C. (2008). Human exonuclease 1 and BLM helicase interact to resect DNA and initiate DNA repair. Proc Natl Acad Sci U S A *105*, 16906-16911.
Patel, S.S., and Picha, K.M. (2000). Structure and function of hexameric helicases. Annu Rev Biochem *69*, 651-697.
Paull, T.T., and Gellert, M. (1998). The 3' to 5' exonuclease activity of Mre11 facilitates repair of DNA double-strand breaks. Mol Cell *1*, 969-979.
Paull, T.T., and Gellert, M. (1999). Nbs1 potentiates ATP-driven DNA unwinding and endonuclease cleavage by the Mre11/Rad50 complex. Genes & Dev *13*, 1276-1288.
Paull, T.T., and Gellert, M. (2000). A mechanistic basis for Mre11-directed DNA joining at microhomologies. Proc Natl Acad Sci U S A *97*, 6409-6414.
Peak, M.J., Robb, F.T., and Peak, J.G. (1995). Extreme resistance to thermally induced DNA backbone breaks in the hyperthermophilic archaeon Pyrococcus furiosus. J Bacteriol *177*, 6316-6318.

Pellegrini, L., Yu, D.S., Lo, T., Anand, S., Lee, M., Blundell, T.L., and Venkitaraman, A.R. (2002). Insights into DNA recombination from the structure of a RAD51-BRCA2 complex. Nature *420*, 287-293.

Prinz, S., Amon, A., and Klein, F. (1997). Isolation of COM1, a new gene required to complete meiotic double-strand break-induced recombination in Saccharomyces cerevisiae. Genetics *146*, 781-795.

Puapaiboon, U., Jai-Nhuknan, J., and Cowan, J.A. (2001). Characterization of a multi-functional metal-mediated nuclease by MALDI-TOF mass spectrometry. Nucleic Acids Res *29*, 3652-3656.

Quaiser, A., Constantinesco, F., White, M.F., Forterre, P., and Elie, C. (2008). The Mre11 protein interacts with both Rad50 and the HerA bipolar helicase and is recruited to DNA following gamma irradiation in the archaeon Sulfolobus acidocaldarius. BMC Mol Biol *9*, 25.

Richard, D.J., Bolderson, E., Cubeddu, L., Wadsworth, R.I., Savage, K., Sharma, G.G., Nicolette, M.L., Tsvetanov, S., McIlwraith, M.J., Pandita, R.K., *et al.* (2008). Single-stranded DNA-binding protein hSSB1 is critical for genomic stability. Nature *453*, 677-681.

Rothenberg, M., Kohli, J., and Ludin, K. (2009). Ctp1 and the MRN-complex are required for endonucleolytic Rec12 removal with release of a single class of oligonucleotides in fission yeast. PLoS Genet *5*, e1000722.

Sartori, A.A., Lukas, C., Coates, J., Mistrik, M., Fu, S., Bartek, J., Baer, R., Lukas, J., and Jackson, S.P. (2007). Human CtIP promotes DNA end resection. Nature *450*, 509-514.

Seitz, E.M., Brockman, J.P., Sandler, S.J., Clark, A.J., and Kowalczykowski, S.C. (1998). RadA protein is an archaeal RecA protein homolog that catalyzes DNA strand exchange. Genes Dev *12*, 1248-1253.

Seitz, E.M., Haseltine, C.A., Kowalczykowski, S.C., and Paul, B. (2001). DNA recombination and repair in the Archaea. In Adv Appl Microbiol (Academic Press), pp. 101-169.

Shiloh, Y. (2003). ATM and related protein kinases: safeguarding genome integrity. Nat Rev Cancer *3*, 155-168.

Shiotani, B., and Zou, L. (2009). Single-stranded DNA orchestrates an ATM-to-ATR switch at DNA breaks. Mol Cell *33*, 547-558.

Shrivastav, M., De Haro, L.P., and Nickoloff, J.A. (2008). Regulation of DNA double-strand break repair pathway choice. Cell Res *18*, 134-147.

Shroff, R., Arbel-Eden, A., Pilch, D., Ira, G., Bonner, W.M., Petrini, J.H., Haber, J.E., and Lichten, M. (2004). Distribution and dynamics of chromatin modification induced by a defined DNA double-strand break. Curr Biol *14*, 1703-1711.

Singleton, M.R., Dillingham, M.S., Gaudier, M., Kowalczykowski, S.C., and Wigley, D.B. (2004). Crystal structure of RecBCD enzyme reveals a machine for processing DNA breaks. Nature *432*, 187-193.

Sinha, K.M., Unciuleac, M.C., Glickman, M.S., and Shuman, S. (2009). AdnAB: a new DSB-resecting motor-nuclease from mycobacteria. Genes Dev *23*, 1423-1437.

Sirover, M.A., and Loeb, L.A. (1976). Infidelity of DNA synthesis in vitro: screening for potential metal mutagens or carcinogens. Science *194*, 1434-1436.

Smith, G.R. (2001). Homologous recombination near and far from DNA breaks: alternative roles and contrasting views. Annu Rev Genet *35*, 243-274.
Sonoda, E., Hochegger, H., Saberi, A., Taniguchi, Y., and Takeda, S. (2006). Differential usage of non-homologous end-joining and homologous recombination in double strand break repair. DNA Repair (Amst) *5*, 1021-1029.
Spies, M., Amitani, I., Baskin, R.J., and Kowalczykowski, S.C. (2007). RecBCD Enzyme Switches Lead Motor Subunits in Response to [chi] Recognition. Cell *131*, 694-705.
Spies, M., Bianco, P.R., Dillingham, M.S., Handa, N., Baskin, R.J., and Kowalczykowski, S.C. (2003). A molecular throttle: the recombination hotspot chi controls DNA translocation by the RecBCD helicase. Cell *114*, 647-654.
Spies, M., and Kowalczykowski, S.C. (2006). The RecA binding locus of RecBCD is a general domain for recruitment of DNA strand exchange proteins. Mol Cell *21*, 573-580.
Spycher, C., Miller, E.S., Townsend, K., Pavic, L., Morrice, N.A., Janscak, P., Stewart, G.S., and Stucki, M. (2008). Constitutive phosphorylation of MDC1 physically links the MRE11-RAD50-NBS1 complex to damaged chromatin. J Cell Biol *181*, 227-240.
Sun, H., Treco, D., Schultes, N.P., and Szostak, J.W. (1989). Double-strand breaks at an initiation site for meiotic gene conversion. Nature *338*, 87-90.
Sun, H., Treco, D., and Szostak, J.W. (1991). Extensive 3'-overhanging, single-stranded DNA associated with the meiosis-specific double-strand breaks at the ARG4 recombination initiation site. Cell *64*, 1155-1161.
Symington, L.S. (2002). Role of RAD52 Epistasis Group Genes in Homologous Recombination and Double-Strand Break Repair. Microbiol Mol Biol Rev *66*, 630-670.
Takata, M., Sasaki, M.S., Sonoda, E., Morrison, C., Hashimoto, M., Utsumi, H., Yamaguchi-Iwai, Y., Shinohara, A., and Takeda, S. (1998). Homologous recombination and non-homologous end-joining pathways of DNA double-strand break repair have overlapping roles in the maintenance of chromosomal integrity in vertebrate cells. EMBO J *17*, 5497-5508.
Tauchi, H., Kobayashi, J., Morishima, K., Matsuura, S., Nakamura, A., Shiraishi, T., Ito, E., Masnada, D., Delia, D., and Komatsu, K. (2001). The Forkhead-associated Domain of NBS1 Is Essential for Nuclear Foci Formation after Irradiation but Not Essential for hRAD50/hMRE11/NBS1 Complex DNA Repair Activity. J Biol Chem *276*, 12-15.
Tauchi, H., Kobayashi, J., Morishima, K., van Gent, D.C., Shiraishi, T., Verkaik, N.S., vanHeems, D., Ito, E., Nakamura, A., Sonoda, E., *et al.* (2002). Nbs1 is essential for DNA repair by homologous recombination in higher vertebrate cells. Nature *420*, 93-98.
Taylor, A.F., and Smith, G.R. (1995). Strand specificity of nicking of DNA at Chi sites by RecBCD enzyme. Modulation by ATP and magnesium levels. J Biol Chem *270*, 24459-24467.
Taylor, A.F., and Smith, G.R. (2003). RecBCD enzyme is a DNA helicase with fast and slow motors of opposite polarity. Nature *423*, 889-893.

Trujillo, K.M., Roh, D.H., Chen, L., Van Komen, S., Tomkinson, A., and Sung, P. (2003). Yeast xrs2 binds DNA and helps target rad50 and mre11 to DNA ends. J Biol Chem *278*, 48957-48964.

Trujillo, K.M., and Sung, P. (2001). DNA structure-specific nuclease activities in the Saccharomyces cerevisiae Rad50/Mre11 complex. J Biol Chem *13*, 13.

Trujillo, K.M., Yuan, S.S., Lee, E.Y., and Sung, P. (1998). Nuclease activities in a complex of human recombination and DNA repair factors Rad50, Mre11, and p95. J Biol Chem *273*, 21447-21450.

Tseng, S.F., Chang, C.Y., Wu, K.J., and Teng, S.C. (2005). Importin KPNA2 is required for proper nuclear localization and multiple functions of NBS1. J Biol Chem *280*, 39594-39600.

Tsubouchi, H., and Ogawa, H. (1998). A novel mre11 mutation impairs processing of double-strand breaks of DNA during both mitosis and meiosis. Mol Cell Biol *18*, 260-268.

Usui, T., Ohta, T., Oshiumi, H., Tomizawa, J., Ogawa, H., and Ogawa, T. (1998). Complex formation and functional versatility of Mre11 of budding yeast in recombination. Cell *95*, 705-716.

Vermote, C.L., and Halford, S.E. (1992). EcoRV restriction endonuclease: communication between catalytic metal ions and DNA recognition. Biochemistry (Mosc) *31*, 6082-6089.

White, M.F., and Bell, S.D. (2002). Holding it together: chromatin in the Archaea. Trends Genet *18*, 621-626.

Williams, R.S., Dodson, G.E., Limbo, O., Yamada, Y., Williams, J.S., Guenther, G., Classen, S., Glover, J.N., Iwasaki, H., Russell, P., *et al.* (2009). Nbs1 flexibly tethers Ctp1 and Mre11-Rad50 to coordinate DNA double-strand break processing and repair. Cell *139*, 87-99.

Williams, R.S., Moncalian, G., Williams, J.S., Yamada, Y., Limbo, O., Shin, D.S., Groocock, L.M., Cahill, D., Hitomi, C., Guenther, G., *et al.* (2008). Mre11 dimers coordinate DNA end bridging and nuclease processing in double-strand-break repair. Cell *135*, 97-109.

Woods, W.G., and Dyall-Smith, M.L. (1997). Construction and analysis of a recombination-deficient (radA) mutant of Haloferax volcanii. Mol Microbiol *23*, 791-797.

Wu, L., Luo, K., Lou, Z., and Chen, J. (2008). MDC1 regulates intra-S-phase checkpoint by targeting NBS1 to DNA double-strand breaks. Proc Natl Acad Sci U S A *105*, 11200-11205.

Xiao, Y., and Weaver, D.T. (1997). Conditional gene targeted deletion by Cre recombinase demonstrates the requirement for the double-strand break repair Mre11 protein in murine embryonic stem cells. Nucleic Acids Res *25*, 2985-2991.

Yamaguchi-Iwai, Y., Sonoda, E., Sasaki, M.S., Morrison, C., Haraguchi, T., Hiraoka, Y., Yamashita, Y.M., Yagi, T., Takata, M., Price, C., *et al.* (1999). Mre11 is essential for the maintenance of chromosomal DNA in vertebrate cells. EMBO J *18*, 6619-6629.

Yang, S.W., and Nash, H.A. (1994). Specific photocrosslinking of DNA-protein complexes: identification of contacts between integration host factor and its target DNA. Proc Natl Acad Sci U S A *91*, 12183-12187.

You, Z., Chahwan, C., Bailis, J., Hunter, T., and Russell, P. (2005). ATM activation and its recruitment to damaged DNA require binding to the C terminus of Nbs1. Mol Cell Biol *25*, 5363-5379.
You, Z., Shi, L.Z., Zhu, Q., Wu, P., Zhang, Y.W., Basilio, A., Tonnu, N., Verma, I.M., Berns, M.W., and Hunter, T. (2009). CtIP links DNA double-strand break sensing to resection. Mol Cell *36*, 954-969.
Yu, M., Souaya, J., and Julin, D.A. (1998). The 30-kDa C-terminal domain of the RecB protein is critical for the nuclease activity, but not the helicase activity, of the RecBCD enzyme from Escherichia coli. Proc Natl Acad Sci U S A *95*, 981-986.
Yuan, S.S., Lee, S.Y., Chen, G., Song, M., Tomlinson, G.E., and Lee, E.Y. (1999). BRCA2 is required for ionizing radiation-induced assembly of Rad51 complex in vivo. Cancer Res *59*, 3547-3551.
Yun, M.H., and Hiom, K. (2009). CtIP-BRCA1 modulates the choice of DNA double-strand-break repair pathway throughout the cell cycle. Nature *459*, 460-463.
Zhang, S., Wei, T., Hou, G., Zhang, C., Liang, P., Ni, J., Sheng, D., and Shen, Y. (2008). Archaeal DNA helicase HerA interacts with Mre11 homologue and unwinds blunt-ended double-stranded DNA and recombination intermediates. DNA Repair (Amst) *7*, 380-391.
Zhang, X., and Paull, T.T. (2005). The Mre11/Rad50/Xrs2 complex and non-homologous end-joining of incompatible ends in S. cerevisiae. DNA Repair (Amst) *4*, 1281-1294.
Zhu, J., Petersen, S., Tessarollo, L., and Nussenzweig, A. (2001). Targeted disruption of the Nijmegen breakage syndrome gene NBS1 leads to early embryonic lethality in mice. Curr Biol *11*, 105-109.
Zhu, Z., Chung, W.H., Shim, E.Y., Lee, S.E., and Ira, G. (2008). Sgs1 helicase and two nucleases Dna2 and Exo1 resect DNA double-strand break ends. Cell *134*, 981-994.
Zierhut, C., and Diffley, J.F. (2008). Break dosage, cell cycle stage and DNA replication influence DNA double strand break response. EMBO J *27*, 1875-1885.

Vita

Ben Barrett Hopkins was born in Penang, Malaysia on the 19th of March 1980. He is the son of Corrinne and Fred Hopkins. He attended the International School of Bangkok in Bangkok, Thailand and graduated in 1998. He then went to the University of California, Santa Barbara where he received his B.S. in Microbiology in 2002 and his M.S. in Chemistry in 2004. He enrolled in the Microbiology Ph.D. program at the University of Texas, Austin in the Fall of 2004.

Permanent address: 4600 Avenue C, Austin, TX 78751

This dissertation was typed by Ben Barrett Hopkins